GEMS&GEMOLOGY

TABLE OF CONTENTS

pg. 245

pg. 266

pg. 281

pg. 310

ABOUT THE COVER: The effect of blue fluorescence on the appearance of faceted diamonds is a controversial topic in the trade today. Yet inert and fluorescent diamonds are commonly placed next to each other in contemporary jewelry. Half the necklace and one earring in this composite photo are shown under normal lighting conditions (left), and the other half of the necklace and the same earring are shown as they appear under a long-wave ultraviolet lamp (right). For a complete view of the necklace and earrings under both lighting environments, see page 258. The diamonds in the necklace weigh a total of 132 ct, and the pear-shaped center stone in the earring weighs 3.20 ct. Courtesy of Harry Winston, Inc., New York.

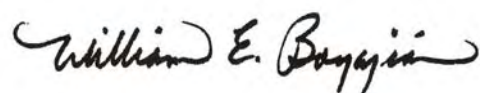*Photo by Harold & Erica Van Pelt—Photographers, Los Angeles, CA.*

The Impact of Fluorescence in Diamonds:
A Different Research Perspective

*T*he effect of ultraviolet fluorescence on diamond appearance has been hotly debated for at least the past decade. Opinions of even the most experienced tradespeople vary widely. With great conviction, some say that blue fluorescence of different strengths typically enhances a diamond's overall appearance. Others, as convincingly, say that it has a negative effect. To address this controversy, researchers at the GIA Gem Trade Laboratory conducted an experiment on the effects of long-wave ultraviolet radiation on the color appearance and transparency of gem diamonds. Their results are reported in this issue.

This study challenges the perception held by many in the trade that UV fluorescence generally has a negative effect on the overall appearance of a diamond. In fact, the results support the age-old belief that strong or even very strong blue fluorescence can improve appearance rather than detract from it, especially in diamonds with faint yellow body color. This result is consistent with the slightly higher "asking" prices reported for these stones. While the apparent benefits of blue fluorescence are less obvious in colorless to very near-colorless diamonds, they still were evident in the study. This should bring into question the trade's lower "bid" prices for moderate to highly fluorescent diamonds in the better colors. It also makes us question the source of the present controversy surrounding fluorescent diamonds. It may be the result of trademembers' misunderstanding of the complexity of the issue, or the extreme price sensitivity in the highest color grades (where there are fewer stones and distinctions are more subtle). Or it may be the fact that it is simply easier to move goods without the encumbrance of a reported fluorescence.

To some extent, this type of research project is unusual in gemology, in that human observation rather than instrumental analysis is the key tool. Yet evaluation of this human element is just the kind of important research that is needed to help resolve misunderstandings and false perceptions among members of the trade and even the consuming public. Gemological research involves not only the physical, optical, and chemical nature of gems, but also the visual assessment of stones in buying and selling situations. GIA will never alter its course of promoting the scientific examination of gem materials to seek knowledge and understanding, but we also want to encourage more research studies that address important trade concerns.

Thus, we believe that the diamond fluorescence article is as significant a contribution to gemology as the synthetic moissanite and synthetic emerald articles also featured in this issue. After all, the science of gemology is not just about R.I.'s and S.G.'s, or even sophisticated chemical and spectral analysis. It is also about dispelling (or, in some cases, confirming) beliefs that have been perpetuated over the years, and about separating bias and tradition from reality in the gem industry.

William E. Boyajian
President, Gemological Institute of America

A Contribution to Understanding the Effect of Blue Fluorescence on the Appearance of Diamonds

By Thomas M. Moses, Ilene M. Reinitz, Mary L. Johnson, John M. King, and James E. Shigley

Some gem diamonds fluoresce, most commonly blue, to the concentrated long-wave ultraviolet radiation of a UV lamp. There is a perception in the trade that this fluorescence has a negative effect on the overall appearance of such a diamond. Visual observation experiments were conducted to study this relationship. Four sets of very similar round brilliant diamonds, covering the color range from colorless to faint yellow, were selected for the different commonly encountered strengths of blue fluorescence they represented. These diamonds were then observed by trained graders, trade professionals, and average observers in various stone positions and lighting environments. For the average observer, meant to represent the jewelry buying public, no systematic effects of fluorescence were detected. Even the experienced observers did not consistently agree on the effects of fluorescence from one stone to the next. In general, the results revealed that strongly blue fluorescent diamonds were perceived to have a better color appearance when viewed table-up, with no discernible trend table-down. Most observers saw no relationship between fluorescence and transparency.

ABOUT THE AUTHORS

Mr. Moses is vice-president of identification services, Dr. Reinitz is manager of research and development, and Mr. King is laboratory projects officer at the GIA Gem Trade Laboratory, New York. Dr. Johnson is manager of research and development at the GIA Gem Trade Laboratory, Carlsbad, California, and Dr. Shigley is director of GIA Research in Carlsbad.

Please see acknowledgments at the end of the article.

Many factors influence the color appearance of colorless to faint yellow diamonds. Typically, such diamonds are quality graded for the absence of color according to the D-to-Z scale developed by the Gemological Institute of America in the 1940s (Shipley and Liddicoat, 1941). By *color appearance*, however, we mean the overall *look* of a polished diamond's color that results from a combination of factors such as bodycolor, shape, size, cutting proportions, and the position and lighting in which it is viewed. When exposed to invisible ultraviolet (UV) radiation, some diamonds emit visible light, which is termed *fluorescence* (figure 1). This UV fluorescence arises from submicroscopic structures in diamonds. Various colors of fluorescence in diamond are known, but blue is by far the most common.

The response of a diamond to the concentrated radiation of an ultraviolet lamp is mentioned as an *identifying characteristic* (rather than a grading factor) on quality-grading reports issued by most gem-testing laboratories. Other light sources—such as sunlight or fluorescent tubes—also contain varying amounts of UV radiation. Although there have been instances where the color and strength of the fluorescence seen in diamonds observed in these other light sources are also believed to influence color appearance, in recent years the fluorescence noted on grading reports has been singled out by many in the diamond trade and applied across the board as a marker for pricing distinctions. Generally, these distinctions are applied in the direction of lower offering prices for colorless and near-colorless diamonds that exhibit fluorescence to a UV lamp (Manny Gordon, pers. comm., 1997). Other trade members contend that the overall color appearance of a diamond typically is not adversely affected by this property (William Goldberg, pers. comm., 1997); many even say that blue fluorescence enhances color appearance.

Figure 1. Blue is by far the most common fluorescence color encountered in gem diamonds when they are exposed to the concentrated long-wave ultraviolet radiation of a UV lamp. In recent years, this property of many diamonds has been the subject of much debate with regard to its effect on appearance and value. Photo by Harold & Erica Van Pelt.
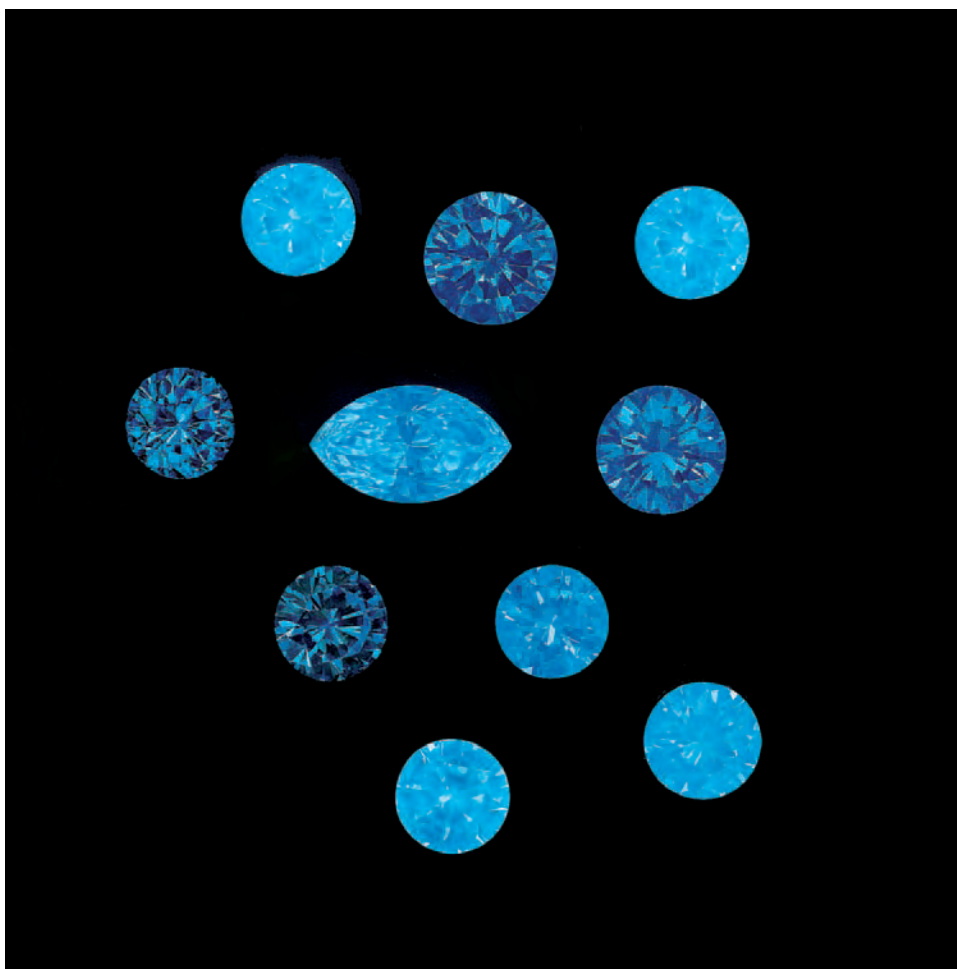
To date, however, there have been no studies that examine the influence of blue fluorescence on the appearance of a diamond under normal viewing conditions. To this end, we identified certain fundamental variables that we needed to investigate as a first step in understanding this complex issue. For example, a grading laboratory such as the GIA Gem Trade Laboratory (GIA GTL) assesses color under carefully controlled lighting and viewing conditions and mainly with the diamond positioned table-down. In a retail jewelry store, when a diamond is examined for its overall color appearance in mounted jewelry, viewing normally occurs with the diamond table-up in any of a variety of lighting conditions, as it does for the wearing of jewelry. Also, because it is within the D through J range that fluorescence has become a greater influence on pricing (Don Palmieri, pers. comm., 1997), we decided to focus our initial investigation on diamonds that represent this end of the color scale. Thus, the purpose of this study was to explore the perceived influence of reported blue fluorescence in colorless to faint

yellow diamonds when viewed in different positions and under different lighting conditions by observers from both within and outside the diamond industry.

BACKGROUND

Industry Perception of Fluorescence in Diamonds. Historically, the trade has given names to certain types of fluorescent diamonds based on the mines that produced significant numbers of such stones. The term *premier*, for example, has been used to describe light yellow diamonds with strong blue fluorescence, because such diamonds were often recovered from South Africa's Premier mine. The term *jager* has been used to describe colorless stones with strong blue fluorescence; the name originates from the Jagersfontein mine in South Africa, where such diamonds were once common (Bruton, 1978). Historically, some diamond merchants would seek out near-colorless to light yellow diamonds with strong blue fluorescence because they

BOX A: FLUORESCENCE IN DIAMOND

Fluorescence is a form of luminescence. For the purposes of this paper, *luminescence* is defined as the emission of light by a substance that has absorbed UV radiation. A substance is *fluorescent* if the emission of light stops when the energy source causing it is removed. (In contrast, if a substance continues to glow after the energy source is removed, it is *phosphorescent*.)

In a luminescent substance, the absorption of UV radiation causes an electron to move from its stable low-energy position ("ground state") into a temporary high-energy ("excited") state (figure A-1). This high-energy state is unstable, so the electron relaxes into a lower-energy excited state that is slightly more stable. As the electron falls back to the ground state, the substance emits light. This emitted energy is always less than excitation energy. Since wavelength increases as energy decreases, emission occurs at longer wavelengths than the excitation wavelength (again, see figure A-1). Submicroscopic structures that allow this movement of electrons are called *luminescence centers.* These centers arise from certain defects in the crystal lattice, such as electrically charged ions, or atomic vacancies or substitutions (see Nassau, 1983; Waychunas, 1988).

Gem diamonds typically contain a variety of structural defects, most involving impurity atoms such as nitrogen, hydrogen, and boron. Nitrogen-related defects are the most common of these, and only some of the resulting defects cause luminescence (Clark et al., 1992; Collins, 1992; see also Davies et al., 1978). The nitrogen-related defects, and their association with fluorescence, are described as follows:

• A single nitrogen atom substituting for carbon in a diamond that is partly type Ib (see, e.g., Fritsch and Scarratt, 1992) produces orangy yellow fluorescence.
• A group of two nitrogen atoms, the A aggregate, tends to quench—that is, extinguish—fluorescence.
• A group of three nitrogen atoms is called the N3 center, and produces blue fluorescence.
• A group of four nitrogen atoms is called the B aggregate, and is not known to cause luminescence.
• A lens-shaped cluster of nitrogen atoms is called a platelet, and is associated with yellow fluorescence.
• A single nitrogen atom trapped near a carbon vacancy causes bright orange fluorescence.
• A vacancy trapped near an A or B aggregate is called the H3 (H4) center, and generates green fluorescence.

A single diamond may contain several different kinds of defects, leading to a range of complex relationships between nitrogen content, nitrogen aggregation state, diamond color, and fluorescence color and strength. A diamond may also display two different fluorescence colors, either clearly zoned or closely mixed together. As described in the Background section of the text, of 5,710 colorless to near-colorless diamonds that fluoresced a noticeable color, 97% showed blue fluorescence, which is caused by the N3 center. Of 16,835 diamonds in the same study that did not fluoresce, many contained N3 centers, but they also contained enough A aggregates to prevent any visible luminescence. The existence of N3 centers in these diamonds is suggested by their yellow bodycolor (most commonly caused by "Cape" absorption bands, which are related to these centers); the existence of A aggregates (or other centers that quench luminescence) is evident from the fact that the stones do not fluoresce. These complexities confound the trade notion that nonfluorescent diamonds are more "pure" than those that fluoresce, since there are nitrogen-related centers that extinguish fluorescence, as well as those that cause blue fluorescence.
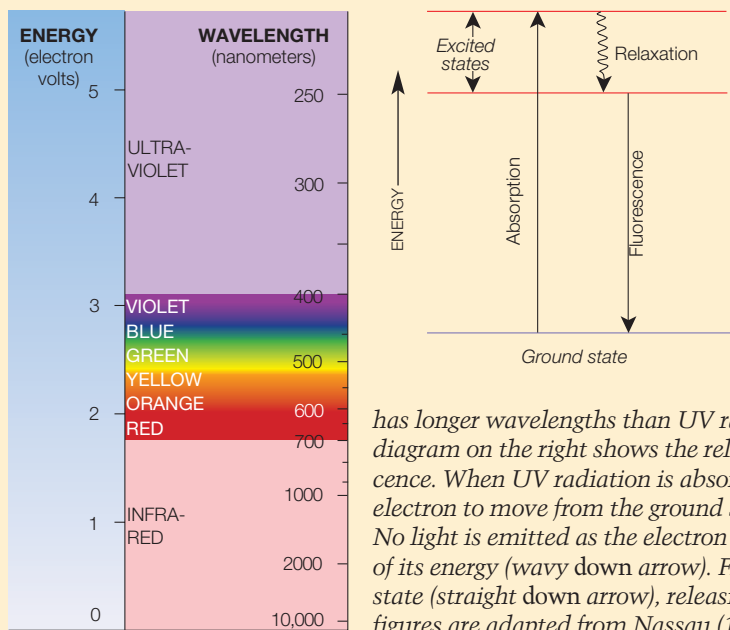
Figure A-1. The diagram on the left shows the relationship of visible light to ultraviolet and infrared radiation. The wavelength of light is related to its energy in an inverse manner: the longer the wavelength, the lower the energy. Visible light has longer wavelengths than UV radiation, but is lower in energy. The energy diagram on the right shows the relationship between absorption and luminescence. When UV radiation is absorbed at a luminescence center, it causes an electron to move from the ground state to an excited state (straight up *arrow). No light is emitted as the electron moves to a slightly lower state, losing some of its energy (wavy* down *arrow). From this lower state it returns to the ground state (straight* down *arrow), releasing energy as fluorescence (visible light). Both figures are adapted from Nassau (1983).*

believed that such fluorescence gave rise to a diamond that appeared "more colorless" (i.e., "less yellow") under lighting with a high UV content. Firms such as C. D. Peacock were known to actively look for such fluorescent diamonds (Joe Samuel Jr., pers. comm., 1997). Often these diamonds were marketed as "blue-white," a term that was prohibited by U.S. Trade Practice Rules in 1938 (U.S. Federal Trade Commission, 1938). Recognizing that some highly fluorescent diamonds might have a slightly different color appearance when viewed under light sources with differing UV content, Shipley and Liddicoat (1941) emphasized the importance of controlled lighting conditions for consistent color grading of faceted diamonds.

Tradespeople further observed that some gem diamonds with a hazy appearance also fluoresced strong blue to UV radiation. In the dynamic market of the late 1970s, some dealers began offering substantially lower prices for what they called "milky Ds" (diamonds with a color grade of D, very strong blue fluorescence, and reduced transparency). Over the next decade, the perceived negative impact of fluorescence spread down the color grade scale (as far as F) and eventually also included stones with weaker fluorescence (M. Rapaport, pers. comm., 1997). In recent years, fluorescence has had more impact as a value factor because of the influx of large quantities of high-quality diamonds from Russia. Many of these diamonds exhibit moderate to strong blue fluorescence to the UV lamp (Kevo Ayvazian, pers. comm., 1997).

The concerns about fluorescence can be attributed to a number of factors. These include notions that: (1) nonfluorescent diamonds are more "pure" than those that fluoresce, (2) nonfluorescent diamonds (in the colorless range [D–F]) are rarer than fluorescent diamonds in the same color range, and (3) the hazy appearance seen in some strongly fluorescent diamonds must exist in more weakly fluorescent diamonds as well. With the airing of a television "exposé" in South Korea in 1993 (*We Want to Know That*), the negative image of fluorescent diamonds was brought to the attention of consumers as well.

An indication of the extent to which fluorescence influences market value is found in the *Rapaport Diamond Report* weekly price guide. In the November 7, 1997, *Report*, for example, some higher-color (D-H) diamonds with very strong fluorescence were listed for up to 15% less than compa-rable nonfluorescent stones. From the spring of 1993 until the present time, the *Report* has stated that "the impact of blue fluorescence on price depends on its noticeability." Although the fluorescence description (which is based on observations made under a long-wave UV lamp) can be read from a laboratory grading report, "noticeability" refers to the direct observation of the diamond under the lighting conditions of a normal trading environment. In that same issue of the *Report*, lower-color (I–N) diamonds with very strong fluorescence carried a *premium* of up to 4% over similar nonfluorescing stones. This may be due to the continuing perception of many in the trade that blue fluorescence acts to mask or offset the faint to very light yellow bodycolor of some gem diamonds.

Observation of Fluorescence. Fluorescence is the "emission of visible light by a material such as diamond when it is stimulated by higher-energy X-rays, ultraviolet radiation, or other forms of radiation. Fluorescence continues only as long as the material is exposed to the radiation" (Liddicoat, 1993, p. 91). In gem testing, the ultraviolet unit that is commonly used provides two types of UV radiation. These two types are normally referred to by their most intense excitation wavelengths: 365 nm, or long-wave UV (also an important component of daylight); and 254 nm, or short-wave UV. Although the latter provides identification data for the laboratory, it is long-wave UV fluorescence that is meant when *fluorescence* is discussed in the diamond trade or described on a diamond grading report. (For more on fluorescence in diamonds, see Box A.)

Depending on the viewing conditions and the observer's visual perception, the reaction of a diamond to long-wave UV radiation may vary in both strength and hue. Both colorless and colored diamonds can fluoresce several hues, most commonly blue, yellow, orange, and white. Some pink (and, on rare occasions, colorless and near-colorless) diamonds fluoresce bright orange. Some blue diamonds, such as the Hope, fluoresce (and phosphoresce) red to short-wave UV. These different colors of UV fluorescence arise either from trace impurities (mainly nitrogen and boron, possibly hydrogen) or from other submicroscopic defects in the diamond crystal structure (again, see Box A). In the experience of GIA GTL, strength of fluorescence does not directly correlate to either color or clarity. For example, a diamond with a clarity grade of

internally flawless and a color grade of D can exhibit the same strength of blue fluorescence as another diamond with a clarity of I_1 and a color grade of J.

A gemological report assigns grades so that the quality of one diamond may be assessed relative to others, but it also provides information that describes the stone and helps separate it from other diamonds. *At GIA GTL, the fluorescence entry on a diamond grading report is considered to be a description, not a grade.* In fact, the laboratory has used fluorescence to help clients recover diamonds that were lost or stolen.

At GIA GTL, the standard procedure for observing UV fluorescence includes use of a long-wave UV lamp in a darkened viewing environment. Factors such as the distances and viewing angles between the UV lamp, the diamond, and the observer are specified to maintain consistency between observers. A set of reference diamonds is used to establish the intensity of the fluorescence exhibited by a stone within the ranges none, faint, medium, strong, and very strong. In a procedure similar to that employed for color grading with the D-to-Z scale, the diamond being examined is placed table-down and moved between the reference stones until the intensity of the fluorescence is stronger than the

Figure 2. As with diamond color grading, both the control of observation variables (light source, environment, viewing geometry) and the use of known reference stones are required to make consistent fluorescence observations. At GIA GTL, the diamond being examined is placed table-down and moved between the fluorescence reference stones until the intensity of the fluorescence is stronger than the reference stone on the left, and weaker than the reference stone on the right. Photo by Maha DeMaggio.

reference stone on the left, and weaker than the reference stone on the right (figure 2). As with color grading, the trained eye adjusts for differences in facet arrangement, size, and shape between the diamond and the reference stones. This procedure follows the standard methodology recommended by the American Society for Testing and Materials (ASTM, 1996) for comparing the colors of objects.

To better understand how common UV fluorescence is among colorless to faint yellow diamonds, we reviewed a random sample of 26,010 GIA GTL grading reports for diamonds in this range. The data revealed that approximately 65% of these diamonds had no reported fluorescence to long-wave UV radiation. (Note that a report description of "none" means that any fluorescence exhibited is weaker than that of the reference stone that marks the none/faint boundary.) Of the 35% (9,175 diamonds) for which fluorescence was reported, 38% (3,465) were described as having faint fluorescence and 62% (5,710) had descriptions that ranged from medium to very strong. Of the 5,710 diamonds with medium to very strong fluorescence, 97% (5,533) fluoresced blue (in varying intensities) and only 3% (162 stones) fluoresced another color (yellow, white, or orange; no color is reported for descriptions of faint fluorescence.). Therefore, only 35% of the 26,010 diamonds fluoresced, and less than 1% fluoresced a color other than blue. Of the 11,901 diamonds in the D-to-F range, a similar proportion fluoresced (4,250 diamonds, 36% of the total).

Although yellow fluorescence is also a concern in the industry (see, e.g., the June 1997 issue of the *Diamond Value Index*), our decision to limit the present study to diamonds with blue fluorescence was based on the preponderance of such diamonds and the difficulty of finding sufficient numbers of yellow-fluorescent stones to conduct a parallel study. Diamonds with extremely strong blue fluorescence and a distinctive oily or hazy appearance, often referred to as "overblues," are also a concern to the industry. In our experience, however, they are even rarer than diamonds with yellow fluorescence.

MATERIALS AND METHODS

Diamond Samples. From an initial population of more than 1,000 diamonds made available for study, we identified approximately 300 stones with varying degrees of blue fluorescence. From these, we assembled four sets of six stones each that were very similar to one another in all respects except their fluorescence (see figure 3 and table 1). Based on
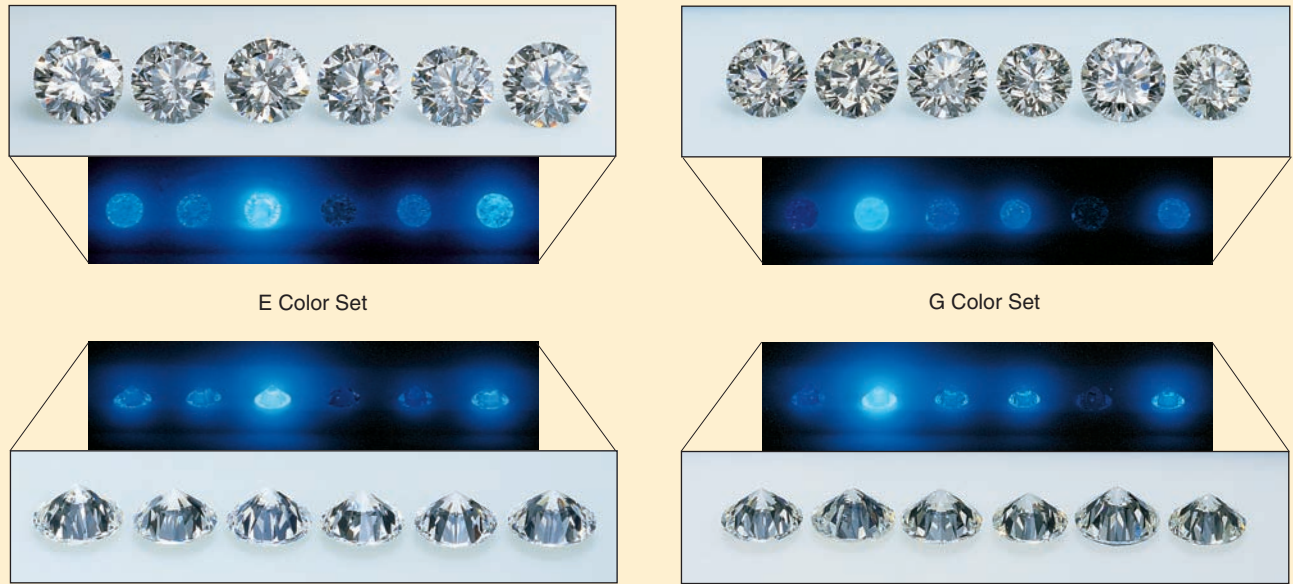
Figure 3. The four color sets of diamonds used for the observation experiments are seen here table-up and table-down under normal lighting conditions, and under the long-wave UV lamp used to make fluorescence determinations in the laboratory. See table 1 for precise descriptions of these stones as they are presented here, which is the same arrangement within each set shown to the observers. From left to right, top to bottom: the six stones in the E set show strong, medium, very strong, none, faint, and strong fluorescence; the G set stones show faint, very strong, medium, medium, none, and strong fluorescence; the I set stones show medium, very strong, faint, strong, none, and strong fluorescence; and the K set stones show very strong, faint, strong, strong, faint, and strong fluorescence. (Because of the inherent difficulties of controlling color in printing, the colors in this illustration may differ from the actual colors of the stones.) Photos of diamonds in normal light are by Harold & Erica Van Pelt; and in UV light, by Maha DeMaggio.
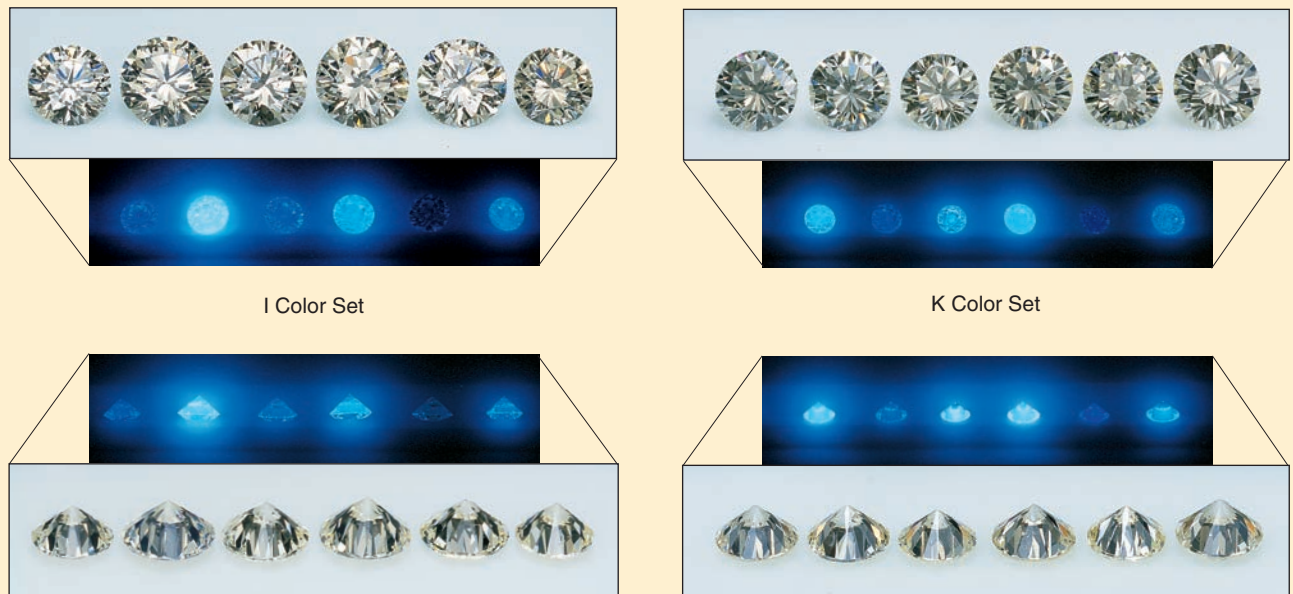
TABLE 1. Description of the 24 faceted diamonds used in this study.[a]

Letter	E color (Set 3)			G color (Set 2)			I color (Set 1)			K color (Set 4)		
	Fluor.[b]	Clarity	Wt. (ct)	Fluor.	Clarity	Wt. (ct)	Fluor.	Clarity	Wt. (ct)	Fluor.	Clarity	Wt. (ct)
A	Strong	VS_1	0.76	Faint	VVS_1	0.60	Medium	SI_1	0.79	V. strong	SI_2	0.56
B	Medium	VVS_1	0.68	V. strong	VS_2	0.62	V. strong	VS_2	1.15	Faint	SI_1	0.56
C	V. strong[c]	IF	0.70	Medium	IF	0.63	Faint	VS_1	1.01	Strong	VS_2	0.47
D	None	VVS_1	0.69	Medium	VS_2	0.50	Strong	VS_1	1.19	Strong	SI_1	0.59
E	Faint	VS_1	0.65	None	IF	0.72	None	VS_1	1.03	Faint	VS_2	0.48
F	Strong	VVS_1	0.77	Strong	VS_1	0.51	Strong	VS_2	0.80	Strong	VS_2	0.65

[a]The letters represent how the diamonds were referred to in answering our questionnaire and their order from left to right as they were placed in trays or ring mounts for viewing (i.e., the diamond labeled "A" was on the left,"B" next, etc.). The set numbers refer to the order in which each color set was given to the observer. For all four sets of diamonds, polish and symmetry were good, very good, or excellent.
[b]Fluor. = strength of fluorescence to a long-wave ultraviolet lamp.
[c]V. Strong = very strong.

our experience grading millions of diamonds, the selection was typical of those encountered in the trade. All 24 diamonds were round brilliants; most had clarity grades at or above the VS range, were of good or better symmetry and polish, had similar proportions, and fell within similar size ranges. Each set comprised a different color grade—E, G, I, and K—representing important commercial breakpoints. Within each of the four sets, the six diamonds represented a wide range of intensity of blue UV fluorescence (from none to very strong). For all observations, the diamonds were arranged in each set so that there was no particular order to the strength of their fluorescence. As noted above, we did not include those diamonds with extremely strong blue fluorescence and a hazy appearance ("overblues"—see, e.g., figure 4), because we could not obtain sufficient numbers of such stones. However, the diminished transparency of these extreme examples prompted us to investigate transparency as well as color in this study. Although we would have preferred a larger sample of diamonds, we felt that this initial study should focus on controlling those other variables that could affect appearance, leaving fluorescence as the variable to be studied. Despite the large number of blue fluorescent diamonds that were available, potentially influential factors such as size, proportions, polish, symmetry, and clarity considerably narrowed our final selection.

Viewing Environments and Methodology. Because faceted diamonds are observed under different lighting and viewing situations in different parts of the trade, we identified five representative viewing environments for this experiment (see table 2 and figure 5). These environments cover the range of lighting and viewing situations commonly encountered in the industry. (Although incandescent lights are frequently used in retail jewelry stores for display purposes, diamond value judgments made by jewelers are typically made with daylight or fluorescent light.) The viewing environments that we used fall into two general categories: "grading environments" and "appearance environments."

In *grading environments*, an attempt is made to control, as much as possible, all observation variables to achieve consistent, repeatable results during the evaluation of a diamond's color grade. Here, as in standardized GIA color grading, the faceted diamonds were viewed table-down through the pavilion facets, so that the effects of cutting, such as facet reflections, would be minimized. Two such environments were used:

1. A GIA GEM DiamondLite viewing unit, with a nonfluorescent white interior and two overhead Verilux (daylight equivalent) fluorescent tube-type lamps, was placed in an otherwise darkened room. In this configuration, the six diamonds in each set were positioned table-down on the floor of the viewing box, 5–10 cm (2–4 inches) below the lamps, with the observer looking at the diamonds in profile view (again, see figure 5). This is the standard position and environment for color grading diamonds in the D-to-Z range at GIA GTL.

2. An overhead, desk-mounted, Phillips F15T8/D 15-watt (daylight equivalent) fluorescent tube-type lamp was placed in a standard office setting. In such an environment, there may or may not be ambient light sources nearby (in this instance, there were). The diamonds were positioned table-down in a grooved, white, nonfluorescent plastic tray and observed in profile

Figure 4. The 127 ct Portuguese diamond at the Smithsonian Institution in Washington, DC, is a classic example of a blue fluorescent diamond referred to as an "overblue." These diamonds of extremely strong blue fluorescence may exhibit a noticeable oily or hazy appearance when excited by any of a number of light sources. Although diamonds described on a laboratory report as having very strong blue fluorescence are routinely seen in the trade, a true "overblue" is not commonly encountered and was not part of our study. Photo © Harold & Erica Van Pelt.

view. (Although many diamond dealers regularly use a folded business card for such observations, most white card stock itself fluoresces bluish white and thus adds its own emitted light to the diamond being observed, potentially altering the color appearance.) This is the standard position and environment for diamond color grading used in diamond bourses around the world and in retail jewelry stores.

In *appearance environments*, there is less attempt (or opportunity, or perceived need) to control the observation variables that can affect the diamond's color appearance. Typical situations include: informal color grading of D-to-Z diamonds; observations of color appearance made at the time a diamond is bought or sold; and, for the jewelry-buying public, how a diamond might appear when worn in jewelry. Here, the diamond is viewed *table-up through the crown facets*, where the cutting style has more influence on the perceived color. Three such environments were used in our experiment:

3. Observations were made with an overhead, desk-mounted, Sylvania Cool White F15T8/CW 15-watt (daylight equivalent) fluorescent tube-type lamp in a standard trading environment. (Recognizing that different offices have different overhead fluorescent lighting, we felt that the use of different bulbs for environments 2 and 3 provided a broader representation of trade environments. Again, in such a setting, there may or may not be ambient light sources nearby. In this environment, we did not have ambient light.) For this experiment, the diamonds were observed table-up in a grooved, white, nonfluo-

TABLE 2. The five viewing environments used in this study.

No.	Lighting environment	Light source	Observer type (no.)	Stone orientation	Distances: light-to-object / observer-to-object
1	DiamondLite, in a darkened room	Verilux type fluorescent tubes (2)	Laboratory grader (5) Trade grader (2)	Table-down, floor of viewing box	2–4 in. / 12–18 in. (5–10 cm / 30–45 cm)
2	Overhead desk-mounted light, in a lighted room	18" Phillips F15T8/D 15-watt fluorescent tube	Laboratory grader (6) Trade observer (4)	Table-down, grooved tray	12–18 in. / 6–18 in. (30–45 cm / 15–45 cm)
3	Overhead desk-mounted light, in a darkened room	18" Sylvania F15T8/CW 15-watt fluorescent tube	Laboratory grader (8) Trade grader (2) Trade observer (2)	Table-up, grooved tray	12–18 in. / 6–18 in. (30–45 cm / 15–45 cm)
4	Ceiling-mounted room lighting	Phillips FB40CW/6 40-watt fluorescent tubes	Laboratory grader (6) Trade grader (1) Average observer (5)	Table-up in ring, ring tray	Approx. 6 ft. / 6–18 in. (Approx. 2 m / 15–45 cm)
5	Window (indirect sunlight)	South daylight (1:00–4:00 pm, July, in New York City)	Laboratory grader (3) Average observer (6)	Table-up in ring, ring tray	Not applicable / 6–18 in. (NA / 15–45 cm)

rescent plastic tray. This is a standard environment for evaluating diamonds in the trade.

4. Observations took place in a room with Phillips FB40CW/6 40-watt fluorescent tube-type ceiling lights. Each of the diamonds was placed in a spring-loaded white metal display mounting, and each set was placed in a neutral gray ring tray. This also is a standard condition for buying and selling diamonds in the trade; in addition, it approximates the lighting conditions for typical indoor wearing of diamond jewelry.

5. Observations were made in a room where the only light was external, indirect sunlight coming through a window (July afternoon daylight, on a sunny day, from a southerly direction in New York City). Each of the diamonds was placed in a spring-loaded white metal display mounting, and each set was placed in a neutral gray ring tray. This is a standard position and environment for buying and selling diamonds in the retail jewelry industry. Although partial filtering of UV radiation occurs through a window, this approximates typical outdoor wearing of diamond jewelry.

Because different intensities of ultraviolet radiation in the light sources could affect the diamonds' fluorescence reaction, we used a UVX digital radiometer manufactured by Ultraviolet Products, Inc., to measure the UV content in each of the light sources chosen. The measurements revealed no appreciable differences in long-wave UV content from one fluorescent light source to the next. They also revealed that these light sources emit approximately 5% as much UV radiation as the UV lamp, at the light-to-object distances used in the laboratory. According to our measurements, indirect daylight through our windows has about as much UV radiation as the fluorescent light sources.

Observers. We assembled four groups of observers, a total of 46 individuals, to represent both the diamond industry and the diamond-buying public, as follows:

1. Laboratory Graders (25 total)—trained individuals employed by GIA GTL, who routinely perform diamond color grading using the D-to-Z scale and GIA's standard grading procedure. Because of their experience in diamond grading and the fact that they are constantly monitored for consistency, we felt that the members of this group would best be able to make the dis-

tinctions we were investigating. Consequently, members of this group participated in every viewing environment.

2. Trade Graders (5 total)—trained individuals employed by diamond manufacturers, who routinely perform diamond color grading using the D-to-Z scale and a standard grading procedure.

3. Trade Observers (5 total)—individuals employed by diamond manufacturers or diamond brokers, who have a working knowledge of diamond color-grading practices but either do not carry out color grading on a daily basis or, if they do color grade, they use less stringent guidelines than those used by the Laboratory and Trade Graders.

4. Average Observers (11)—individuals who represent the diamond-buying public. Some of these had limited knowledge of diamond color-grading procedures, while others had none. In either case, none of these individuals had previously made observations of color appearance in diamond in any systematic way.

We asked these four sets of observers to view the four sets of diamonds in one or more of the viewing environments. Because some observers brought their own trade practices to the experiment, and others had no prior experience with some of the environments, we did not ask all observers to make observations in each type of environment. Nor do we have equal numbers of observations for each group of observers and viewing environment. However, we did ask four observers (three Laboratory Graders and one Trade Observer) who had both laboratory and extensive trade experience to look at the diamonds in more than one viewing environment. All told, the final data represent a total of 50 observations for each of the four sets of diamonds (i.e., 46 observers, four of whom viewed the diamonds in two environments).

Observer Questionnaires. We gave each observer a sheet of instructions that briefly stated that the research project concerned diamond fluorescence and then asked questions regarding his or her observations (table 3). The observer was verbally instructed not to alter the geometry of the environment (the arrangement of the light source, diamond, and eye) in which the observation was being made. Terms such as *hue* (color), *depth* (strength) *of color*, and *transparency* (in this instance, the presence or
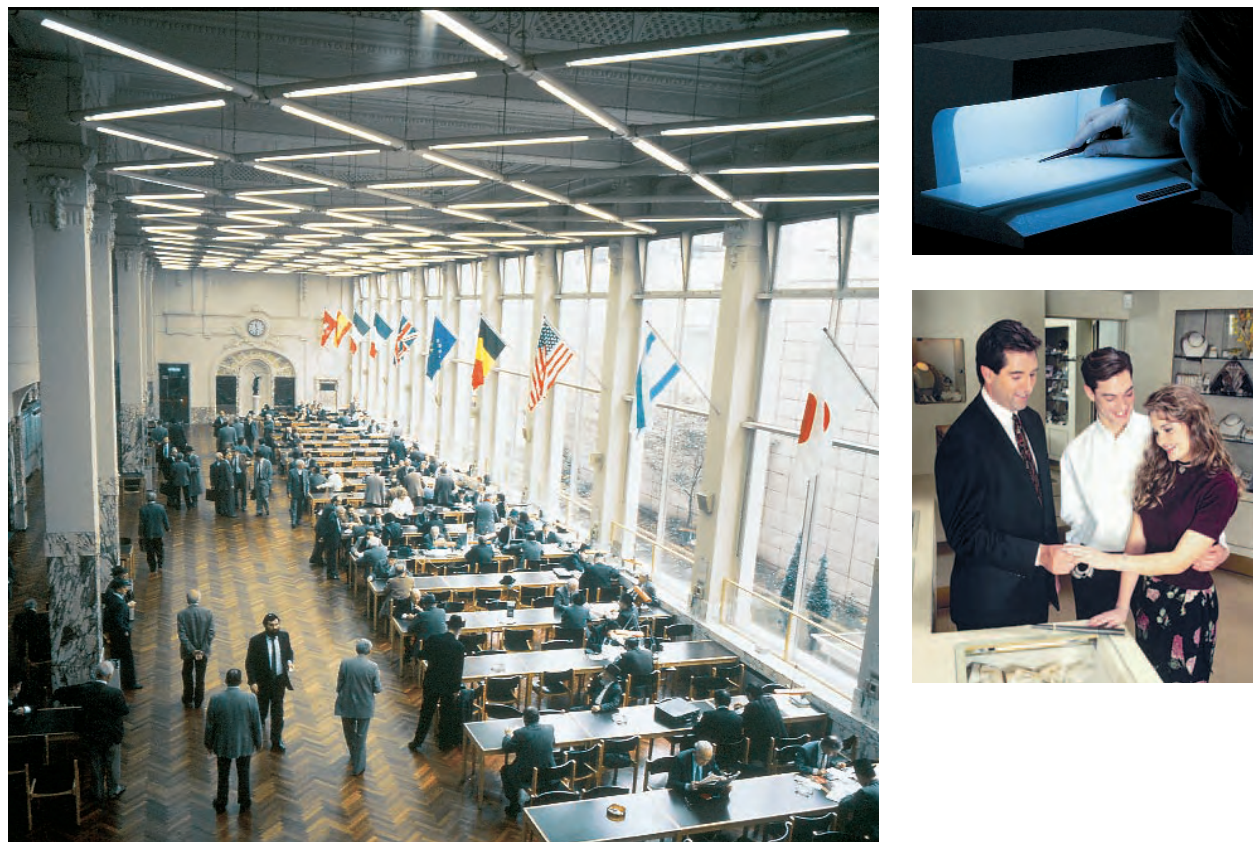
Figure 5. Gem diamonds are viewed in various environments and positions. These range from a highly controlled grading environment (DiamondLite, upper right) through more variable environments such as the diamond bourse (at Antwerp, above left) to the more generalized environment of the retail jewelry store (lower right). DiamondLight photo by Maha DeMaggio, jewelry store photo by James Aronovsky, and bourse photo courtesy of the Diamond Bourse, Antwerp.

absence of haziness or oiliness) were defined so that all observers were responding to the same characteristics. Our concern was to determine whether these observers could perceive any effect from fluorescence on the appearance of the diamonds (that is, more or less colored or more or less transparent) under normal lighting conditions.

We presented the diamonds to each observer one set at a time, and then asked the individual to answer the same group of questions for each set. Observers were allowed to select more than one stone as "most colored," "least colored," etc. No time limit was given to view the sets of diamonds.

RESULTS

Analysis of the Data. Questions 1, 2, and 6 were designed to focus the observer's attention on the properties we wanted to test: color and transparency. Questions 3 and 4 provided us with quantifiable data on color that could be statistically analyzed.

The answers to question 5 were not statistically meaningful. Questions 7 and 8 provided quantifiable data for transparency.

We analyzed the combined results for all observers and all viewing environments to see whether there was an overall trend in (A) perceived strength or weakness of color in relation to fluorescence; and (B) perceived transparency in relation to fluorescence. Next, for questions 3, 4, 7, and 8 (again, see table 3), we tallied the number of observers who chose a particular diamond in response to each question. Since we had different numbers of stones in each fluorescence category (e.g., two diamonds with "strong fluorescence" in the E color set), we used a statistical normalizing technique to correct for the number of observations, so that each fluorescence category had the same chance of being considered as most colored, least colored, most transparent, or least transparent. This normalization was important because certain fluo-

rescent stones were picked more often than others of equal fluorescence strength in the same color set. We also adjusted the totals where needed to account for a single observer "splitting his or her ballot"—that is, choosing more than one stone as most colored, least colored, most transparent, or least transparent. We used this corrected data set to build distributions of the number of observations versus fluorescence strength, for each question and a variety of groupings (across observer types and viewing environments).

With this analytical technique, key trends in the data can be readily discerned. These trends are best seen as bar graphs of the (normalized) number of observations for each fluorescence category. The answers to the two questions "most colored" and "least colored" (or "most transparent" and "least transparent") actually constitute *one set* of observations; that is, if a fluorescent effect exists, it should be evident in the choice of both "most color" and "least color." To see this, the data are plotted on the same graph, with more desirable attributes (least color and most transparency) plotted above the axis, and less desirable attributes (most color and least transparency) plotted below the axis (see, e.g., figure 6). A trend is indicated when the averages for each category (above and below the axis) form a sloped line. For instance, figure 7A does not show a trend, whereas the trend in figure 8A is pronounced.

We first compared the Laboratory Grader responses to questions 3, 4, 7, and 8 to those of each of the other groups (Trade Graders, Trade Observers, and Average Observers). We found that the observations by the Trade Graders and Trade Observers showed trends similar to the observations by Laboratory Graders. However, observations by Average Observers were randomly distributed (that is, even in a color set and viewing environment where trained Laboratory Graders detected a trend in stone color or transparency, average observers did not). Therefore, the results for Average Observers were excluded from the remainder of the analysis. It is apparent that the Average Observers were not able to consistently discriminate any fluorescence-related effects in the viewing environments most similar to those in which jewelry is purchased and worn.

Assessing the Fluorescence Effect. Questions 1 and 6 provided a general measure of the strength of the effect fluorescence *might* have on color and transparency. Seventy-one percent of all observers (excluding Average Observers), across all environments and sets, said that stones in a given set appeared to have different depths of color. Twenty-nine percent reported that all the stones in a set had the same color appearance. However, when the answers for each color set were examined separately, it became evident that these results were related to color grade: 46% of the observations indicate no difference for the E-color diamonds, 41% for the G-color diamonds, 15% for the set with an I color grade, and 10% for K color. No difference in transparency was reported by 62% of the observers in response to question 6. This result also varied by color set, from 72% for the E set to 56% for the I set.

The data revealed a weak "fluorescence effect" in color appearance over all five viewing environments considered together (figure 6). Although responses to strongly fluorescent stones were mixed, in general, observers were more likely to

---

TABLE 3. The observer questionnaire.

Name: _____

Viewing Method: _____

Diamond Series: _____

1. Do all the diamonds in this group appear to have the same depth of color? (Yes No)

    If yes, please proceed to question 6.

    If not, circle the corresponding letter for the one or ones which appear different.

    A   B   C   D   E   F

2. Do any of the diamonds have a different hue (color)? (Yes No)

    If yes, which one or ones?

    A   B   C   D   E   F

3. Which diamond (or diamonds) has the most color?

    A   B   C   D   E   F

4. Which diamond (or diamonds) has the least color?

    A   B   C   D   E   F

5. Of the diamonds that remain, are any more colored than the rest? (Yes No)

    If yes, which one or ones?

    A   B   C   D   E   F

6. Is there a difference in the transparency of any of these diamonds? (Yes No)

    If yes, please answer the next two questions.

7. Which diamond (or diamonds) appears the most transparent?

    A   B   C   D   E   F

8. Which diamonds appear the least transparent?

    A   B   C   D   E   F

choose inert and faintly fluorescent stones as "most colored" and very strongly fluorescent stones as "least colored" within each color set. For transparency, the "fluorescence effect" appears even weaker, since most observers detected no effect at all.

Because all the viewing environments were included in the above analyses, further evaluation was needed to determine whether any particular factor—viewing position, light source, and/or stone color—influenced the perceived effects of fluorescence on color and transparency.

Viewing Position. Observations made with similar lighting conditions, but with the stones observed table-down in environment 2 and table-up in environment 3, showed noticeably different results. Table-down yielded no trend in color with respect to increasing strength of blue fluorescence. However, table-up showed a trend of better color appearance with greater strengths of fluorescence. We then grouped the color observations for all light sources for each of the two positions, with the results shown in figures 7a and 8a. Viewed table-down, neither the most colored nor the least colored choices show a trend with fluorescence. In the table-up position, there is a clear trend for strongly fluorescent diamonds to look less colored, and for diamonds with no to weak fluorescence to look more colored.

Across both viewing positions, most observers saw no effect of fluorescence on transparency. Half the observers saw no difference in transparency in the table-down position; the other half observed a clear trend toward lower transparency with stronger fluorescence (figure 7b). As seen in figure 8b, 71% of the observers saw no difference in transparency table-up in similar lighting, and there was no discernible trend in the observations of those who did perceive a difference.

Light Source. We saw no difference in the relationship between apparent color and strength of fluorescence in diamonds observed table-down in a DiamondLite unit (environment 1) as compared to fluorescent overhead illumination (environment 2). Nor did we see different relationships between color and fluorescence in stones viewed table-up with fluorescent overhead illumination as compared to external window light (environments 3, 4, and 5). In other words, there did not appear to be any difference among the light sources we used in their effect on perceived color relative to fluorescence.
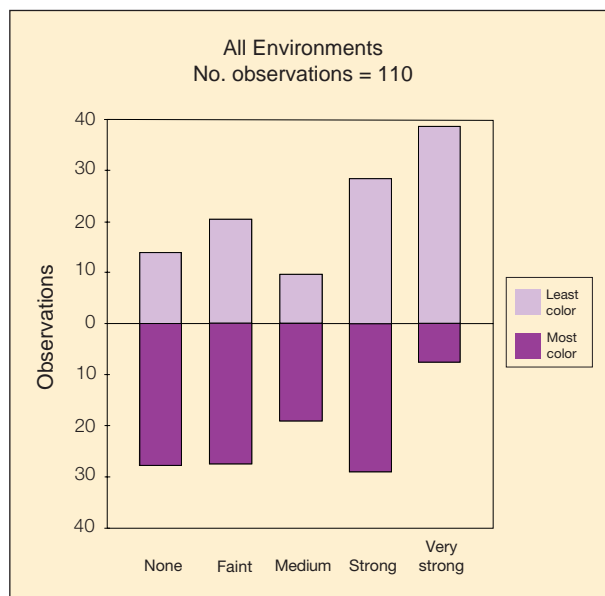

Figure 6. This bar graph illustrates the observations of color appearance in which color differences were noticed, for the various fluorescence categories across all color sets and all experienced observers. Strongly fluorescent diamonds are more likely to be considered "least colored"—that is, to have a better color appearance—in contrast to weakly fluorescent stones, which were somewhat likelier to be considered "most colored."

By contrast, the results for transparency suggested a difference between daylight (environment 5) and artificial light (environments 1–4). Non-fluorescent and weakly fluorescent stones were reported by some observers to be more transparent table-down in artificial light (environments 1 and 2; figure 7b), but less transparent table-up in indirect sunlight (environment 5; figure 8c). Although we were not able to make any definitive conclusions because of the limited number of usable observers for the indirect sunlight environment, the preliminary correlation of greater transparency with stronger fluorescence in the table-up position merits further investigation.

Diamond Color. For each of the four color sets (E, G, I, and K) taken separately, we also saw no relationship between strength of fluorescence and color appearance with the diamonds viewed table-down, but we again saw a trend toward better color appearance with stronger fluorescence when the diamonds were viewed table-up, regardless of light source. It
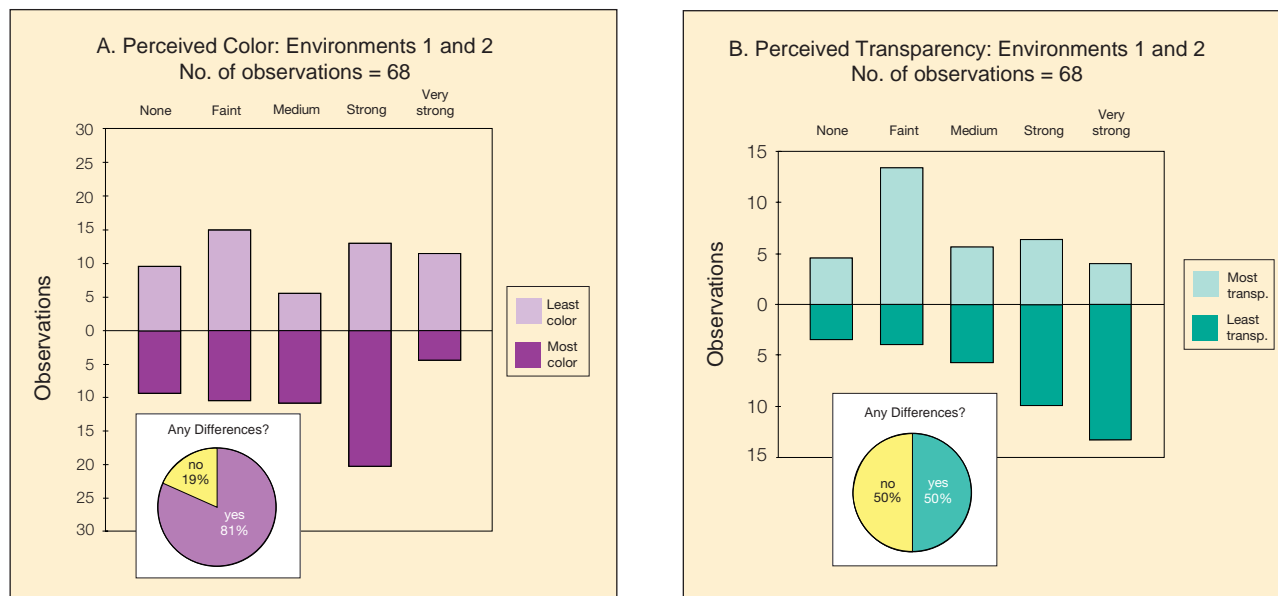
Figure 7. These graphs show the results of the observations on the diamonds positioned table-down. (A) Although color differences were seen in most cases (across all experienced observers and color sets), as indicated by the pie chart, there is no clear trend in color appearance with strength of the fluorescence. (B) In half the cases, no differences in transparency were seen in the diamonds positioned table-down; however, the remaining observations showed a clear trend for weakly fluorescent diamonds to be considered more transparent than strongly fluorescent stones.

appears that fluorescence had a weaker effect on table-up color appearance for the diamonds in the E and G color sets than for those in I and K. However, as there were far fewer observations for a single color set than for all sets taken together, these results are less definitive.

DISCUSSION

For the observers in this study, the effect of blue fluorescence on color appearance and transparency in colorless to faint yellow diamonds was subtle. In fact, our results indicate that Average Observers could not make the fine distinctions sought in this study. Of the experienced observers, most saw an effect on color appearance, but far fewer saw any difference in transparency. Even among the experienced observers, responses varied from stone to stone. Because some highly fluorescent diamonds in a set were singled out and others were not, it is possible that other factors are affecting color appearance more strongly than fluorescence strength.

The results of this study indicate that there is a perceptible relationship between blue fluorescence and color appearance, which depends on viewing position. On average, strongly fluorescent diamonds have a better color appearance table-up, and this effect is most noticeable at lower color grades. Most observers did not detect any differences in transparency among diamonds in a given color set. Of those who did see a difference under fluorescent lighting, it was only apparent in the table-down position. These results challenge the notion that strongly fluorescent diamonds typically have a hazy appearance.

Classic examples of fluorescent and nonfluorescent diamonds that have similar color appearance and transparency can be seen in many pieces of fine jewelry. Figure 9 shows two complete views of the diamond necklace and earrings from the cover of this issue: one view under normal lighting conditions and the other under the long-wave UV lamp. Clearly, there is a range of fluorescence strengths to the diamonds brought together in these pieces; however, there is a generally uniform overall appearance to the diamonds under normal lighting conditions.

CONCLUSION

Documenting the effects of blue fluorescence on the appearance of gem diamonds is a difficult and complex process. In this study, we screened more than 1,000 polished diamonds to find 24 that fit the chosen color grades, clarity, cutting style and quality,

A. Perceived Color: Environments 3, 4, and 5
No. of observations = 90

B. Perceived Transparency: Environments 3 and 4
No. of observations = 64

C. Perceived Transparency: Environment 5
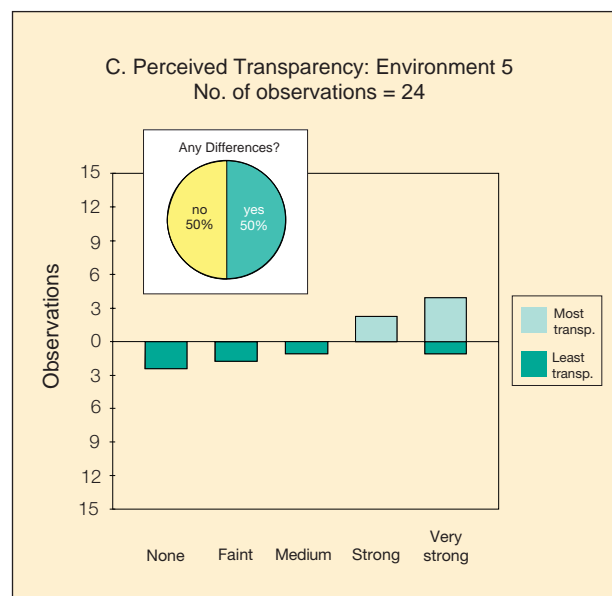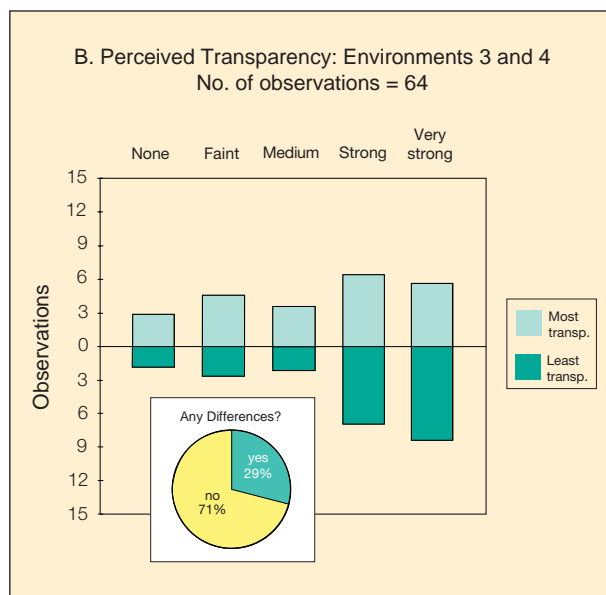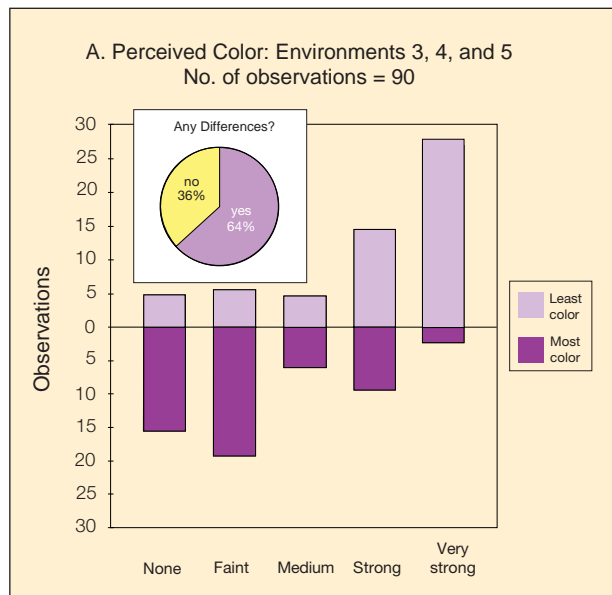No. of observations = 24

Figure 8. The results were also graphed for observations on diamonds positioned table-up with the different types of fluorescent light and indirect sunlight. (A) Differences in color appearance were noted in all three environments; they showed a clear trend for strongly fluorescent diamonds to be considered less colored than weakly fluorescent stones. (B) In most cases, no differences in transparency were seen for diamonds positioned table-up in fluorescent light environments; for observations in which differences were noted, no trend was seen. (C) In half the observations, no differences in transparency were seen; for diamonds positioned table-up in indirect sunlight, the few observations in which differences were seen suggest that strongly fluorescent diamonds were likelier to be considered most transparent.

and size range while representing the various strengths of fluorescence. Although yellow fluorescent diamonds and "overblues" are also of concern in the trade, such stones are so rare that we could not assemble appropriate examples to perform a comparable study. We obtained the cooperation of 46 observers from a wide variety of trade and nontrade backgrounds. One interesting aspect of this study was that the nontrade observers could not make meaningful distinctions. For this group, which would be considered most representative of the jewelry-buying public, fluorescence had no overall effect on color appearance or transparency.

For the experienced observers, we found that, in general, the strength of fluorescence had no widely perceptible effect on the color appearance of diamonds viewed table-down (as is typical in laboratory and trade grading). In the table-up position (as is commonly encountered in jewelry), diamonds described as strongly or very strongly fluorescent were, on average, reported as having a better color appearance than less fluorescent stones. In this study, blue fluorescence was found to have even less effect on transparency. These observations confirm GIA GTL's experience grading millions of diamonds over the decades.

Figure 9. The necklace and earrings reproduced on the cover of this issue of Gems & Gemology *are seen here in their entirety under normal lighting conditions (left) and under the long-wave UV lamp (right). Quite often, diamonds in a range of fluorescent strengths and colors are placed next to inert diamonds, yet the piece maintains a uniform overall appearance under normal lighting conditions. The diamonds in the necklace weigh a total of 132 ct; the diamonds in the earrings weigh 23 ct, with the two large pear shapes 3.04 and 3.20 ct. Jewelry courtesy of Harry Winston, Inc.; photos by Harold & Erica Van Pelt.*

Although we identified general tendencies across all diamonds and experienced observers, we also identified apparent variations in fluorescence effect for different color sets. For instance, the effect of fluorescence on color was most noticeable in the lower (I and K) colors, although in the marketplace the influence on price is greater in the higher (D through H) colors.

Unlike the notion held by many in the trade, fluorescent diamonds are not as prevalent as nonfluorescent stones, as the GIA Gem Trade Laboratory sample data for more than 26,000 diamonds showed. The present study also challenges the trade perception that fluorescence usually has a negative effect on better-color diamonds. Our results show that the diamond industry would be better served by considering each individual diamond on its own visual merits.

REFERENCES

American Society for Testing and Materials (1996) *ASTM Standards on Color and Appearance Measurement*, 5th ed., ASTM, Philadelphia, PA, D1729-89: Standard practice for visual evaluation of color difference of opaque materials, pp. 82–84.

Bruton E. (1978) *Diamonds*, 2nd ed. N.A.G. Press, London, 532 pp.

Clark C.D., Collins A.T., Woods S.G. (1992) Absorption and luminescence spectroscopy. In J. Field, Ed., *Properties of Natural and Synthetic Diamond*, Academic Press, London, pp. 35–80.

Collins A.T. (1992) The characterisation of point defects in diamond by luminescence spectroscopy. *Diamond and Related Materials*, Vol. 1, Nos. 5-6, pp. 457–469.

Davies G., Welbourne C.M., Loubser J.H.N. (1978) Optical and electron paramagnetic effects in yellow type Ia diamonds. *Diamond Research 1978*, pp. 23–30.

Fritsch E., Scarratt K. (1992) Natural-color nonconductive gray-to-blue diamonds. *Gems & Gemology*, Vol. 28, No. 1, pp. 35–42.

Liddicoat R.T., Ed. (1993) *GIA Diamond Dictionary*, 3rd ed. Gemological Institute of America, Santa Monica, CA, 275 pp.

Nassau K. (1983) *Physics and Chemistry of Color*, John Wiley & Sons, New York, 454 pp.

Shipley R.M., Liddicoat R.T. Jr. (1941) A solution to diamond color grading problems. *Gems & Gemology*, Vol. 3, No. 11, pp. 162–167.

U.S. Federal Trade Commission (1938) *Trade Practice Rules for the Wholesale Jewelery Industry*. Rule No. 6, p. 4, as promulgated March 18, 1938.

Waychunas G.A. (1988) Luminescence, X-ray Emission and new spectroscopies. In F.C. Hawthorne, Ed., *Reviews in Mineralogy*, Vol. 18, Spectroscopic Methods in Mineralogy and Geology, Mineralogical Society of America, Washington, DC, pp. 639–698.

We Want to Know That (1993) SBA-TV, South Korea, broadcast May 9.

SYNTHETIC MOISSANITE:
A NEW DIAMOND SUBSTITUTE

By Kurt Nassau, Shane F. McClure, Shane Elen, and James E. Shigley

A new diamond imitation, synthetic moissanite (silicon carbide), is now being produced by C3 Inc. in near-colorless form for jewelry purposes. With refractive indices of 2.648 and 2.691, a dispersion of 0.104, a hardness of 9¼ on the Mohs scale, and a specific gravity of 3.22, synthetic moissanite is much closer to diamond in overall appearance and heft than any previous diamond imitation. The thermal properties of synthetic moissanite are also so close to those of diamond that the thermal probes currently on the market react to synthetic moissanite as if it were "diamond." This new material can be readily separated from diamond on the basis of its anisotropic optical character, which produces a doubling in the appearance of facet junctions. A new instrument manufactured by C3 Inc. solely to distinguish synthetic moissanite from diamond was also examined for this study.

ABOUT THE AUTHORS

Dr. Nassau, retired from his position as Distinguished Scientist at AT&T Bell Laboratories, is now a freelance writer, consultant, and expert witness living in Lebanon, New Jersey. He is on the Board of Directors of C3 Inc. Mr. McClure is manager of Identification Services at the GIA Gem Trade Laboratory, Carlsbad, California. Mr. Elen is a research technician, and Dr. Shigley is director, at GIA Research, Carlsbad.

*T*o the long list of diamond simulants currently available in the jewelry market, a new one has been added: synthetic moissanite. As typically happens with the introduction of a synthetic or simulant, there is considerable concern in the jewelry trade about this diamond imitation and its identification. One particular problem with synthetic moissanite is that its thermal properties are so close to those of diamond that it passes as "diamond" when tested with a thermal probe.

This article reports on the examination of several samples of near-colorless synthetic moissanite (figure 1), both to characterize this material and to determine how it can be identified by standard gem-testing methods. The authors also evaluate a testing instrument developed by C3 Inc., which is intended to be used in conjunction with a thermal probe to distinguish this new simulant from diamond.

BACKGROUND

Diamond Imitations. All diamond imitations known to date have significant deficiencies. For example, synthetic spinel, colorless sapphire, and YAG (yttrium aluminum garnet) are much less brilliant than diamond. Synthetic rutile and strontium titanate are much too soft and display too much dispersion ("fire"). GGG (gadolinium gallium garnet) and CZ (cubic zirconia) have very high specific gravities, and the latter is somewhat brittle. Synthetic moissanite, by contrast, has gemological properties that are generally closer to those of diamond (table 1).

Silicon Carbide. Since it was first manufactured a century ago, silicon carbide (SiC) has played an important industrial role as an abrasive. The growth of single crystals of silicon carbide has been studied for many years for two possible end uses: as a semiconductor material, and as a diamond substitute in jewelry. In fact, the promise of synthetic moissanite as a diamond imitation has been described several times in the gemological and related literature. Some of these publications included enthusiastic descriptions of faceted colored material (usually blue to green) and premature claims that

Figure 1. Near-colorless synthetic moissanite is being marketed for jewelry purposes as a diamond imitation. The faceted pieces shown here, weighing from 0.09 to 0.57 ct, illustrate the appearance of this material. Because synthetic moissanite is doubly refractive, one can sometimes see doubling of the back facet junctions even with the unaided eye (particularly noticeable in the large round brilliant on the upper right). Photo © GIA and Tino Hammid.

colorless material was available (see, e.g., De Ment, 1948, 1949; Mitchell, 1962; McCawley, 1981). One of the authors (KN) noted the potential value of silicon carbide as a gem simulant 17 years ago. Referring to some pale tan to green to black centimeter-size crystals and faceted stones as large as half a carat, he stated that "these synthetic moissanites are quite attractive, and might provide a superb diamond imitation if they could only be made colorless" (Nassau, 1980, p. 253). At that time, however, a way had not been found to control either the color or the growth process to make synthetic crystals suitable for the gem industry.

Only recently, as described below, has the controlled growth of synthetic moissanite actually been achieved. Material that may appear near-colorless face-up in jewelry is now available for gemological use. It is being produced by Cree Research Inc. of Durham, North Carolina, and distributed by C3 Inc. A preliminary note on the new C3 material has appeared in this journal (Johnson and Koivula, 1996).

Early work on silicon carbide was summarized by Mellor (1929; see also Powell, 1956). Edward G. Acheson (1893) appears to have been the first to recognize its hardness and potential as an abrasive. He made silicon carbide accidentally while trying to grow diamond by passing an electric arc between carbon electrodes through a mixture of carbon and molten clay (an aluminum silicate). He named the new substance "carborundum" (later to become a trade name). Subsequently, he obtained a better yield by using a mixture of carbon and sand. This same "Acheson" process is still used today in slightly modified form for the manufacture of silicon carbide for abrasive products (Divakar et al., 1993).

Shortly thereafter, the Nobel prize-winning

TABLE 1. Characteristics of "colorless" diamond and "colorless" simulants.

Material[a]	Mohs hardness	Toughness	R.I.	Birefringence	Dispersion	S.G.	Optic character	Pavilion flash colors
Diamond	10	Good to excellent	2.417	None	0.044 (moderate)	3.52	Singly refractive (isotropic)	Orange and blue on a few facets
Syn. moissanite	$9\frac{1}{4}$	Excellent	2.648, 2.691	0.043 (moderate)	0.104 (strong)	3.22[c]	Doubly refractive (uniaxial +)	Orange and blue
Syn. corundum	9	Excellent	1.770, 1.762	0.008– 0.010 (weak)	0.018 (weak)	4.00	Doubly refractive (uniaxial –)	Not diagnostic
Cubic zirconia[d]	$8–8\frac{1}{2}$	Good	2.150– 2.180	None	0.058– 0.066 (moderate)	5.56– 6.00	Singly refractive (isotropic)	Orange over most of pavilion
Yttrium aluminum garnet (YAG)	$8\frac{1}{4}$	Good	1.833	None	0.028 (weak)	4.55	Singly refractive (isotropic)	Blue, violet, some orange
Syn. spinel	8	Good	1.728	None	0.020 (weak)	3.64	Singly refractive (isotropic)	Blue over most of pavilion
Gadolinium gallium garnet (GGG)	$6\frac{1}{2}$	Fair to good	1.970	None	0.045 (moderate)	7.05	Singly refractive (isotropic)	Blue, some orange
Syn. rutile	$6–6\frac{1}{2}$	Poor to fair	2.616, 2.903	0.287 (v. strong)[e]	0.330 (v. strong)	4.26	Doubly refractive (uniaxial +)	Various spectral colors, widespread
Strontium titanate	5–6	Fair	2.409	None	0.190 (v. strong)	5.13	Singly refractive (isotropic)	Spectral colors, widespread

References: GIA Gem Property Chart A *(1992)*, GIA Gem Reference Guide *(1988)*, Harris *(1995)*, Hobbs *(1981)*, Nassau *(1980)*, von Muench *(1982)*, and this study.
[a]*Glass and colorless minerals, such as zircon, topaz, and quartz, are not included in this table because they are rarely encountered today.*
[b]*All but one sample of synthetic moissanite were inert to short-wave UV radiation.*

chemist Henri Moissan discovered natural silicon carbide in the Canyon Diablo meteorite (Moissan, 1904). Kunz (1905) applied the name *moissanite* to the natural mineral in Moissan's honor.

Since then, moissanite reportedly has been found in tiny amounts in other meteorites as well as in many terrestrial occurrences (e.g., Obukhov, 1972; Vigorova et al., 1978; Hallbauer et al., 1980; Moore et al., 1986; Rodgers et al., 1989; Mathez et al., 1995). Some or all of these occurrences may have been spurious, with the material derived from the older cutting wheels used to section mineral, rock, and meteorite specimens (Mason, 1962; Milton and Vitaliano, 1984; Milton, 1986), or from contamination by the huge amounts of silicon carbide produced industrially. (More than 36,000 tons were produced domestically, and 159,000 tons were imported into the United States, during the first seven months of 1997 [Balaziak, 1997].) However, the identification of moissanite as inclusions in diamond crystals before they were broken (Moore et al., 1986), and the determination of their abnormal isotopic composition (Mathez et al., 1995), confirm the occurrence of moissanite as a natural mineral.

The Structure of Moissanite. At first, considerable confusion resulted when investigators found a variety of different crystal structures for moissanite, including those having cubic (C), hexagonal (H), and rhombohedral (R) symmetries. This complexity results from the existence of *polytypes*, which represent different stacking sequences of hexagonal layers of atoms. More than 150 polytypes are known in the case of silicon carbide, all of which are properly designated as "moissanite" (Thibault, 1944; Ramsdell, 1947; Verma and Krishna, 1966).

At present, only the 4H and 6H polytypes of alpha-SiC can be grown in bulk form (i.e., as boules). Both polytypes are hexagonal, and both yield near-colorless material. The near-colorless synthetic moissanite described here is the 6H form. The 4H polytype, which has properties very close to those of the 6H polytype, is currently being produced for semiconductor uses, but not in near-colorless form. A key distinction from the 6H polytype is the much weaker absorption below 425 nm in the visible spectrum (Harris, 1995). Beta-SiC, which is the 3C polytype, is cubic and has a crystal structure even closer to that of diamond than the 4H or 6H

Long-wave UV fluorescence[b]	Absorption spectrum	Polish luster	Read-through effect	Relief in 3.32 S.G. liquid	Magnification
Inert or (usually) blue; sometimes yellow	"Cape" lines at 415 and 478 nm, sometimes no sharp lines	Adamantine	None	High	Included crystals, feathers, graining, bearding, naturals, waxy to granular girdle surface, sharp facet junctions
Inert to orange	Absorption below 425 nm; no sharp lines	Subadamantine	None	High	Doubling in appearance of facet junctions, whitish or reflective needles, rounded facet junctions, surface pits, polish lines
Inert	Not diagnostic	Vitreous to subadamantine	Very strong	Moderate	Gas bubbles, sharp facet junctions
Greenish yellow or yellowish orange	Not diagnostic	Subadamantine	Slight	Moderate	Gas bubbles, unmelted zirconium oxide powder, sharp facet junctions
Orange, sometimes inert	Not diagnostic	Subadamantine to vitreous	Strong	Low	Gas bubbles, sharp facet junctions
Weak green or inert	Not diagnostic	Vitreous to subadamantine	Very strong	Low	Gas bubbles
Pinkish orange or inert	Not diagnostic	Adamantine to vitreous	Moderate	Low	Gas bubbles, metallic platelets, rounded facet junctions, polishing marks
Inert	Absorption below 430 nm	Subadamantine to submetallic	None	High	Doubling in appearance of facet junctions, gas bubbles, rounded facet junctions, polishing marks
Inert	Not diagnostic	Vitreous to subadamantine	None	High	Gas bubbles, rounded facet junctions, polishing marks, scratches, abrasions

cSynthetic moissanite will float in methylene iodide (S.G. 3.32), while diamond and the other diamond imitations listed in this table will sink.
dCubic zirconia varies in chemical composition, so the properties will vary somewhat.
ev. strong = very strong.

polytypes. However, it cannot be grown in bulk form at present and it is inherently yellow (von Muench, 1982).

Single Crystal (Bulk) Growth of Synthetic Moissanite. Growth techniques for silicon carbide have been studied for many decades (O'Connor and Smiltens, 1960; Verma and Krishna, 1966; Smoak et al., 1978; von Muench, 1984; Wilke, 1988; Davis et al., 1990; Divakar et al., 1993). Of these, only a seeded sublimation process, derived from the "Lely" approach, has proved viable for the controlled growth of large single crystals of synthetic moissanite (Davis et al., 1990; Nakashima et al., 1996).

In his original work, Lely (1955) used a cylinder, made of lumps of SiC, that had a cavity. This cylinder was heated in a sealed graphite crucible to 2500°C, at which point SiC crystals grew inside the cavity. Difficulties with controlling the chemical purity and the specific polytypes formed have led to many modifications. In particular, the use of carefully controlled atmospheres and temperature gradients, as well as the addition of a thin, porous graphite tube to line the cavity (which, through dif-

fusion, provides improved control of the sublimation) have resulted in better control of the crystals that grow inside the tube. Many types of heating systems have been used, including radio frequency and resistance heating. Significant advances in the Lely process were reported in the USSR (Tairov and Tsvetkov, 1981).

The final breakthrough in the Lely process is revealed in a patent of Davis et al. (1990), where controlled growth of SiC occurs by sublimation from a feed powder, diffusion through graphite, and growth directly from the vapor phase on a seed crystal. With a sublimation process, the silicon carbide vaporizes and then recrystallizes without ever passing through a liquid stage. Details of this growth process as used for the near-colorless synthetic moissanite being distributed by C3 Inc. have not been released.

However, Davis et al. (1990) reported the growth of a 6H-polytype synthetic moissanite crystal (of gem quality, but not colorless) that was 12 mm in diameter and 6 mm thick during a six-hour growth period at the time of the initial patent filing in 1987. One of many recent papers in Nakashima

et al. (1996), on various aspects of synthetic moissanite growth and its applications to the electronics industry by Cree Research, mentions the availability of 50-mm-diameter boules of 6H moissanite in 1994 (Tsvetkov et al., 1996). Such a boule could conceivably permit the manufacture of a brilliant-cut synthetic moissanite 50 mm in diameter and 28 mm high that would weigh about 380 carats! No production figures have been released on the amount of material that is currently available or could be made available for jewelry purposes. However, in December 1997, the senior author saw more than 1,000 faceted synthetic moissanites in the offices of C3 Inc. The company has stated that it plans to focus its marketing on near-colorless faceted material, with a release to the trade in early 1998, in a price range of 5%–10% of the average retail price of comparable diamonds (J. Hunter, pers. comm., 1997).

The hardness of synthetic moissanite is listed as 9¼ on the Mohs scale, which may be misleading. As shown in figure 2, the Mohs scale above a hardness value of 8 is disproportionately compressed when compared to a quantitative linear hardness scale such as that of Knoop (Bruton, 1978), which measures indentation hardness. The Knoop hardness of the 6H polytype of moissanite is reported to be in the range 2917–2954 kg/mm^2 (2.91–2.95 Gpa) on the c crystal face (von Muench, 1984). The difference in Knoop hardness between corundum (Mohs 9) and moissanite (Mohs 9¹¹⁄₄₄) is larger than the difference between corundum and topaz (Mohs 8). Because of this disparity, synthetic moissanite cannot be polished by conventional techniques. The complex cutting process requires an additional, proprietary step (J. Hunter, pers. comm., 1997).

MATERIALS AND METHODS

Twenty-three faceted "near-colorless" synthetic moissanites were made available to GIA by C3 Inc. for this study; we had requested a representative range of the colors and qualities that could be produced. The samples weighed from 0.09 to 1.12 ct, and were polished in round brilliant, emerald cut, and square-modified-brilliant styles. In addition, C3 Inc. supplied a 3.79 ct polished rectangular light green piece that had been optically oriented for spectroscopy. A 71.4 gram piece of boule and two 7 mm cubes were used for a precise specific gravity determination and a cleavage experiment. (However, C3 Inc. has stated that rough material will not be available to the trade for the time being.)
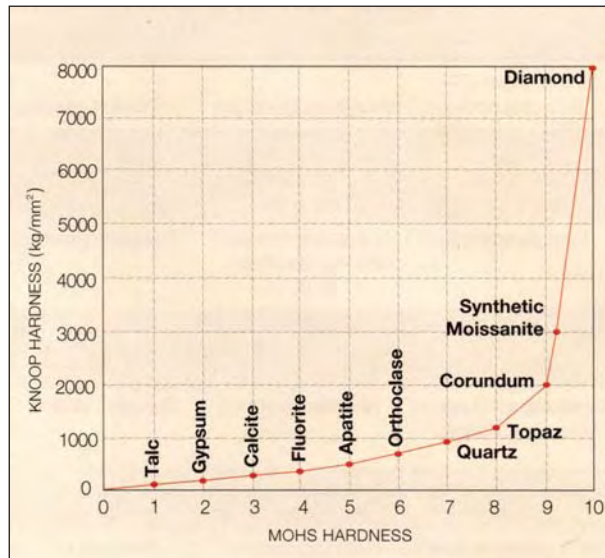

Figure 2. This diagram compares the Mohs and Knoop (indentation) hardness scales. The Knoop scale better illustrates the relationship in hardness for diamond, synthetic moissanite, and corundum. Diagram modified after Bruton, 1978, p. 402.

In addition to the samples studied at GIA, one of the authors (KN) examined approximately 1,000 faceted synthetic moissanites and 100 preformed cubes at C3 Inc. The faceted samples included a 4.92 ct round brilliant, with a diameter of 11.9 mm and an approximate color grade of N, and a green round brilliant of 17.31 ct with a diameter of 17.5 mm. The faceted pieces studied at GIA were representative of this larger group of cut stones examined at C3 Inc. Also seen were 13 pieces of jewelry, which contained a total of 38 stones and included the ring discussed below.

Standard gemological equipment used for all 23 main samples included a Gemolite Mark V binocular microscope, a polariscope, a desk-model spectroscope, and a short-wave (254 nm) and long-wave (365 nm) ultraviolet lamp. Approximate refractive index values were measured for 11 of these samples with a Jemeter Digital 90 infrared reflectometer. For research purposes only (the GIA Gem Trade Laboratory does not grade diamond simulants), trained graders used standard GTL procedures to try to assign diamond-equivalent color grades to the 18 samples that weighed more than 0.20 ct. Specific gravity measurements were obtained by the hydrostatic method on these same 18 samples, as well as the large piece of rough described above.

Because the thermal inertia ranges of diamond (0.55–1.7 cal/cm °C) and moissanite (1.6–4.8 cal/cm °C) overlap (Hoover, 1983; Harris, 1995), GIA

researchers performed thermal inertia testing on the 23 core samples using a Ceres CZeckpoint, a Ceres Diamond Probe II, a GIA GEM DiamondMaster, and a GIA GEM Mini-DiamondMaster. For comparison, the following "colorless" gem materials were also tested using the same four instruments (with the number of samples in parentheses): diamond (types Ia [5 samples] and IIa [1]), sapphire (3), zircon (2), cubic zirconia (2), strontium titanate (2), synthetic spinel (2), synthetic rutile (7), yttrium aluminum garnet (2), gadolinium gallium garnet (2), "paste" (glass—2), and quartz (1). Thirteen colorless to yellow diamonds, with color grades ranging from E to Fancy Light Yellow, were also tested with the GIA Gem DiamondMaster. The senior author made thermal inertia measurements on 10 additional synthetic moissanites with a Ceres CZeckpoint, a Ceres Diamond Probe, a Presidium tester, and a Diamond Guard. Electrical conductivity of the 23 main synthetic moissanite samples was measured using a GIA GEM Instruments conductometer.

The ultraviolet transparency of a diamond was compared to that of several synthetic moissanites in a specially designed viewing box, using a concept similar to that suggested by Yu and Healey (1980). X-ray transparency was recorded photographically using an HP Faxitron X-ray machine. Visual observation of the luminescence to X-rays of both materials (one diamond and 11 synthetic moissanites) was performed with a Picker portable X-ray unit adapted for this purpose.

Semiquantitative chemical analysis of eight of the synthetic moissanites examined at GIA was performed with a Tracor Spectrace 5000 energy-dispersive X-ray fluorescence (EDXRF) system. Several sets of excitation conditions were used to detect the widest possible range of chemical elements. Operating conditions yielded a lower limit of detection for transition metals of about 0.01 wt.%.

Absorption spectra for eight of the GIA samples were obtained in the ultraviolet-visible range (250–750 nm) at room temperature using a Hitachi U4001 spectrophotometer, and in the infrared range using a Nicolet Magna 550 spectrometer. Raman spectra were recorded with a Renishaw System 2000 instrument. For details on any of these experimental procedures, please contact the GIA authors.

A small instrument has been developed by C3 Inc. for the specific and limited purpose of distinguishing synthetic moissanite from diamond (see figure 3). Marketing of the Colorless Moissanite/ Diamond Tester Model 590 is expected to start

early in 1998, at approximately the same time that synthetic moissanite is released to the jewelry trade (J. Hunter, pers. comm., 1997).

The C3 tester determines relative transparency in the near-ultraviolet, where diamond transmits and synthetic moissanite absorbs. The accompanying instructions clearly state that this new instrument is to be used *only in conjunction with* a standard thermal inertia tester. Any unknown near-colorless gem should *first* be tested with a thermal inertia probe. Only those samples that the thermal inertia tester indicates are "diamond" would need to be tested with the C3 instrument, which would then identify whether any were synthetic moissanite. With the C3 instrument, the gem sample is illuminated at an angle by a small, high-intensity halogen lamp. Radiation from the lamp is transmitted and reflected within the sample, and the near-ultraviolet radiation that emerges from the table facet is detected by the instrument.

Use of the instrument is fairly simple. The operator brings the polished facet of a diamond or synthetic moissanite (loose or mounted) in contact with a fiber-optic probe that is located on the side of the instrument. As soon as the sample touches the probe, the instrument emits a sound (and an indicator light illuminates) if any material other than moissanite is detected; there is no sound or response from the indicator light if the item is synthetic moissanite. The synthetic moissanites, dia-

Figure 3. The Colorless Moissanite/Diamond Tester Model 590 was designed and built by C3 Inc. for the sole purpose of rapidly distinguishing synthetic moissanite from diamond only after a stone has been identified as "diamond" on a thermal probe. Photo by Maha DeMaggio.

Figure 4. This 14k gold ring contains two rows of faceted light-green synthetic moissanites, which were mounted in wax and then cast in place with no apparent damage to the material. All of the stones reacted as synthetic moissanite on the Model 590 tester. Ring courtesy of C3 Inc.; photo by Maha DeMaggio.

monds, and other near-colorless gem materials listed above for the thermal probe testing were also tested with this instrument. In addition, the C3 instrument was used to test 13 pieces of jewelry containing synthetic moissanites, including the ring in figure 4.

RESULTS

Table 2 summarizes some of the gemological properties—i.e. those data that were found to vary from one sample to the next—of the 23 synthetic moissanites examined in detail during this study.

Visual Appearance. The samples examined at GIA (reportedly representing the range of color that can be produced at present) were near-colorless to light yellow, green, and gray. Those samples that appeared to be in the I-to-K range all looked colorless in the face-up position, but around the L-to-N range they started to show face-up color. The one U-V stone was obviously gray face-up, which made it appear dark. Because many of these samples had grayish or greenish hues, it was difficult to arrive at an exact color grade on the traditional D-to-Z scale, which is comprised of predominantly yellowish stones. In the color grading of diamonds, grayish or greenish hues such as these fall outside normal procedures. However, when compared to diamonds that do fall on the D-to-Z scale, the 18 faceted synthetic moissanites above 0.20 ct ranged from the lower end of the "near-colorless" (G-to-J) category, with the best color being equivalent to I, to U-V in the "light" category of the scale. Synthetic moissan-

ites representing this approximate range of colors are illustrated in figure 5.

At first overall observation with the unaided eye, this material looks like a believable diamond imitation (see again figure 1). There were no eye-visible inclusions in any of the samples (on the diamond clarity grading scale, these synthetic moissanites would fall into the VVS to SI grades). They displayed no "read-through" effect, as can be seen in most other diamond imitations, which have lower refractive indices (see Hobbs, 1981). The samples showed moderate to high dispersion (greater than that of diamond or CZ, but less than that of synthetic rutile). Their brilliance appeared to be slightly less than that of diamond.

Gemological Properties. The refractive indices of synthetic moissanite are over the limit of a conventional refractometer (that is, greater than 1.81). Measurements with the Jemeter reflectivity meter revealed an R.I. range of 2.59–2.64. Refractive index values of $\omega=2.648$ and $\varepsilon=2.691$ (with a birefringence of 0.043 and dispersion of 0.104) have been measured using precision optical techniques on synthetic moissanite (von Muench, 1982; Harris, 1995).

When they were observed under crossed polarizers in a polariscope, all of the synthetic moissanites remained dark when rotated in a face-down position. This singly refractive reaction is to be expected, since all of the samples were oriented with the c-axis (optic axis) perpendicular to the table facet. These samples had to be examined in several directions, most notably through the girdle, to obtain a doubly refractive reaction. Checking stones in several orientations in the polariscope is a wise precaution in any case, but it is particularly important for the separation of synthetic moissanite from diamond (which is singly refractive in all orientations). We did obtain a uniaxial optic interference figure in most of the samples (although with some difficulty), and we did not observe any strain pattern such as might be seen in diamond.

The hydrostatic specific gravity measurements ranged from 3.20 to 3.24 (again, see table 2), which is significantly lower than the 3.52 value typical of diamond. A precision density performed on the 71.4 gram piece of rough gave a value of 3.224. Because of the difference in specific gravity, a diamond and a synthetic moissanite faceted as round brilliants of the same diameter and the same proportions will have different carat weights (e.g., a 6.50-mm-diameter round brilliant diamond will weigh about 1.00

TABLE 2. Selected gemological properties of the synthetic moissanites examined in this study.

Weight (ct)	Equivalent color grade[a]	S.G.	Long-wave UV fluorescence[b]	Short-wave UV fluorescence	Luminescence to X-rays	Electrical conductivity
1.12	O-P (grayish green)	3.22	Wk. orange	Inert	nd	No
1.05	M-N (grayish yellow)	3.23	Inert	Inert	nd	Yes
0.74	U-V (gray)	3.22	Inert	Inert	nd	No
0.67	S-T (greenish gray)	3.22	Inert	Inert	nd	No
0.66	S-T (gray)	3.21	Inert	Inert	nd	No
0.57	I-J (yellow)	3.22	Wk. orange	Inert	Wk. yellow	Yes
0.57	M-N (gray)	3.20	Inert	Inert	nd	No
0.53	K-L (green yellow)	3.22	Inert	Inert	Inert	Yes
0.53	L-M (brownish yellow)	3.21	Inert	Inert	nd	No
0.44	M-N (brownish yellow)	3.22	Inert	Inert	nd	Yes
0.43	L-M (brownish yellow)	3.24	Inert	Inert	nd	Yes
0.35	M-N (brownish yellow)	3.21	Inert	Inert	nd	Yes
0.33	L-M (brownish yellow)	3.22	Inert	Inert	nd	Yes
0.33	M-N (greenish brownish yellow)	3.22	Inert	Inert	nd	Yes
0.27	J-K (yellow)	3.23	Inert	Inert	Inert	No
0.22	L-M (green)	3.21	Mod. orange	Wk. orange	Mod. yellow	Yes
0.21	S-T (gray)	3.24	Inert	Inert	Inert	No
0.20	K-L (yellow)	3.24	Inert	Inert	Inert	No
0.19	nd[c]	nd	Inert	Inert	Inert	No
0.10	nd	nd	Inert	Inert	Inert	Yes
0.10	nd	nd	Inert	Inert	Inert	Yes
0.09	nd	nd	Inert	Inert	Inert	Yes
0.09	nd	nd	Wk. orange	Inert	Inert	Yes

[a]Color grades are approximate; see discussion in text. [b]Wk. = weak; Mod. = moderate. [c]nd = not determined.

ct., whereas a synthetic moissanite of identical diameter and cut will weigh about 0.91 ct).

When examined with a desk-model spectroscope, the samples exhibited no sharp bands, but each displayed a cutoff below about 425 nm. This is in contrast to near-colorless to light yellow diamonds, which usually show the "Cape" line at 415 nm. This feature could be useful for gemologists with considerable spectroscopic experience, but it should be noted that it can be easy to confuse a 425 nm cutoff with the general darkening in the blue portion of the spectrum.

On all of the different thermal inertia instruments used for testing, every synthetic moissanite in this study registered as "diamond." Note that 13 samples displayed some electrical conductivity (unlike most near-colorless diamonds, although some light gray or blue diamonds are electrically conductive).

Microscopic Examination. When we examined the main sample of 23 synthetic moissanites with a microscope or loupe, we saw several distinctive characteristics. The most obvious feature seen

Figure 5. The synthetic moissanites examined at GIA ranged in color from approximately I to U-V on the GIA color-grading scale for diamonds. This range was most evident when the samples were placed table-down and viewed side-by-side in a white plastic tray, as illustrated here. All of the stones had a somewhat gray, green, or yellow appearance. The two largest samples shown here are 1.12 and 1.05 ct. Photo by Shane F. McClure.

Figure 6. Because of its anisotropic optical character, synthetic moissanite exhibits double refraction depending on the orientation in which a sample is examined. In this view of a faceted synthetic moissanite through the crown main facets, doubling of the facets is readily apparent. Photomicrograph by Shane Elen; magnified 10×.

when the samples were examined through the crown facets was an apparent doubling of the pavilion facet junctions (conversely, when viewed through the pavilion, of the crown facet junctions). This is due to double refraction, which is readily apparent in synthetic moissanite in directions other than parallel to the optic axis (figure 6). All 23 samples were faceted with the c-axis oriented perpendicular to the table facet; consequently, when viewed along this direction, they showed no doubling. When the synthetic moissanites were viewed at any other angle, however, doubling was clearly visible. Doubling could even be seen when these samples were viewed perpendicular to the table by focusing past the culet and looking for secondary reflections of the table and crown facets (figure 7). Orange or blue dispersion colors (Hobbs, 1981) were sometimes evident on pavilion facets, but these were much less distinct than similar colors seen on faceted CZ.

In general, the synthetic moissanites we examined were not as well polished as a typical diamond. Many had rounded facet junctions, in contrast to the sharp junctions seen on a diamond (figure 8). The girdles of most of the synthetic moissanites were frosted, polished, or striated (figure 9), similar to those of some CZ. No bearding along the girdle was seen. Some of the samples acquired late in the study showed better polish and sharper facet junctions, indicating improved manufacturing techniques.

One test that is commonly used to identify CZ can also help with synthetic moissanite. Because we have no polishing compounds harder than diamond, and because diamond's hardness varies depending on its crystallographic orientation, the cutter must constantly adjust the polishing direction during manufacturing. This is not necessary for

Figure 7. Although synthetic moissanite is typically faceted with the table perpendicular to the c-axis to minimize the effects of double refraction, focusing past the culet will allow doubling to be seen in the reflections of the table and crown facets (left, at 17× magnification). This is significantly different from the singly refractive appearance of the facets in diamond (right, at 12× magnification). Photomicrographs by Shane F. McClure.
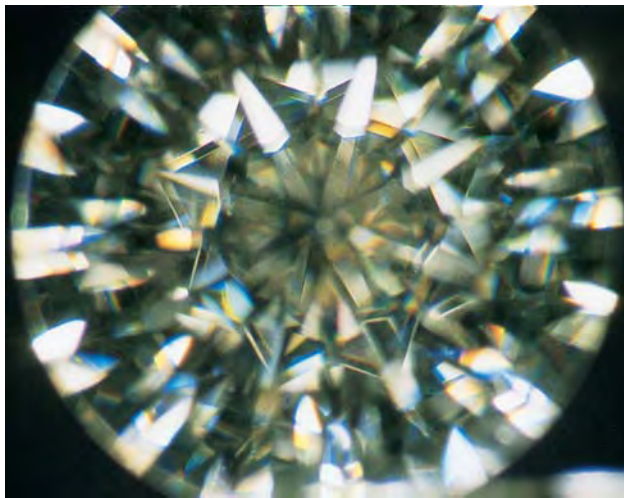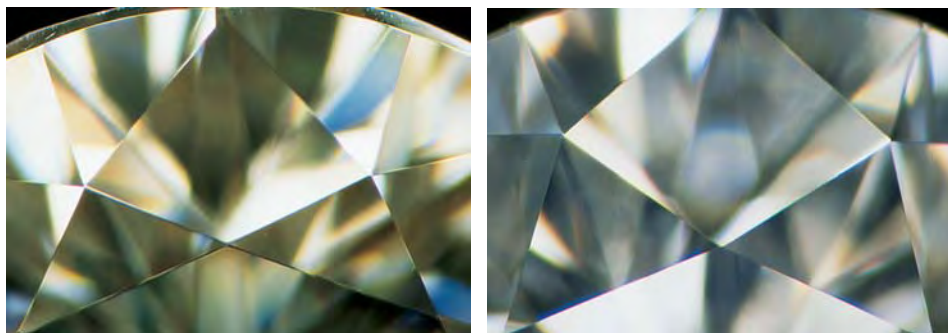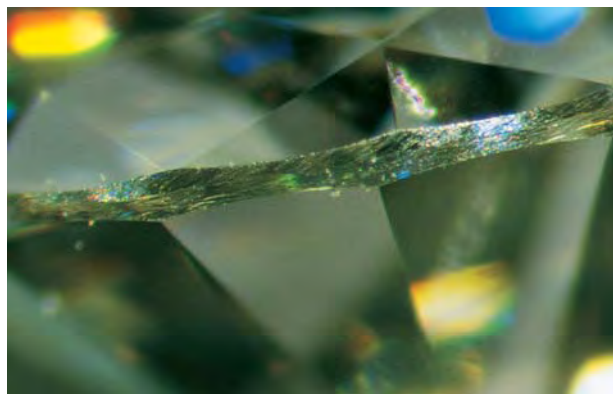
Figure 8. Most of the cut synthetic moissanites examined had somewhat rounded facet junctions (left), as compared to the sharp facet junctions of diamond (right). Photomicrographs by Shane F. McClure; magnified 34×.

any other materials, including synthetic moissanite. Therefore, if the polishing lines on individual facets (as observed in the microscope) all run in the same direction, the stone cannot be a diamond (figure 10). This test will not establish that the stone is synthetic moissanite, but in many instances just knowing it is not a diamond may be enough.

With magnification, we observed inclusions in almost all of the samples, although typically the samples were fairly clean. The most common inclusions were white-appearing needles that were subparallel to one another (see figure 11) and parallel to the c-axis (i.e., perpendicular to the table facet). Less prevalent, and somewhat less visible, were very fine, subparallel reflective stringers that were also oriented parallel to the c-axis (figure 12). These were best seen using fiber-optic illumination. Some samples contained scattered pinpoint inclusions, which in a few cases formed clouds. Several were large enough to resemble small crystals or gas bubbles when viewed with a loupe. We did not see fractures in any of the samples. On some facets, we saw cavities and/or smaller "whitish" pits or indentations with surrounding white-stained areas (see figure 13).

Quite unexpected, and apparently not previously reported for silicon carbide, were triangular pits that resemble the "trigons" characteristic of diamond crystal surfaces. One of the authors (KN) observed these on some samples of boules that he examined at C3. The pits range from less than a millimeter to 6 mm (figure 14) in longest dimension.

Fracture, Cleavage, and Twinning. Several cleavage directions have been reported in thin, hexagonal, carborundum-type plates of synthetic moissanite crystals (R.W. Keyes, in O'Connor and Smiltens, 1960). The possible cleavage of synthetic moissanite is significant not only because of the effect its presence would have on durability, but also because it would be another similarity to diamond.

To investigate whether cleavage was present in synthetic moissanite, we attempted to induce the reported cleavages in a 7 mm cube. When these attempts proved unsuccessful, we placed the cube on a steel plate and hit it several times with a large

Figure 9. Parallel striations across the girdle of this synthetic moissanite readily separate it from diamond. Photomicrograph by Shane Elen; magnified 15×.

Figure 10. Whereas the manufacturer must repeatedly adjust the polishing orientation for diamond because of its directional hardness, synthetic moissanite can be polished in a single direction. This is typically evident in the polishing lines on adjacent facets. Photo by Shane F. McClure; magnified 32×.
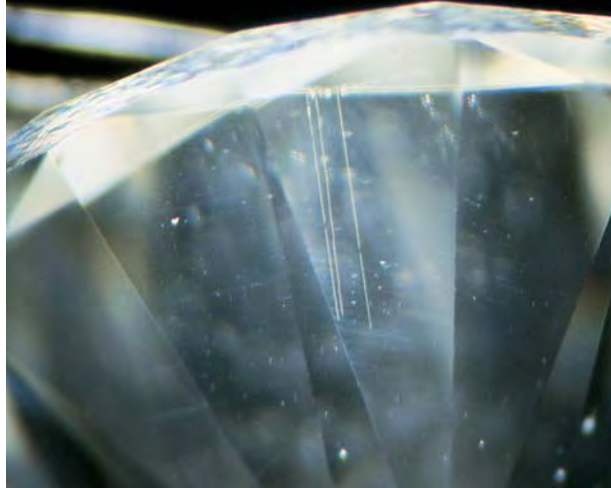
Figure 11. All of the synthetic moissanite samples examined contained some inclusions; the most common were these white needles that are subparallel to one another. Photomicrograph by John Koivula; magnified 20×.
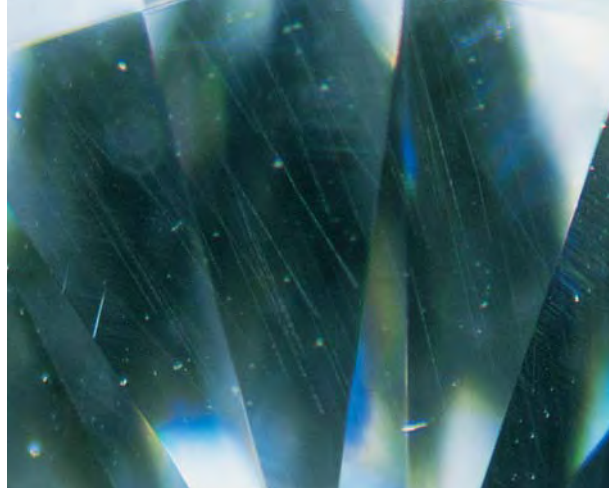

Figure 12. Also seen in some of the samples were these very fine, subparallel, reflective stringers. Photomicrograph by Shane F. McClure; magnified 40×.

hammer until it shattered. Careful visual examination of the fragments revealed extensive conchoidal fracturing, but no cleavage. Accordingly, conchoidal fracturing could be expected to occur at the girdle of faceted synthetic moissanites if they were subjected to hard wear, but there do not appear to be any planes of weakness due to prominent cleavage.

The plates tested by Keyes (O'Connor and Smiltens, 1960) frequently contain a mixture of polytypes, which is a type of twinning (Verma and Krishna, 1966). It is possible that the "cleavage" previously reported in the carborundum-type crystal plates was actually parting along twinning planes created by undetected regions of other SiC polytypes. However, twinning was not observed in any of the synthetic moissanite studied. Information provided by the manufacturer indicates that the growth technique used avoids the occurrence of twinning (J. Hunter, pers. comm, 1997).

The C3 Testing Instrument. The Colorless Moissanite/Diamond Tester Model 590 provided correct results for all synthetic moissanite samples ranging from less than 0.10 ct to over 17 ct. The testing operation was rapid (only a second or so per sample, similar to the time needed with a thermal probe). As noted earlier, the C3 instrument is designed to be used only on samples that test positive for diamond with a standard thermal probe. This procedure is important, because most of the near-colorless gem materials that were examined with the new C3 instrument were found to respond as if they were "diamond" (i.e., they activated the instrument's light and beeper). The one exception was synthetic rutile: Seven samples elicited the same reaction on the C3 instrument as "synthetic

moissanite" (i.e., the instrument's light and beeper did not activate). However, synthetic rutile would not register as "diamond" on a thermal probe.

Even the 13 diamonds with increasing yellow color elicited a "diamond" reaction with the C3 instrument. Conversely, all 38 synthetic moissanites mounted in the ring shown in figure 4, plus the 13 other pieces of jewelry, were detected correctly with the C3 tester.

Two nonfaceted composite samples, consisting of 1 mm diamond macle tops cemented over cube-shaped pieces of synthetic moissanite, were prepared by one of the authors (KN) specifically to test their response with the C3 instrument. One was cemented with epoxy, the other with an "instant" cyanoacrylate. In both instances, the instrument gave a "moissanite" response, because the near-ultraviolet was absorbed by the underlying synthetic moissanite. A separate test indicated that neither cement absorbed in this region of the spectrum.

Luminescence. Four of the 23 core synthetic moissanite samples fluoresced to long-wave UV radiation (one moderate orange, and three weak orange), while the remainder were inert (note that many near-colorless diamonds fluoresce, mainly blue, to long-wave UV). Only one of these four samples fluoresced (weak orange) to short-wave UV. In all cases, the fluorescence was evenly distributed across the sample, and there was no phosphorescence. When exposed to a beam of X-rays, one sample (of 11 tested) displayed moderate yellow fluorescence, one was weak yellow, and the rest were inert.

Testing with Advanced Instrumentation. The UV-visible absorption spectra for the eight samples tested were identical: All showed a distinct increase in absorption at about 425 nm (figure 15), which corre-

sponds to the region of absorption from 400 to 425 nm seen with a hand spectroscope. No sharp bands were recorded. In contrast, the spectra of near-colorless type Ia diamonds typically exhibit one or more sharp absorption bands of the "cape" series (with the most intense band being at 415 nm); otherwise, they are increasingly transparent down to about 330 nm in the ultraviolet. Type IIa colorless diamonds lack these cape lines in their visible spectra.

The infrared spectra of the same eight synthetic moissanites again revealed identical features, with absorption below 1800 cm^{-1}; several strong, sharp peaks between 2600 and 2000 cm^{-1}; and several barely perceptible peaks between 3200 and 3000 cm^{-1} (figure 16). In contrast, the spectra of type Ia and IIa diamonds exhibit distinctly different characteristic sets of absorption features.

A Raman spectrum recorded for a polished cube of synthetic moissanite revealed a series of features that vary depending on the optical orientation of the sample. Nevertheless, the Raman spectra of synthetic moissanite are significantly different from those of diamond (figure 17).

The EDXRF spectra of the same eight samples showed the presence of silicon, a major constituent of synthetic moissanite, and no trace elements (figure 18). Note that carbon is not present in this spectrum because EDXRF does not detect light ele-

ments. Untreated natural diamonds do not exhibit Si, although the presence of a silicon-containing mineral inclusion, such as garnet, could show up in the spectra. In the latter event, however, the inclusion would have to be so large that it was eye-visible.

Other Identification Tests. Because of the absorption below 425 nm, synthetic moissanite is much less transparent in the ultraviolet region than near-colorless diamond is. For example, it is more opaque than diamond when exposed to long-wave UV radiation. In terms of transparency to X-rays under the exposure conditions that render diamond more transparent, the synthetic moissanite appears more opaque. Both techniques allow several samples to be tested at the same time.

A previous study (Nassau and Schonhorn, 1977) published data on a "surface tension" test using the measurement of the contact angle of a drop of water on a facet as a means of identifying high-R.I. gem materials, and, in particular, separating diamonds from many colorless imitations. As reported in that study, diamond and synthetic moissanite have nearly the same contact angle; as a result, one cannot rely on either this test or use of a "diamond pen," which tests for this property.

Figure 13. When viewed in reflected light, this small depression appears to be a white pit accompanied by a large stain. Photomicrograph by Shane Elen; magnified 20×.
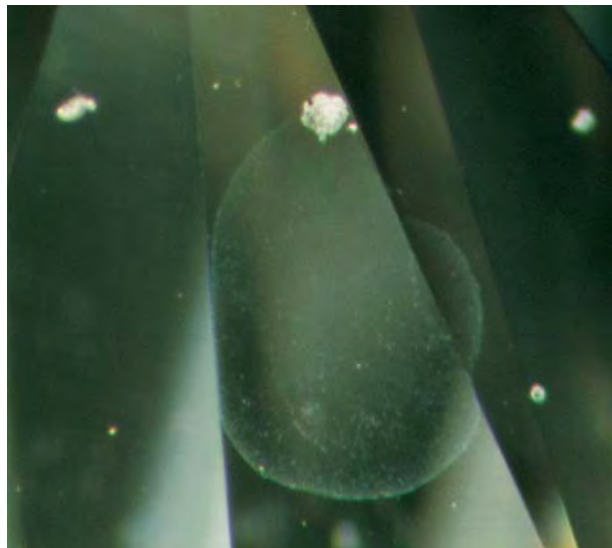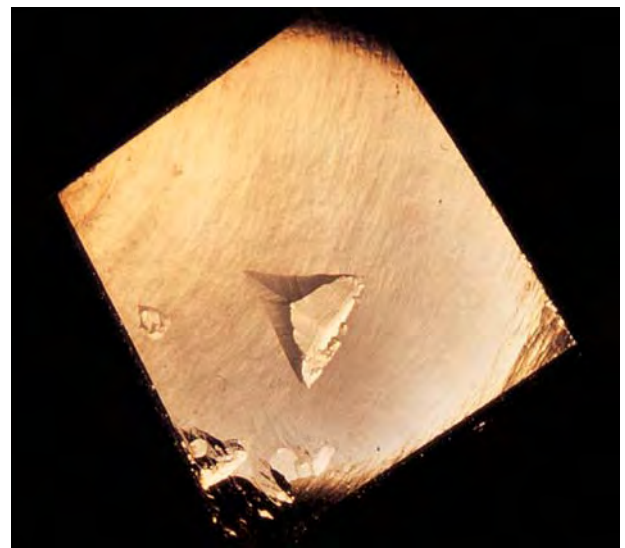

Figure 14. This triangular pit on the surface of a 71.4 gram synthetic moissanite boule resembles one of the trigons commonly seen on diamond crystals. The pit has 6-mm-long sides and a depth of less than 0.25 mm. Photo by K. Nassau.
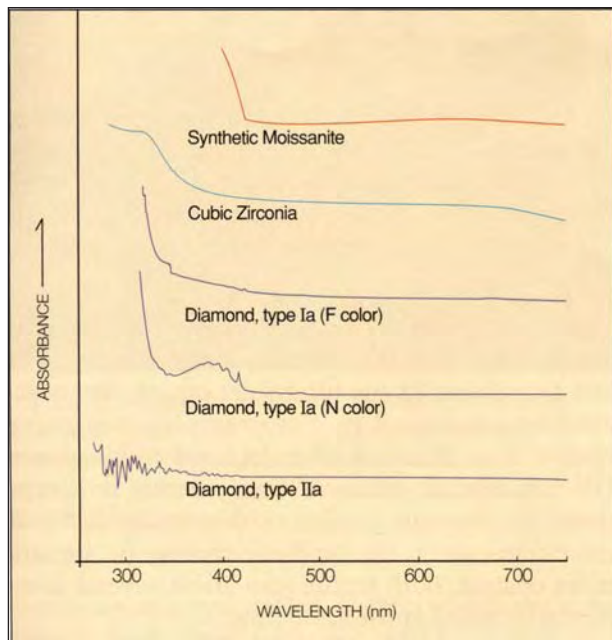
Figure 15. Illustrated here are the visible and near-ultraviolet absorption spectra of a near-colorless synthetic moissanite, a colorless cubic zirconia, two type Ia diamonds, and a colorless type IIa diamond. Note that the synthetic moissanite has no sharp bands, but does show a region of intense absorption beginning at about 425 nm and extending into the ultraviolet. It is this region of absorption, absent in the spectrum of diamond, that gives rise to the great difference in UV transparency between diamond and synthetic moissanite.

DISCUSSION

Synthetic moissanite is a believable imitation of diamond. However, it may exhibit slightly less brilliance; it has more dispersion, a lower S.G., and a higher R.I.; and it is less hard and nonisotropic. Nevertheless, diamond and synthetic moissanite have overlapping thermal inertia ranges, because of which they both react as "diamond" with a thermal probe.

The various gemological and other physical characteristics of the synthetic moissanites described in this article do not vary significantly from one sample to the next because the material is of fixed (i.e., stoichiometric) chemical composition, according to C3 Inc. (J. Hunter, pers. comm., 1997). (For the phase diagram of silicon carbide, see R. I. Scace and G. A. Slack in O'Connor and Smiltens, 1960.) Synthetic moissanite is a semiconductor material like diamond; the main differences in chemical composition in both materials involve only very small amounts of nitrogen and boron that can substitute in the crystal. This situation is quite different from cubic zirconia, where variable

amounts of stabilizers, and even different stabilizers, lead to considerable variation in composition, and hence, to broad ranges in its properties.

Synthetic moissanite is reportedly stable in air to 1700°C (3092°F); in vacuum to 2000°C; and is inert to well over 1000°C to most chemicals, except fluorine, chlorine, molten alkalis, and some molten metals (Divakar et al., 1993). In view of this high stability in air, even *in situ* soldering of broken prongs, as is done with diamond jewelry, should present no problem when synthetic moissanite is used in a mounting. In fact, the small synthetic moissanites in the 14k gold ring shown in figure 4 were cast in place, a practice used in manufacturing

Figure 16. The mid-infrared spectrum of synthetic moissanite is very different from the spectra of cubic zirconia and especially diamond.
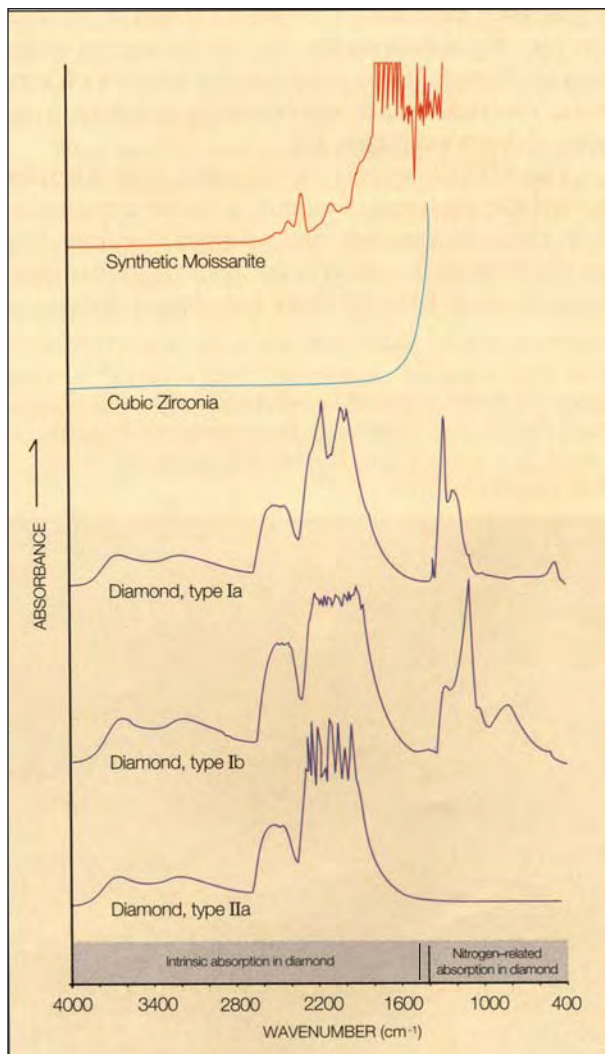
some commercial-quality jewelry, without any apparent damage to the samples. No durability testing was done during this study because no material was made available for this purpose. However, the manufacturer reports that no problems have arisen with conventional setting, repairing, and cleaning (J. Hunter, pers. comm., 1997).

Identifying Single Stones. Simple tests to separate synthetic moissanite from diamond include examination with a loupe or gemological microscope to look for double refraction (i.e., doubling of the facets). Distinctive subparallel needle-like inclusions and stringers oriented perpendicular to the table may be present, as well as rounded facet junctions, polishing lines that run in the same direction on adjacent facets, and an undiamond-like girdle appearance. Also, the synthetic moissanites in this

Figure 17. The 1332 cm⁻¹ peak characteristic of diamond is absent in the Raman spectra of synthetic moissanite, regardless of orientation.
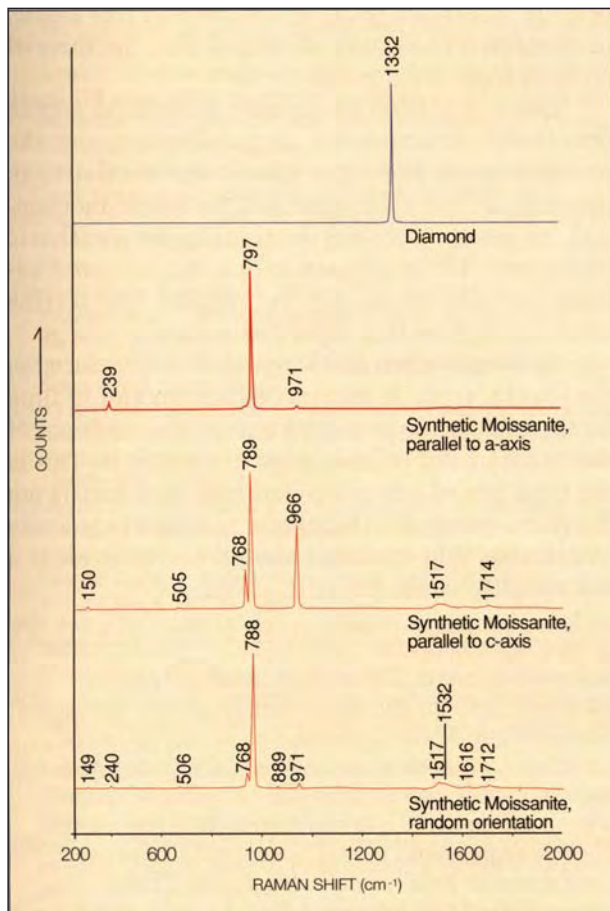
study did not show any of the strain, fractures, cleavage, or mineral inclusions that are typical of diamond.

With a desk-model spectroscope, the absorption below about 425 nm is distinctive, since most colorless to near-colorless diamonds display a sharp 415 nm band or are transparent in this region. However, features at the blue end of the visible spectrum may be difficult to see with this instrument.

The electrical conductivity evident in many of the near-colorless synthetic moissanite samples examined is an indication, but not diagnostic since such behavior is occasionally encountered in near-colorless natural diamonds. Specific gravity, however, is diagnostic. Testing with a reflectivity meter can also give diagnostic results, but great care must be taken when using this instrument.

Although testing with a conventional thermal probe is by itself not sufficient to identify synthetic moissanite, the use of a thermal inertia probe in conjunction with the C3 Inc. tester will conclusively separate synthetic moissanite from diamond quickly and without extensive training.

It should be noted that no single test will conclusively identify a material as synthetic moissanite. Many tests will prove that an unknown is not a diamond (which in many cases may be sufficient), but it would be necessary to consider additional features discussed in this article to conclude that a diamond simulant is moissanite.

Figure 18. The EDXRF spectrum of synthetic moissanite shows the X-ray fluorescence peak for silicon, a major constituent in silicon carbide, which would not be found in a natural, untreated diamond. Note that this method does not detect carbon, a major constituent in both materials.
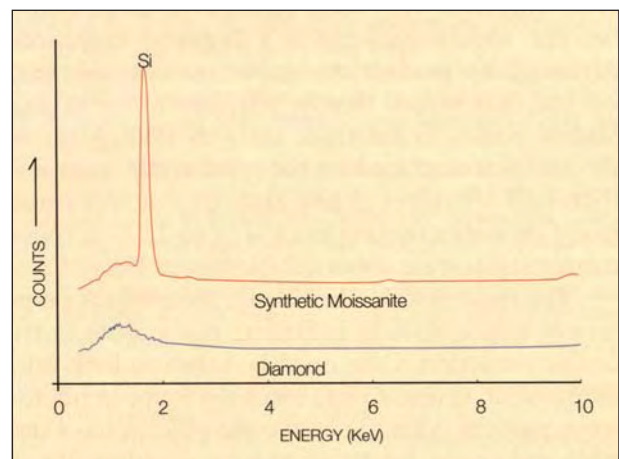
Figure 19. These round brilliants are the three largest synthetic moissanites studied at GIA. They ranged from 0.74 to 1.12 ct. The square modified brilliants represent some of the most attractive samples examined. Photo by Maha DeMaggio.

Identifying Synthetic Moissanite When Mixed with Other Stones. It may be necessary to separate synthetic moissanite from polished diamonds in a mixed parcel. One quick and reliable method is to use specific gravity, employing an appropriate heavy liquid (such as methylene iodide, S.G. 3.32): The less-dense synthetic moissanites will float, while the denser diamonds will sink (as always, care must be taken when handling heavy liquids due to their toxicity). Another approach is to take advantage of the great difference in near-ultraviolet and ultraviolet transparency, which offers a means to view a parcel of cut stones and separate them depending on whether they appear more transparent (diamond) or less transparent (synthetic moissanite).

CONCLUSION

Near-colorless synthetic moissanite soon could become widely available as a diamond imitation. Although no production figures are available yet, C3 Inc. has stated that it will begin marketing faceted stones to the trade early in 1998. Most of the samples examined for the main study were less than half a carat, but the authors did test three round brilliants ranging from 0.74 to 1.12 ct; other cutting styles were also available (figure 19).

The most readily identifiable gemological property of near-colorless synthetic moissanite is its double refraction. Care must be taken to look into the stone at an angle, or to focus the loupe or microscope past the culet to observe the reflections of the table and crown facets, since facet doubling is not usually evident in a sample face-up when viewed perpendicular to the table facet. Specific gravity is also diagnostic: Synthetic moissanite floats in 3.32 liquid, while diamond sinks. If an appropriate reflectivity meter is available, the difference in RI between diamond and synthetic moissanite will separate them as well (with proper precautions).

Features seen with magnification may be indicative, but they should be considered diagnostic only for the most experienced gemologist. Electrical conductivity is also indicative, but it should never be considered diagnostic.

It must be stated emphatically that the thermal inertia probes currently in wide use, which jewelers have relied on for many years to separate diamond from its simulants, must now be employed with great caution. Synthetic moissanite could be misidentified as diamond by a jeweler relying solely on these probes. Indeed, this has already been done experimentally, with the unfortunate results being televised in the United States on a news program that the Discovery Channel broadcast nationally on December 12, 1997. It is essential that the jeweler perform additional tests, as described in this article, to conclusively identify all stones that the thermal probe detects as diamond.

There is a need to develop additional simple gem-testing instruments, or possibly improve the existing thermal probes (given the similarity in thermal inertia of diamond and synthetic moissanite), to assist jewelers in testing for synthetic moissanite. The combination of a thermal probe followed by use of the C3 Inc. Model 590 testing instrument provides a rapid distinction.

As always when a new material is introduced to the jewelry trade, it takes a certain amount of time for the industry to become aware of the existence of the material and to learn how to identify it. This is the time period when jewelers and gemologists are the most vulnerable. Synthetic moissanite is easily identifiable, and mistakes should not be made if a few simple procedures are followed.

REFERENCES

Acheson E.G. (1893) U.S. Patent 492,767, February 28, 1893.

Balaziak R. (1997) Manufactured abrasives in the third quarter of 1997. *Mineral Industry Surveys,* U.S. Department of the Interior, U.S. Geological Survey, Reston, VA.

Bruton E. (1978) *Diamonds,* 2d ed. Chilton Book Co., Radnor, PA.

Davis R.F., Carter C.H., Hunter C.E. (1990) *Sublimation of Silicon Carbide to Produce Large, Device-Quality Single Crystals of Silicon Carbide.* U.S. Patent Re. 34,861, February 14, 1995; reissue of U.S. Patent 4,866,005, September 12, 1989; reissue application filed October 26, 1990.

De Ment J. (1948) New gem superior to diamond. *The Mineralogist,* Vol. 16, pp. 211–218.

De Ment J. (1949) Silicon carbide—Rival to the diamond, in brilliancy. *The Gemmologist (London),* Vol. 17/18, pp. 53–59.

Divakar R., Chia K.Y., Kunz S.M., Lau S.K. (1993) Carbides (silicon): Silicon carbide. In M. Howe-Grant, Ed., *Kirk-Othmer Encyclopedia of Chemical Technology,* 3rd ed., John Wiley & Sons, New York, Vol. 4, pp. 891–911.

GIA Gem Reference Guide (1988) Gemological Institute of America, Santa Monica, CA.

Hallbauer D.K., Kable E.J., Robinson D.N. (1980) The occurrence of detrital diamond and moissanite in the Proterozoic Witwatersrand conglomerates, and their implication for crustal evolution. *Berliner Geowissenschaftliche Abhandlungen, Series A, Geologie und Paleontologie,* Vol. 19, pp. 67–68.

Harris G.L., Ed. (1995) *Properties of Silicon Carbide.* Electronic Materials Information Service, Vol. 13, Institute of Electrical Engineers (INSPEC), London.

Hobbs J. (1981) A simple approach to detecting diamond simulants. *Gems & Gemology,* Vol. 17, No.1, pp. 20–33

Hoover D.B. (1983) The Gem DiamondMaster and the thermal properties of gems. *Gems & Gemology,* Vol. 19, No. 2, pp. 77–86.

Johnson M.L., Koivula J.I., Eds. (1996) Gem news: Synthetic moissanite as a diamond simulant. *Gems & Gemology,* Vol. 32, No. 1, pp. 52–53.

Kunz G.F. (1905) "Moissanite." *American Journal of Science,* Series 4, Vol. 19, pp. 396–397.

Lely J.A. (1955) Darstellung von Einkristallen von Silicium-carbid und Beherrschung von Art und Menge der eingebauten Verunreinigungen. *Berichte der Deutschen Keramischen Gesellschaft,* Vol. 32, pp. 229–231.

Mason B. (1962) *Meteorites.* John Wiley & Sons, New York, p. 61.

Mathez E.A., Fogel R.A., Hutcheson I.D., Marshintsev V.K. (1995) Carbon isotopic composition and origin of SiC from kimberlites of Yakutia, Russia. *Geochimica et Cosmochimica Acta,* Vol. 59, No. 4, pp. 781–791.

McCawley E.L. (1981) Cubic moissanite—a gem mineral of the diamond family. *Lapidary Journal,* Vol. 34, No. 10 (January), pp. 2244–2247.

Mellor C. (1929) *A Comprehensive Treatise on Inorganic and Theoretical Chemistry.* Longmans, Green & Co., London, Vol. 5, pp. 875–887.

Milton C. (1986) Moissanite SiC: Yes or no? *Fourteenth General Meeting, International Mineralogical Association, Abstracts,* Stanford University, Stanford , CA, p. 171.

Milton C., Vitaliano D. (1984) Moissanite SiC: A non-existent mineral. *Twenty-Seventh International Geological Congress, Abstracts, Moscow,* p. 89.

Mitchell R.K. (1962) A rare synthetic. *Journal of Gemmology,* Vol. 8, No. 6, pp. 218–220.

Moissan F.F.H. (1904) Étude de la meteorite de Canyon Diablo. *Comptes Rendus de Academie des Sciences, Paris,* Vol. 139, p. 773.

Moore R.O., Otter M.L., Rickord R.S., Harris J.W., Gurney J.J. (1986) The occurrence of moissanite and ferro-periclase as inclusions in diamonds. *Fourth International Kimberlite Conference, Abstracts, Sydney,* Geological Society of Australia, pp. 409–411.

Nakashima S., Matsunami H., Yoshida S., Harima H., Eds. (1996) Silicon carbide and related materials. *Proceedings of the Sixth International Conference, Kyoto, September 18–21, 1995,* Conference Series No. 142, Institute of Physics Publishing, Philadelphia, PA.

Nassau K. (1980) *Gems Made by Man.* Gemological Institute of America, Santa Monica, CA.

Nassau K., Schonhorn H. (1977) The contact angle of water on gems. *Gems & Gemology,* Vol. 15, No. 12, pp. 354–360.

Obukhov A.B. (1972) *Mineralogy of Silicon Carbide: Silicon Carbide in Technical Materials and Rocks* (in Russian). Akademia Nauk SSSR, Leningrad, 140 pp.

O'Connor J.R., Smiltens J. (1960) Silicon Carbide: A High temperature semiconductor. *Proceedings of the Conference on Silicon Carbide,* Boston, MA, April 2–3, 1959, Pergamon Press, New York.

Powell B.W. (1956) The story of silicon carbide. *Lapidary Journal,* Vol. 10, No. 5, pp. 430–438.

Ramsdell L.S. (1947) Studies of silicon carbide. *American Mineralogist,* Vol. 32, No. 1/2, pp. 64–82.

Rodgers K.A., Courtney S.F., Seelye R., McCullock A., Mulholland I. (1989) An occurrence of "moissanite" (SiC) from Seddonville, West Coast, New Zealand. *New Zealand Natural Sciences,* Vol. 16, pp. 105–108.

Smoak R.H., Korzekwa T.M., Kunz S.M., Howell E.D. (1978) Carbides: Silicon Carbide. In D. Eckroth, Ed., *Kirk-Othmer Encyclopedia of Chemical Technology,* 3rd ed., John Wiley & Sons, New York, Vol. 4, pp. 520–535.

Tairov Y.M., Tsvetkov V.F. (1981) Growing large-size, single crystals of various silicon carbide polytypes. *Journal of Crystal Growth,* Vol. 52, pp. 146–150.

Thibault N.W. (1944) Morphological and structural crystallography and optical properties of silicon carbide (SiC). *American Mineralogist,* Vol. 29, No. 7/8, pp. 249–278, and No. 9/10, pp. 327–362.

Tsvetkov V.F., Allen S.T., Kong H.S., Carter C.H. Jr. (1996) Recent progress in SiC crystal growth. In S. Nakashima, H. Matsunami, S. Yoshida, and H. Harima, Eds., *Silicon Carbide and Related Materials. Proceedings of the Sixth International Conference, Kyoto, September 18–21, 1995,* Conference Series No. 142, Institute of Physics Publishing, Philadelphia, PA.

Verma A.R., Krishna P. (1966) *Polymorphism and Polytypism in Crystals.* John Wiley & Sons, New York.

Vigorova V.G., Chashchukhina V.A., Vigorov B.L., Palgueva G.V. (1978) Moissanite from granite of the Urals. *Doklady Akademia Nauk SSSR,* Earth Science Sections,Vol. 241, pp. 182–185.

von Muench W. (1982) Silicon carbide. In O. Madelung, Ed., *Landolt-Boernstein Numerical Data and Functional Relationships in Science and Technology,* New Series, Group III, Vol. 17A, Springer Verlag, New York, pp. 132–142, 442–449.

von Muench W. (1984) Silicon carbide. In M. Schultz and H. Weiss, Eds., *Landolt-Boernstein Numerical Data and Functional Relationships in Science and Technology,* New Series, Group III, Vol. 17C, Springer Verlag, New York, pp. 403–416, 585–592.

Wilke K.-Th. (1988) *Kristallzuechtung.* Verlag Harri Deutsch, Thun, Frankfurt.

Yu R.M., Healey D. (1980) A phosphoroscope. *Journal of Gemmology,* Vol. 17, No. 4, pp. 250–258.

CHARACTERIZATION OF CHINESE HYDROTHERMAL SYNTHETIC EMERALD

By Karl Schmetzer, Lore Kiefert, Heinz-Jürgen Bernhardt, and Zhang Beili

Synthetic emeralds grown hydrothermally in an alkali-free, chlorine-bearing solution have been manufactured in Guilin, China, since 1987. Diagnostic microscopic features include growth and color zoning as well as oriented needle-like tubes and cone-shaped voids ("nailhead spicules") that are typically associated with small chrysoberyl crystals. Also distinctive is the presence of chlorine in this iron- and alkali-free hydrothermal synthetic emerald. In addition, spectroscopic properties in the mid- and near-infrared are useful to characterize this new Chinese product; features in the 2500–3100 cm^{-1} range (also found in other chlorine-bearing synthetic emeralds) help distinguish it from natural emeralds.

ABOUT THE AUTHORS

Dr. Schmetzer is a research scientist residing in Petershausen, near Munich, Germany. Dr. Kiefert is a research scientist at the SSEF Swiss Gemmological Institute, Basel, Switzerland. Dr. Bernhardt is a research scientist at the Institute of Mineralogy of Ruhr University, Bochum, Germany. Professor Zhang is director of the National Gemstone Testing Center, Beijing, China.

Please see acknowledgments at end of article.

During a visit to Beijing in May 1996, one of the authors (KS) was shown several rough and faceted samples of a hydrothermal synthetic emerald that was manufactured in China (see, e.g., figure 1). This synthetic emerald has been produced since 1987 by Professor Zeng Jiliang at the Institute of Geology for Mineral Resources, CNNC, Guilin, Guangxi Province, southern China. It was first commercially released in 1993. At present, production is about 7,500 ct of rough a year, but this amount is expected to increase (Guo Tao, pers. comm., 1996, 1997). Samples have been sold under different trade names (Fritsch, 1996; C. M. Ou-Yang, pers. comm., 1997), but at present only "GJL-Emerald" (Guangxi Jewellery Limited) is used by the manufacturers (C. M. Ou-Yang, pers. comm., 1997).

Hydrothermally grown synthetic emeralds have been commercially available since the early 1960s. They were first produced in Austria (Lechleitner) and later in the United States (Linde, Regency), Australia (Biron), and Russia (Pough, 1965; Flanigen et al., 1965, 1967; Galia, 1972; Nassau, 1976; Brown and Snow, 1984; Kane and Liddicoat, 1985; Bukin et al., 1986; Schmetzer, 1988, 1990; Hosaka, 1990; Koivula et al., 1996). Hydrothermally grown synthetic emeralds from China were first described by Geng and Ou-Yang (1995). They were also briefly mentioned by Fritsch (1996) and Koivula et al. (1996), but to date there has been no comprehensive gemological description of this material.

This article reports on our examination of several crystals and faceted samples of this Chinese hydrothermal synthetic emerald. To help establish criteria by which they can be separated from their natural counterparts, we will describe in detail the mineralogical, gemological, chemical, and spectroscopic characteristics of these new synthetic gems. We will also compare these properties to those of various synthetic

Figure 1. This 4.72 ct crystal (sample H) and the 0.13–0.61 ct faceted samples are some of the hydrothermal synthetic emeralds grown in China that were examined for this study. The wires used to suspend the seed are visible on both ends of the crystal. Photo © GIA and Tino Hammid.

emeralds that have been hydrothermally grown by other commercial producers.

BACKGROUND ON CRYSTAL GROWTH

According to their producer, these Chinese synthetic emeralds are grown in autoclaves with gold liners at a temperature range of 585°–625°C and a pressure of 4.50 kbar (Guo Tao, pers. comm., 1996, 1997). This pressure is much higher than that normally used for the commercial growth of hydrothermal synthetic emeralds—that is, 0.70 to 1.53 kbar, as summarized by Hosaka (1990)—but in a similar temperature range of 500°–620°C. Therefore, the Chinese hydrothermal synthetic emeralds may be the first that are commercially produced at a pressure above 2 kbar.

The high-pressure synthesis of beryl was described by Franz and Morteani (1981) at 2 kbar and a temperature of 700°C as well as at 4 kbar and 500°C. Kodaira et al. (1982) synthesized beryl at an even higher pressure of 10 kbar, at 650°C to 750°C. They obtained prismatic crystals up to 0.3 mm in length.

The Chinese material grows at about 0.5 mm a day in a direction perpendicular to the seed plate. Both natural and synthetic beryl seed plates are used (Fritsch, 1996; Guo Tao and C. M. Ou-Yang, pers. comm., 1997). The producer also stated that he has grown two types of hydrothermal synthetic emerald: one with only chromium used as a color-causing dopant, and the second with chromium, vanadium, and iron compounds in the nutrient

and/or in the solution (Geng and Ou-Yang, 1995). Only the first type is now produced commercially (Guo Tao, pers. comm., 1997).

MATERIALS AND METHODS

For this study, we examined 11 Chinese hydrothermal synthetic emeralds (see table 1): a 12.12 ct crystal (sample A) that was acquired in China from the producer in 1994 by Prof. H. A. Hänni; a 7.40 ct crystal (sample B) and five faceted "stones" (0.31 to 0.50 ct; samples C to G) that the producer made available for the present investigation in 1996; and a 4.72 ct crystal (sample H) and three faceted pieces (0.13 to 0.61 ct; samples I to K) from the GIA Research collection that were obtained from the producer in 1995 by Prof. E. Fritsch.

All 11 samples (most of which are shown in figure 1) were tested by standard gemological methods for optical properties, fluorescence, and specific gravity. Morphological characteristics of the three crystals were determined with a standard goniometer, and the external faces of these crystals as well as the internal growth planes of all 11 samples were examined with a Schneider horizontal (immersion) microscope with a specially designed sample holder and specially designed (to measure angles) eyepieces (Schmetzer, 1986; Kiefert and Schmetzer, 1991). Solid inclusions were identified by Raman spec-

troscopy with a Renishaw Raman microscope (see Hänni et al., 1996, 1997).

For chemical characterization, we first submitted samples A to G for qualitative energy-dispersive X-ray fluorescence (EDXRF) analysis using a Spectrace 5000 Tracor X-ray fluorescence spectrometer with a Tracor Northern Spectrace TX-6100 software system, at SSEF. Quantitative chemical data for Cr, V, and Fe in crystal samples A and B were determined with the same equipment. The quantitative chemical compositions of faceted samples C to G were determined by electron microprobe using a CAMECA Camebax SX 50 instrument, with traverses of 100 point analyses measured across the table of each sample.

For samples A to G, spectroscopic data were recorded with a Leitz-Unicam SP 800 spectrophotometer for the visible and ultraviolet range, and with a Hitachi U 4001 instrument for the UV, visible, and near-infrared range (from 250 to 2500 nm). Infrared spectroscopy for the range $6000\,cm^{-1}$ to $1000\,cm^{-1}$ was performed for the same seven samples on a Philips PU 9800 Fourier-transform infrared (FTIR) spectrometer and a Perkin-Elmer 1760 FTIR spectrometer.

Faceted sample F was cut in two pieces, and one of these pieces was powdered. We used 2 mg of the powder to prepare a KBr compressed disk for infrared spectroscopy in the $4000–2000\,cm^{-1}$ range

TABLE 1. Physical characteristics of Chinese hydrothermal synthetic emerald samples.

Sample	A	B	C	D	E	F	G	H	I[b]	J	K[b]
Description	Crystal	Crystal	Faceted	Faceted	Faceted	Faceted	Faceted	Crystal	Faceted	Faceted	Faceted
Weight (ct)	12.12	7.40	0.50	0.39	0.43	0.41	0.31	4.72	0.13	0.22	0.61
Seed type	Natural colorless beryl	Natural colorless beryl	Synthetic emerald	Not observed	Natural colorless beryl	Synthetic emerald	Not observed	Synthetic emerald	Synthetic emerald	Synthetic emerald	Synthetic emerald
Seed inclination to c-axis	20°	33°	34°	32° bent plane	38°	40°	Not observed	20°	33°	35°	36°, 44° bent plane
Microscopic features[a]	Planar color zoning, irreg. subgrain bounds., small feathers	Planar color zoning, irreg. subgrain bounds., single cones w/ beryl xls, small feathers	Planar color zoning, numerous cones w/ chrysoberyl xls, needles at growth plane, small feathers	Planar color zoning, irreg. subgrain bounds., needles at growth plane	Planar color zoning, single cones w/ beryl xls, numerous cones w/ chrysoberyl xls	Planar color zoning, numerous cones w/ chrysoberyl xls, needles in seed	Irregular color zoning, prominent irreg. subgrain bounds.	Planar color zoning, irreg. subgrain bounds., large feathers	Planar color zoning, irreg. subgrain bounds., numerous cones w/ xls, needles at growth plane	Planar color zoning, irreg. subgrain bounds., numerous cones w/ chrysoberyl xls, needles in seed	Planar color zoning, irreg. subgrain bounds., numerous cones w/ xls

[a]Cones = cone-shaped fluid inclusions; irreg. subgrain bounds. = irregular subgrain boundaries; xls = crystals (minerals identified by Raman spectroscopy); needles = needle-like tubes
[b]In these two samples, the tiny crystals were optically identical to the chrysoberyl crystals identified by Raman spectroscopy in other samples.

using a Nicolet-Impact 400D infrared spectrometer. The remaining 38 mg of powder was used for the quantitative determination of Li_2O and H_2O by wet chemical methods.

For comparison purposes, two of the authors (KS and LK) drew on infrared and EDXRF data gathered for other hydrothermal synthetic emeralds. The senior author (KS) has also examined the microscopic features of about 100 hydrothermal synthetic emeralds from different producers. From these samples, he selected 20 for Raman spectroscopy of nailhead spicules (Linde and Regency, 6; Biron, Pool, and AGEE, 5; and Lechleitner, 9), which was conducted as described above for the Chinese samples. Note that the Lechleitner samples included both the synthetic emerald overgrowth over natural beryl and fully synthetic emeralds. Unless otherwise noted, all references to Lechleitner in this article will refer to both products.

RESULTS

Visual Appearance and Crystallography. When examined with the unaided eye, all the samples appeared an intense, homogeneous green without any prominent color zoning (again, see figure 1). A colorless seed plate was easily seen in crystal samples A and B, and the surface of each had residues of the metallic wire used to hold the seed. Careful examination of crystal sample H showed a green seed. On one end of this seed, residue of a metallic wire was overgrown by synthetic emerald. At the other end of the crystal, a second metallic wire traversed both the seed and the synthetic emerald overgrowth (see figure 1).

All three Chinese crystals showed the basal pinacoid c (0001), two prism faces, m (10$\bar{1}$0) and a (11$\bar{2}$0), as well as the hexagonal dipyramid p (10$\bar{1}$2) (figure 2). In all cases, the seeds were oriented as drawn in figure 3, that is, with angles of 20° or 33° between the seed and the c-axis (optic axis). Only sample A showed the two large uneven faces parallel to the seed (figures 3 and 4) that are commonly observed in hydrothermally grown synthetic emeralds (see Pough, 1965; Lebedev et al., 1986; Hosaka, 1990; Sosso and Piacenza, 1995; Sechos, 1997). Because their seeds had different length-to-width ratios, sample H had only one small face parallel to the seed and sample B had none with that orientation (figure 3).

All three crystals were strongly distorted; that is, the two a (11$\bar{2}$0) prism faces in the a–c seed zone
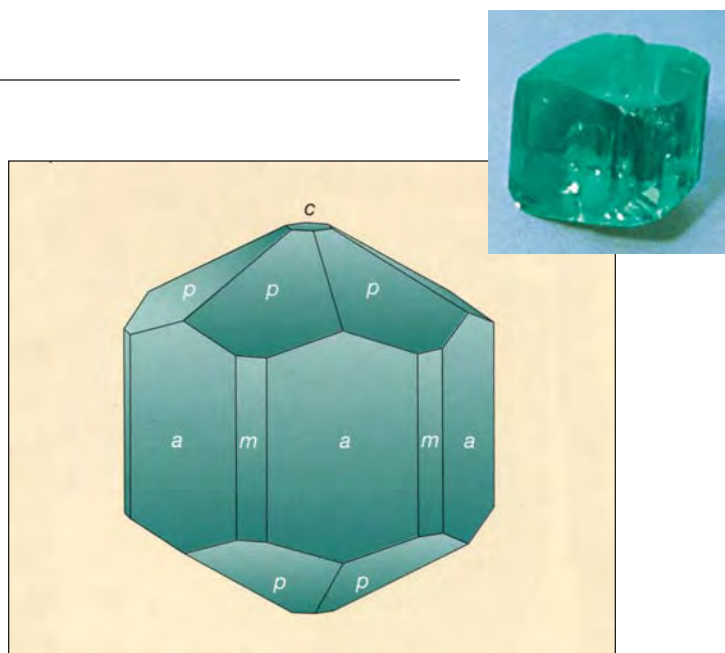

Figure 2. All three crystals of Chninese of Chinese hydrothermal synthetic emerald (see, e.g., 7.40 ct sample B in the inset photo) showed the basal pinacoid c, first-and second-order hexagonal prisms m and a, and the hexagonal dipyramid p, as illustrated in this schematic drawing of an undistorted crystal. Photo by H. A. Hänni

were dominant, and the four symmetrically equivalent a prism faces were distinctly smaller or absent. In addition, on each side, only two of six possible p dipyramids were developed (see figure 3).

Gemological Properties. The gemological properties of our Chinese samples (table 2) overlap those of natural emeralds, especially low-alkali emeralds, from various localities (see, e.g., Schrader, 1983). They are in the range commonly observed for low-iron or iron-free hydrothermally grown synthetic emeralds (see references cited above). Specifically, the values for R.I. and S.G. are similar to those observed for Lechleitner, Linde, Regency, and Biron synthetic emeralds, but they are distinctly lower than those of both types of (high-iron) Russian hydrothermal synthetic emeralds. The moderate fluorescence to UV radiation also indicates the absence of significant iron in the Chinese samples.

Microscopic Characteristics. *Structural Properties.* We observed seeds in six of the eight faceted Chinese samples (again, see table 1). The seed in sample E was colorless beryl (figure 5), similar to crystal samples A and B; as in those crystals (figure 6), the seed was of variable thickness. The other seeds were synthetic emerald, as in crystal sample
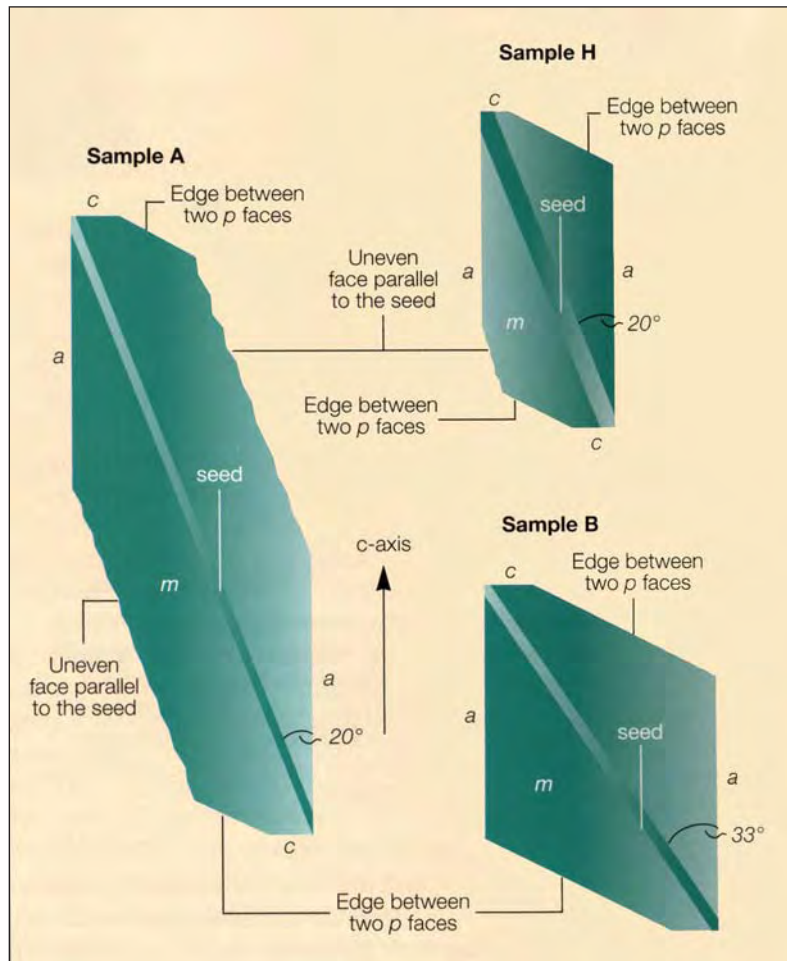
Figure 3. In this illustration (drawn to scale), Chinese hydrothermal synthetic crystal samples A, B, and H are shown as they appear when viewed parallel to the seed. The c-axis is parallel to the prism a *and perpendicular to the basal pinacoid* c; *the seeds are inclined to the c-axis at the angles indicated. Also shown is the edge at which the two* p *faces intersect. Two large uneven faces parallel to the seed are developed in sample A; only one uneven face was seen in sample H and none in sample B. The morphology of the crystals is related to the orientations and sizes of the seeds, which are (length × width × thickness) 21.5 × 8.0 × 0.4 mm in sample A, 13.5 × 11.0 × 0.15 mm in sample B, and 10.6 × 13.6 × 0.5 mm in sample H.*

H. In one of these faceted samples, the seed had a bent surface on one side (figure 7).

In all the Chinese samples found to contain

Figure 4. The face with this uneven, undulating surface was one of two oriented parallel to the seed in Chinese hydrothermal synthetic emerald sample A. Photo by H. A. Hänni; magnified 25×.
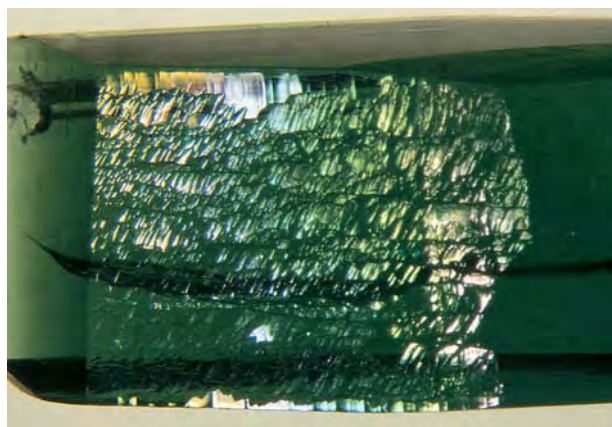
seeds, we observed growth zoning, usually associated with color zoning, that was oriented parallel to the seed (figures 5, 6, and 8). In one sample without a seed, we saw bent zoning similar to that shown in figure 7. In some cases, the growth structures revealed a weak step-like microstructure (again, see figure 6), similar to that seen in various other hydrothermal synthetic emeralds (Galia, 1972; Lebedev and Askhabov, 1984; Schmetzer, 1988).

TABLE 2. Properties of 11 Chinese hydrothermal synthetic emeralds.

Color	Very slightly bluish green
Pleochroism	ω=yellowish green, ε=bluish green
Refractive indices	n_ω=1.576–1.578
	n_ε=1.570–1.572
Birefringence	0.006
Specific gravity	Rough: 2.70–2.71
	Faceted: 2.67–2.69
UV fluorescence	Short-wave: moderate red
	Long-wave: moderate red

Some of the samples revealed irregular boundaries between subindividuals (figure 9), occasionally in the form of an undulating, chevron-like growth pattern. This type of growth structure also is typical of other hydrothermal synthetic emeralds (Lebedev et al., 1986; Schmetzer, 1988; Henn et al., 1988; Hänni, 1993; Sechos, 1997). Note that this growth pattern was not seen in the two samples (E and F) in which the seed was inclined more than 35° to the c-axis, as was also the case for some Russian hydrothermal synthetic emeralds in which the seeds were at an angle of about 45° with the c-axis (Schmetzer, 1996).

Inclusions Related to the Seed or to Growth Planes. We commonly observed three types of elongated inclusions in the Chinese samples. These were related either to the seed or to growth planes in the synthetic emerald overgrowth; they were oriented either inclined to the seed or almost perpendicular to the seed, as illustrated in figure 10. In general, these inclusions appeared as one of two types of cone-shaped spicules (also called nailhead spicules when a crystalline "head" is present) or as needle-like tubes. All were filled with a fluid; some also had a gas bubble.

In the first type of spicule, which occurs as an isolated inclusion oriented parallel to the c-axis, the
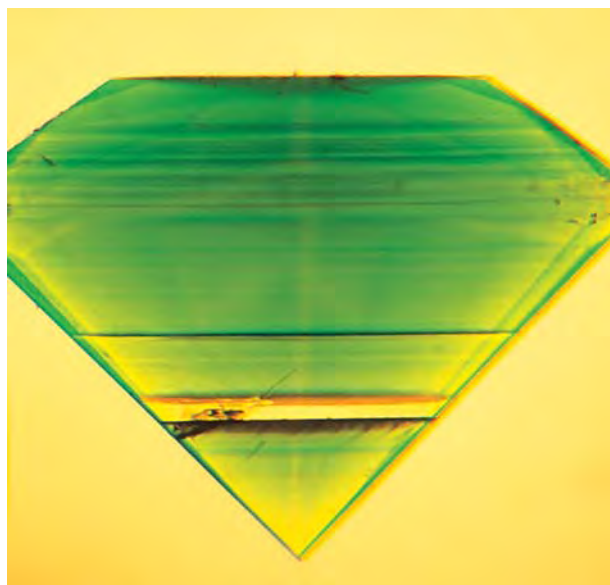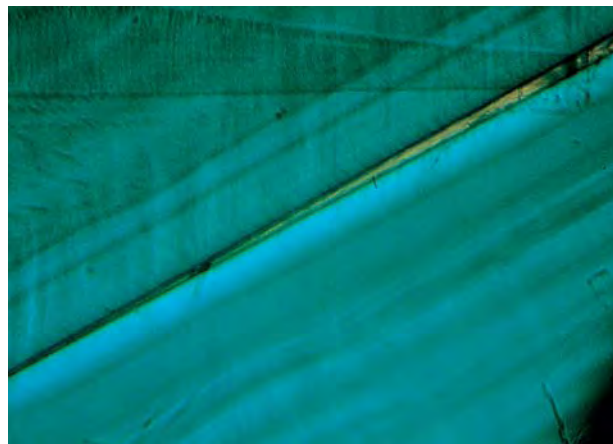

Figure 5. Faceted sample E has a colorless natural beryl seed that almost parallels the table facet, with growth zoning and color zoning parallel to the seed. Note that the seed appears yellow because the stone is immersed in benzyl benzoate. Magnified 35×.

widest end of the cone is in direct contact with a tiny crystal at the seed; the narrower tip pointed in the direction of growth (figures 10A and 11). This general orientation has been described often in the gemological literature (Flanigen et al., 1967; Galia, 1972; Sunagwa, 1982; Hosaka, 1990). The tiny birefringent crystals have a refractive index close to that of the host emerald, so they can be difficult to observe without crossed polarizers.

Figure 6. Some of the colorless seeds in the Chinese synthetic emeralds examined were of variable thickness, as shown here in crystal sample B. Note also the step-like microstructures in the color zoning parallel to the seed, which resembles the irregular growth patterns seen in other hydrothermal synthetic emeralds. Immersion, magnified 50×.

Figure 7. One side of the synthetic emerald seed in faceted sample K is bent. Numerous tiny crystals can be seen throughout both sides of the synthetic seed, as well as cone-shaped spicules oriented parallel to the c-axis. Note also the distinct growth zoning in the seed itself. Immersion, magnified 40×.
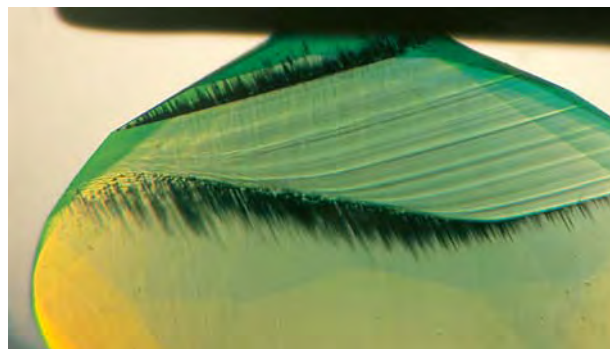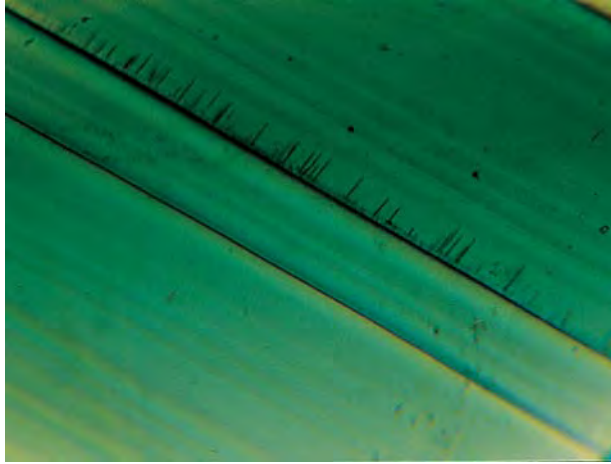
Figure 8. Growth planes, with associated color zoning, were seen oriented parallel to the seed in all of the Chinese samples that had seeds (upper right). Note also in this sample (C) the needle-like tubes that are elongated almost perpendicular to—and end at—one of the growth planes. Immersion, magnified 60×.
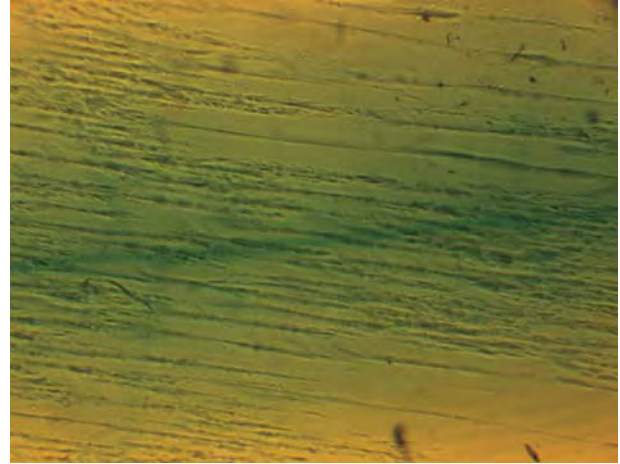

Figure 9. The growth structure of this Chinese hydrothermal synthetic emerald (sample G) revealed irregular boundaries between subindividuals. Immersion, magnified 60×.

The second type of spicule occurs in groups, also parallel to the c-axis, all with their widest ends at or very near the seed (figures 10 and 12). In direct contact with the seed are numerous small crystals (figure 13) that are also birefringent but have a refractive index that is distinctly higher than that of the host beryl.

The needle-like tubes are oriented almost perpendicular (measured at 80° to 85°) to the seed (fig-

Figure 10. This schematic drawing illustrates the different types of characteristic inclusions observed in the Chinese hydrothermal synthetic emeralds: (A) a colorless beryl seed with an isolated beryl crystal and numerous chrysoberyl crystals, both commonly associated with cone-shaped spicules (in all four inclusion types, these spicules parallel the c-axis); (B) a synthetic emerald seed with numerous chrysoberyl crystals— and cone-shaped spicules—on both sides; (C) a synthetic emerald seed with needle-like tubes within the seed (grown in the first autoclave run) and almost perpendicular to its surface, as well as with numerous chrysoberyl crystals on both sides of the seed; (D) a synthetic emerald seed with numerous chrysoberyl crystals and the cone-shaped spicules—a growth plane away from the seed reveals needle-like tubes with an orientation almost perpendicular to the growth plane that end at the growth plane.
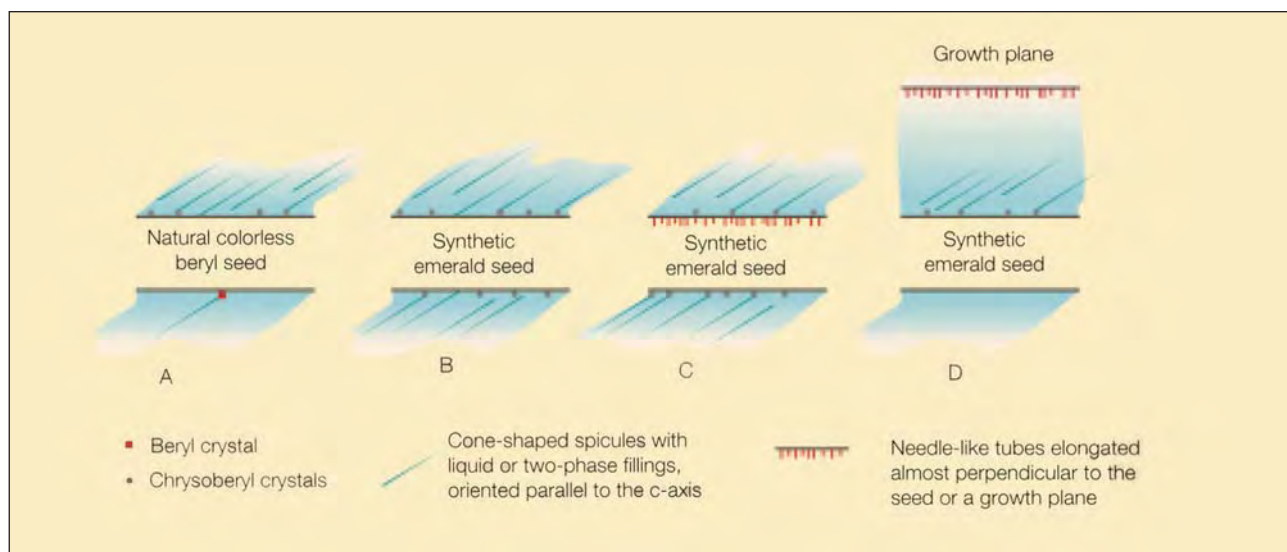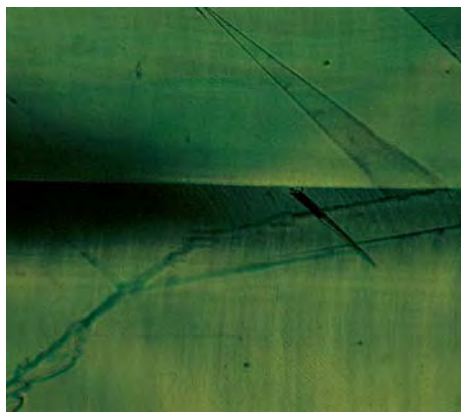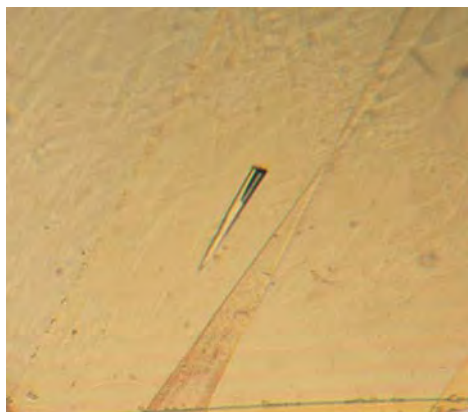
Figure 11. Occasionally seen in the Chinese hydrothermal synthetic emeralds examined were isolated cone-shaped spicules filled with a liquid or liquid and gas (left), and associated with a tiny crystal at their widest ends. The tiny crystal is in contact with the surface of the seed (right). Immersion, magnified 80×.

ures 10C and D, 14)—that is, inclined to the c-axis of the host. One end of the tube is always in direct contact with the seed or a growth plane parallel to the seed. In samples C, D, and I, there were no associated crystalline inclusions at the growth planes (again, see figure 8). In samples F and J, we observed these needle-like tubes *within* the seed, with cone-shaped spicules and birefringent crystals in the adjacent synthetic emerald overgrowth (again, see figure 14).

Other Liquid Inclusions. With the exception of the above-described inclusions, the samples were relatively clean. Only small liquid feathers were observed occasionally.

Figure 12. In the second type of elongated inclusion observed in the Chinese samples, numerous cone-shaped spicules with liquid or two-phase fillings, similar to the isolated inclusions shown in figure 11, also parallel the c-axis. These spicules start at the synthetic emerald seed or at a short distance from the seed; they are associated with numerous tiny crystals that are in contact with the surface of the seed. Note also the distinctive color zoning in the seed. Immersion, magnified 80×.
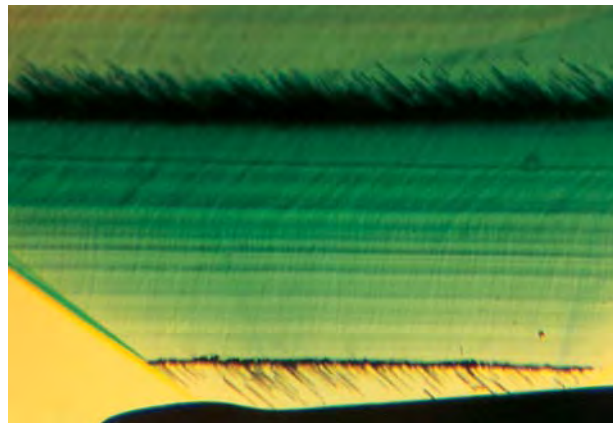
Identification of the Crystalline Inclusions. Tiny crystals at the base of nailhead spicules are common in hydrothermal synthetic emeralds (Pough, 1965; Flanigen et al., 1967; Galia, 1972; Sunagawa, 1982; Brown and Snow, 1984; Kane and Liddicoat, 1985; Gübelin, 1986; Hosaka, 1990; Hänni, 1993). They form when crystal growth starts on a seed plane that is inclined to the c-axis (Flanigen et al., 1967; Schmetzer, 1996). This type of inclusion also forms in flux-grown emerald (Flanigen et al., 1967), but it is commonly seen only in the Nacken products, which were grown in the 1920s on irregularly shaped seeds (Nassau, 1978).

On the basis of their R.I. (above that of beryl) and their crystal morphology, crystalline "nailheads" in hydrothermal synthetic emeralds are generally designated as phenakite (see references cited above). This identification was confirmed for Linde hydrothermal synthetic emerald by Raman spectroscopy (Delé-Dubois et al., 1986a and b). Examination of the inclusions in our Chinese samples, however, did not lead to the same results. Micro-Raman analysis of the birefringent crystals at the broad end of isolated spicules in samples B and E revealed only beryl. Thus, these inclusions are beryl crystals, but with an orientation different from that of the host. However, the Raman spectra of the numerous tiny crystallites that are also in contact with a seed (figure 15) did not match those of either beryl or phenakite; rather, they matched the spectrum of chrysoberyl (figure 16).

Examination of other hydrothermal synthetic emeralds (see Materials and Methods) proved the presence of phenakite in nailhead-type inclusions of several Linde and both types of Lechleitner synthetic emeralds. In the course of this study, with the help of Dr. Graham Brown in selecting the sample at the producer, "nailheads" of chrysoberyl crystals were identified for the first time at the seed of
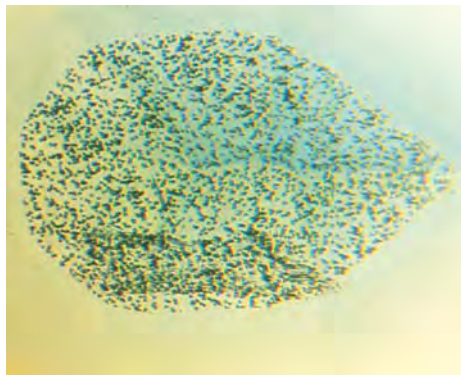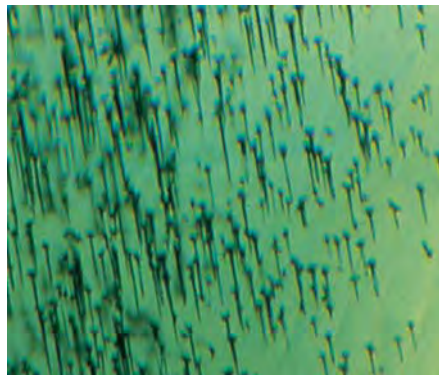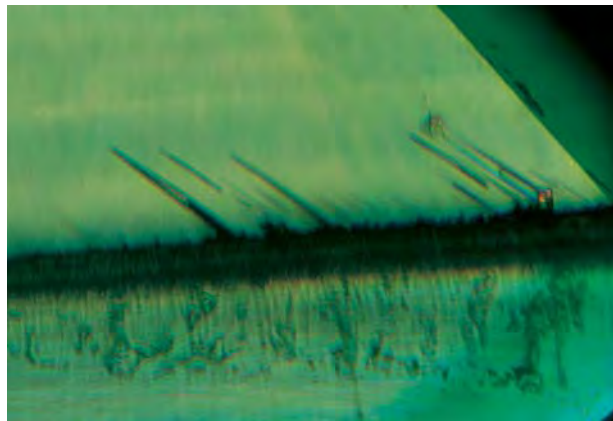
Figure 13. In the Chinese samples, the numerous tiny crystals at the broad ends of the spicules may appear as masses at the surface of the seed (left; immersion, magnified 50×). In a view parallel to the c-axis (i.e., the axis of the spicules), only the "nail-heads" are visible; the cut of the synthetic emerald defines the outline of the seed (right; immersion, magnified 40×).

another hydrothermal synthetic emerald, the Biron product. Raman spectroscopy also identified some of the birefringent and transparent "nailheads" in two Biron synthetic emeralds as beryl, but found no phenakite in the samples analyzed. Interestingly, gold was also identified in these Biron samples; it probably originated from the liner of the autoclave, as indicated by the producer (A. Birkner, pers. comm., 1997) and by Kane and Liddicoat (1985).

Chemistry. The qualitative EDXRF spectra of seven samples indicate distinct amounts of chromium and chlorine as well as the expected silicon and aluminum. Some minor vanadium was observed in one of the crystals.

Quantitative EDXRF and electron microprobe data are summarized in table 3. The microprobe data confirm the EDXRF results. The only color-causing element detected was chromium; vanadium and iron were at the detection limits of the electron microprobe. Alkalis and Mg were also at the detection limits, whereas significant amounts of chlorine and traces of fluorine were found in all samples.

Microprobe traverses indicated that chromium was the only element that varied appreciably from one area of a stone to another. This was most appar-

Figure 14. The third type of elongated inclusion seen in the Chinese samples consists of needle-like tubes with an orientation almost perpendicular to the surface of the synthetic emerald seed (seen at the bottom here). On the other side of this boundary, in the synthetic emerald overgrowth, the cone-shaped spicules are elongated parallel to the c-axis. They start at the seed or at a short distance from the seed, and are often associated with tiny birefringent crystals that are in contact with the seed. (Note that the inclusion above the spicule on the right is not directly related to the spicule.) Immersion, crossed polarizers, magnified 80×.

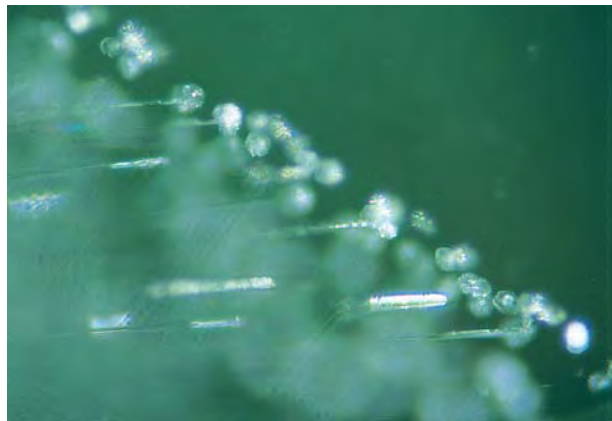*Figure 15. Micro-Raman analysis revealed that the tiny crystals at the broad ends of the numerous one- and two-phase cone-shaped spicules in the Chinese hydrothermal synthetic emeralds were chrysoberyl. Renishaw Raman microscope, magnified 200×.*
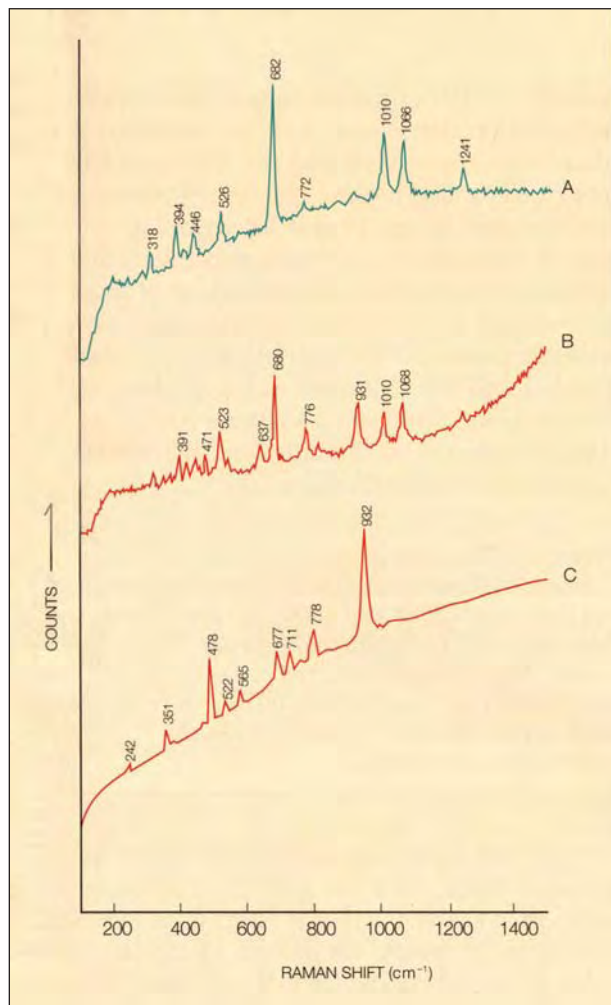
Figure 16. The Raman spectrum of the tiny crystals (B) illustrated in figure 15 match the reference spectrum for chrysoberyl (C). Note that in spectrum B, the lines of the Raman spectrum of the Chinese hydrothermal synthetic emerald host (A) are also present.

ent in samples C and F, where the traverses crossed the table facet, which included several different growth layers and color zones (figure 17).

Wet chemical analyses of sample F indicated a distinct water content of 0.85%, as well as the expected beryllium, but no lithium was found.

Spectroscopy. Because of the orientation of the samples, polarized spectra were measured only for two Chinese hydrothermal synthetic emerald crystals and one faceted sample. Nonpolarized spectra were recorded for four other faceted samples.

Ultraviolet-Visible Spectroscopy. The absorption spectra of all samples were consistent with the

known absorption spectra of chromium in emerald; no absorption bands related to Fe^{2+} or Fe^{3+} were observed (for the exact position of iron absorption bands, see Schmetzer, 1988).

Infrared Spectroscopy. Infrared spectroscopy has been used to separate natural and synthetic emeralds since the late 1960s (Flanigen et al., 1967; Wood and Nassau, 1967, 1968; Nikol'skaya and Samoilovich, 1979; Klyakhin et al., 1981; Lebedev et al., 1986). With modern Fourier-transform infrared spectrometry, it is possible to obtain transmission and/or reflection infrared spectra on faceted samples (Flamini et al., 1983; Leung et al., 1986; Stockton, 1987; Fritsch et al., 1992; Hänni and Kiefert, 1994; Koivula et al., 1996).

The strongest absorption bands of at least two different types of water molecules located in channel sites of the beryl structure (both natural and synthetic) are found in the 3500–4000 cm^{-1} range of the mid-infrared. An extremely intense water absorption was observed in the spectra of the

TABLE 3. Chemical properties of Chinese hydrothermal synthetic emeralds.

Oxide (wt.%)	EDXRF (crystals)		Electron microprobe[a] (faceted stones)				
	A	B	C	D	E	F[b]	G
SiO$_2$			64.78	65.44	64.79	65.45	64.71
TiO$_2$			tr.[c]	tr.	tr.	tr.	tr.
Al$_2$O$_3$			18.37	18.66	18.25	18.46	18.39
Cr$_2$O$_3$	0.74	0.29	0.79	0.62	0.62	0.49	0.82
V$_2$O$_3$	n.d.[d]	0.03	tr.	tr.	tr.	tr.	tr.
FeO[e]	n.d.	n.d.	tr.	tr.	tr.	tr.	tr.
MnO			tr.	tr.	tr.	tr.	tr.
CaO			tr.	tr.	tr.	tr.	tr.
MgO			tr.	tr.	tr.	tr.	tr.
Na$_2$O			0.04	tr.	tr.	tr.	tr.
K$_2$O			tr.	tr.	tr.	tr.	tr.
F			0.04	0.04	0.03	0.04	0.04
Cl			0.67	0.71	0.65	0.69	0.67
Sum[f]			84.69	85.47	84.34	84.13	84.63
Cr$_2$O$_3$ (range)			0.39–1.08	0.54–0.71	0.54–0.73	0.27–0.60	0.69–1.07

[a]Average of 100 point analyses.
[b]Wet chemical analysis gave 0.85 wt.% H_2O; Li_2O was not detected.
[c]tr.=trace (up to 0.02 wt.%).
[d]n.d.=not detected.
[e]Total iron is reported as FeO.
[f]BeO was calculated between 13.45 and 13.95 wt.% for the five samples, assuming 3.0 Be atoms per formula unit.
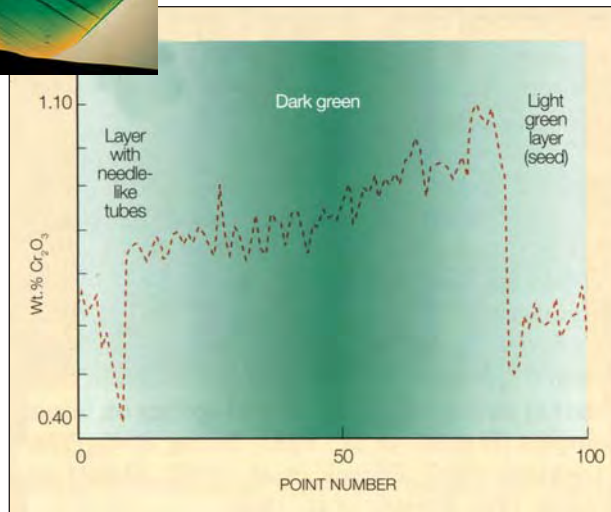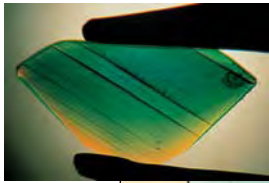
Figure 17. This graph shows the variation in Cr_2O_3 determined by electron microprobe analysis in a scan of 100 analytical points across the table facet (3 mm long) of sample C. Growth layers represented by color zoning in this sample (inset, in immersion, magnified 25×) are exposed at the table, as is the light green seed (on the right). Low levels of chromium are present in the seed, as compared to the remaining dark green area. The discontinuity on the left of this scan was measured at the boundary of another dark green area, close to a growth zone containing numerous needle-like tubes.

Chinese samples (figure 18). Between 5000 and 5500 cm^{-1} are absorption bands of other vibrations of water molecules. All different water absorption bands are strongly polarized (Wood and Nassau, 1968; Koivula et al., 1996), as we observed in the spectra of the Chinese samples.

In the 5000–5500 cm^{-1} region, it is possible to distinguish between the polarized spectra of alkali-free hydrothermal synthetic emeralds, such as our Chinese samples, and those of low-alkali natural emeralds, such as Colombian stones. The spectra must be recorded from oriented samples, because nonpolarized spectra of emeralds in the range of the water absorption bands are not always diagnostic (see Box A).

There is, however, another diagnostic range in the mid-infrared, between 2500 and 3100 cm^{-1}. All of our (chlorine-bearing) Chinese samples revealed a series of three sharp bands at 2746, 2815, and 2887 cm^{-1}, two broad absorption bands at about 2625 and 2970 cm^{-1}, and a smaller shoulder at 2917 cm^{-1} (fig-

ure 19). All five of the absorption bands are strongly polarization dependent: Four are polarized perpendicular to the c-axis, and the 2815 cm^{-1} band is polarized parallel to the c-axis. In nonpolarized spectra (compare figures 19 and 20), the relative intensities of these absorption bands depend on the orientations of the samples. A comparison of these spectra with those of other hydrothermal synthetic emeralds revealed an identical series of absorption bands in all the chlorine-bearing products—Linde, Regency, and Biron (see also figure 20 and Stockton, 1987)—but not in the chlorine-free Russian and Lechleitner synthetic emeralds.

Figure 18. The infrared spectra of faceted Chinese hydrothermal synthetic emerald sample C between 2000 and 6000 cm^{-1} are shown here polarized perpendicular and parallel to the c-axis. Note the water-related peaks in the 3500–4000 cm^{-1} and 5000–5500 cm^{-1} regions, as well as the chlorine-related peaks in the 2500–3100 cm^{-1} region.
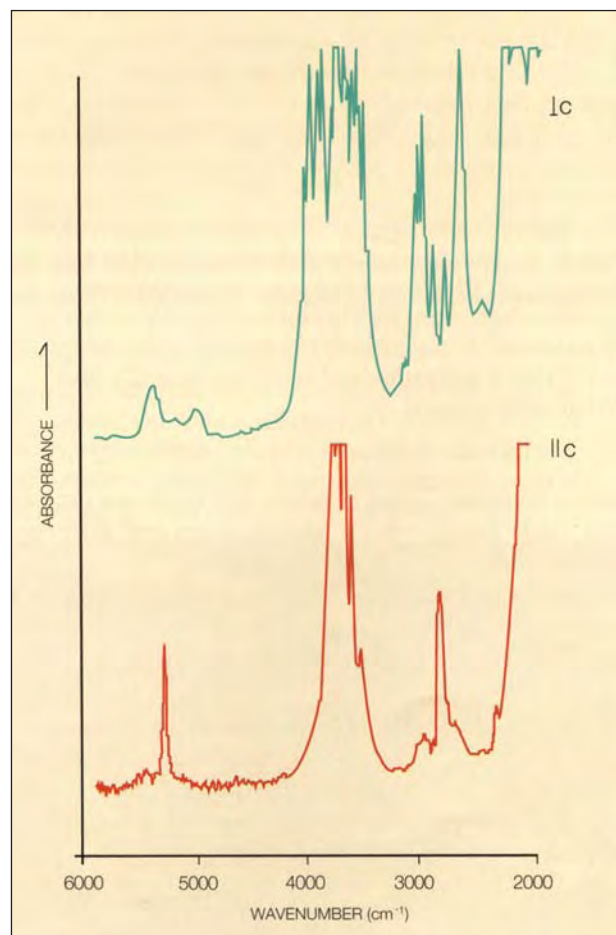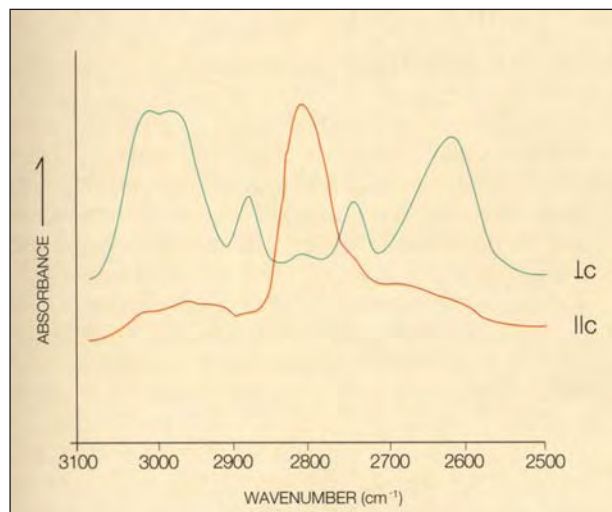
Figure 19. Chlorine-related bands in the 2500–3100 cm^{-1} range of the infrared spectrum, as seen polarized parallel and perpendicular to the c-axis, are diagnostic for the Chinese and other chlorine-bearing hydrothermal synthetic emeralds.

This group of bands is probably related to the chlorine content of these samples. Observation of this series of absorption bands in an unknown sample is sufficient to identify the sample as synthetic; no overlap with any absorption bands seen in natural emeralds is found in the 2500–3100 cm^{-1} range. In addition, polarized spectra are not needed; that is, a sample does not need to be oriented to obtain diagnostic information in this range.

DISCUSSION

Growth Conditions of Chinese Hydrothermal Synthetic Emeralds. The results of our study indicate that Chinese hydrothermal synthetic emeralds belong to the group of chlorine-bearing, alkali-free hydrothermal emeralds that includes two types of products: (1) Linde and Regency (predominantly Cr-bearing); and (2) Biron, Pool, and AGEE (predominantly Cr- and V-bearing). The other group of hydrothermal synthetic emeralds—those that are alkali-bearing and chlorine-free—includes the Lechleitner products and all commercial Russian hydrothermal synthetic emeralds. Samples of the alkali-free group reveal infrared absorption bands of type I water molecules only, whereas samples of the alkali-containing group show bands related to type I and type II water (again, see Box A).

Those Chinese samples that contain a colorless natural seed were grown in a single production step. Those that consist of a green synthetic seed with an overgrowth of synthetic emerald represent two generations of growth: A plate of synthetic emerald was cut from a previously grown crystal, and this plate was used as a seed to grow layers of a second generation (as confirmed by E. Fritsch, pers. comm., 1997, and C. M. Ou-Yang, pers. comm., 1997). This is similar to the procedure used to grow the first hydrothermal synthetic emeralds, such as Lechleitner and Linde, in several subsequent autoclave runs. The morphology of the crystals is dominated by the orientation and size of the seed, especially the relationship of length to width (again, see figure 3).

Samples A and H, which were obtained in 1994 and 1995, respectively, and show irregular growth faces parallel to the seed, probably represent an older type of Chinese synthetic emerald grown with a seed inclined 20° to the optic axis. All other samples were grown with seeds inclined 32° to 40° to the c-axis. According to the producer, he tried to cut the natural beryl plates used as seeds for the first growth step with an orientation of 30° to 35° to the c-axis. However, because of the properties of the natural beryl crystals that were available, he encountered problems orienting them, which

Figure 20. For Biron and Chinese hydrothermal synthetic emeralds in the 2500 and 3100 cm^{-1} range, the relative intensities of the bands seen with polarized spectra (figure 19) are different from those seen here with nonpolarized spectra.
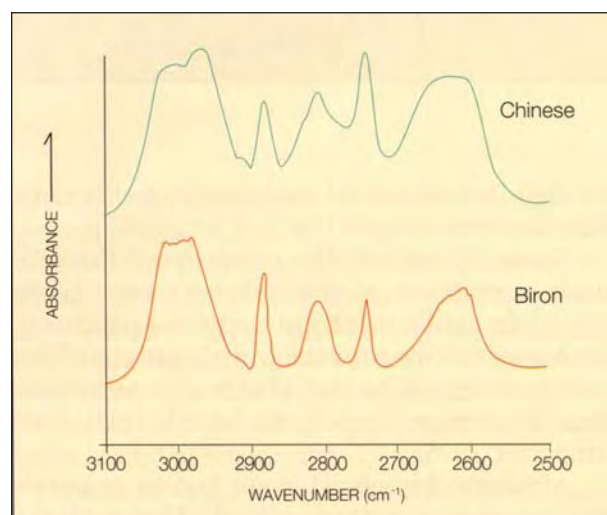
Box A: Distinction of Natural and Synthetic Emeralds by Water Absorption Bands in the Infrared

All natural and hydrothermal synthetic emeralds contain water in the relatively large channels inherent to the structure of beryl. Wood and Nassau (1968) identified two types of water molecules in beryl, as evidenced by absorption features in their infrared spectra. Type I water occurs in low-alkali natural and all hydrothermal synthetic emeralds. Type II water occurs in all alkali-bearing natural emeralds and some hydrothermal synthetic emeralds. Because of the presence of similar amounts of type I and type II water molecules, the absorption spectra of low-alkali hydrothermal synthetic emeralds (Russian samples and Lechleitner fully synthetic emeralds) overlap those of low-alkali natural emeralds such as from Colombia or Zimbabwe (Sandawana) in the 3500–4000 cm^{-1} range. Consequently, only high-alkali natural emeralds without type I water can be easily identified by their infrared spectra in that range (Schmetzer, 1988, 1989, 1990; Kiefert and Schmetzer, 1990).

Because of the high water contents of natural and hydrothermal synthetic emeralds, it is somewhat problematic to obtain the fine structure and exact positions of the absorption maxima of the water-related infrared absorption bands in the 3500–4000 cm^{-1} region from relatively thick crystals or from faceted stones (see text figure 18). The polarized measurement of spectra cannot solve this problem.

The information can be gained by obtaining a small amount of emerald powder (e.g., 2 mg) to prepare a KBr compressed disk, but this is a destructive method that is useful only in a research environment (Flanigen et al., 1967; Schmetzer, 1989; Schmetzer and Kiefert, 1990; Aurisicchio et al., 1994). Nevertheless, to fully characterize the Chinese hydrothermal synthetic emeralds, we obtained such data from sample F, which revealed a single sharp absorption band at 3964 cm^{-1}. This absorption band has been assigned to alkali-free (type I) water molecules in beryl (Wood and Nassau, 1968; Schmetzer, 1989). It is consistent with the chemical composition of sample F (see text table 3), which did not contain significant alkalis.

Even when the diagnostic absorptions in the 3500–4000 cm^{-1} region are too strong to be distinguishable, features in the 5000–5500 cm^{-1} region can usually be resolved. They are, therefore, particularly useful in the separation of natural from hydrothermal synthetic emeralds. In this region, other water vibrations were noted for seven Chinese samples: three distinct absorption maxima, at 5110, 5275, and 5450 cm^{-1}. All three absorption bands can also be assigned to alkali-free (type I) water molecules (Wood and Nassau, 1967, 1968, Nassau and Nassau, 1980; Klyakhin et al., 1981; Kodaira et al., 1982; Flamini et al., 1983; Lebedev et al., 1986; Koivula et al., 1996). This is consistent with the result obtained for sample F using the KBr technique. In some of the spectra obtained by conventional means, the 5275 cm^{-1} absorption band was dominant; in others, the three absorption bands were of similar intensity (figure A-1). The nonpolarized spectra of all seven samples lie between these two basic types, depending on the angle of the beam to the c-axis. However, the polarized spectra of three Chinese samples (figure A-2) revealed that the absorption bands at 5110 and 5450 cm^{-1} are polarized *perpendicular* to the c-axis and the band at 5275 cm^{-1} is polarized *parallel* to the c-axis. This polarization dependency is responsible for the variation in nonpolarized spectra according to the orientation of the sample.

---

resulted in a variety of angles within this range (Guo Tao, pers. comm., 1997).

Seeds inclined to the c-axis more than 35° result in synthetic emeralds that are more-or-less free of irregular internal growth structures. Consequently, the internal growth pattern of this product is similar to that observed in samples of recent Russian production (see Koivula et al., 1996; Schmetzer, 1996).

Although chrysoberyl is not known as a common inclusion in synthetic emerald, Flanigen (1971) mentioned that the formation of impurities such as chrysoberyl and phenakite had been observed during the growth of hydrothermal synthetic beryl. The hydrothermal synthesis of chrysoberyl is also described in the literature in the pressure-temperature range claimed by the producer for these Chinese hydrothermal synthetic emeralds (see, e.g., Franz and Morteani, 1981; Barton, 1986).

The results of our chemical analyses indicated two types of Chinese hydrothermal synthetic emeralds in our study: Most of the samples contained

It is important to note that alkali-bearing natural emeralds exhibit a type II water absorption band at 5275 cm^{-1} with polarization *perpendicular* to the c-axis (Wood and Nassau, 1967, 1968). Similar spectra have been reported for alkali-bearing hydrothermal synthetic emeralds from Russia and for low- to medium-alkali natural emeralds (Klyakhin et al., 1981; Flamini et al., 1983; Lebedev et al., 1986; Koivula et al., 1996). Because of the polarization differences (see figure A-2), it is possible to distinguish between type I and type II water spectra in the 5000–5500 cm^{-1} region.

However, *nonpolarized* spectra of low-alkali natural and synthetic emeralds are almost identical to those of alkali-free synthetic emeralds (again, see figure A-1). Consequently, nonpolarized absorption spectra in the 5000 to 5500 cm^{-1} region are of no diagnostic value. Only moderate- to high-alkali natural emeralds can be identified as natural on the basis of nonpolarized near-IR spectra in which type I absorption bands are absent.

Figure A-1. These nonpolarized infrared spectra of a Chinese hydrothermal synthetic emerald between 5000 and 5500 cm^{-1} were taken in a direction more or less perpendicular to the c-axis (A) and slightly oblique to the c-axis (B). They illustrate how the three main bands—at 5110, 5275, and 5450 cm^{-1}—can vary in intensity depending on the orientation of the sample.

Figure A-2. In these polarized infrared spectra of Chinese hydrothermal synthetic emeralds in the 5000–5500 cm^{-1} region, the band at 5275 cm^{-1} is seen only when the beam is polarized parallel to the c-axis, whereas the bands at 5110 and 5450 cm^{-1} are seen only in spectra polarized perpendicular to the c-axis.
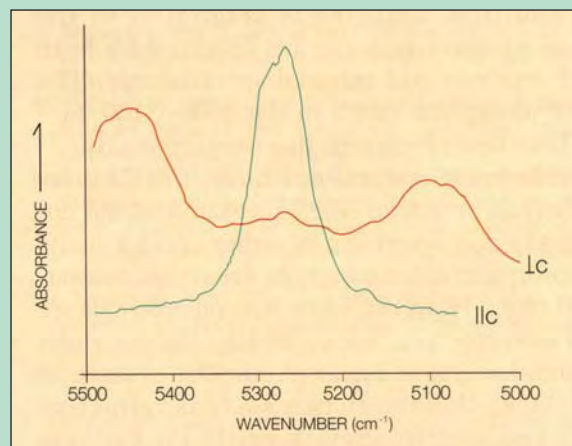
only chromium as the chromophore, but one specimen (sample B) also had small amounts of vanadium. The vanadium-containing specimen may represent the second type of earlier production described by the producer (see Background), but there was no iron present in the specimen we analyzed.

DIAGNOSTIC PROPERTIES

A new type of synthetic emerald is being produced in China by the hydrothermal method. Some of its characteristic properties, such as the use of natural or synthetic seeds, the orientation of seeds and growth planes, as well as a diagnostic chlorine content and the absence of alkalis, are consistent with those known for hydrothermal synthetic emeralds from other producers (e.g., Linde, Biron). Other characteristic features, such as the presence of tiny chrysoberyl crystals on the seeds, have only been identified in Biron hydrothermal synthetic emeralds (as described in this article).

Most of the samples examined revealed microscopic features of diagnostic value, including natu-

ral or synthetic seeds and a characteristic growth zoning parallel to the seed. The characteristic zoning forms an angle to the c-axis of the synthetic emerald, which can be determined easily with a horizontal microscope. This particular angle is diagnostic because no crystal faces of natural beryl are in this range—that is, between 20° and 40° to the c-axis. In addition, the irregular growth pattern characteristic of hydrothermal synthetic beryl was also found in some of the samples examined.

Spicules oriented parallel to the c-axis, commonly associated with tiny chrysoberyl or, rarely, beryl crystals at their widest ends are characteristic for Chinese hydrothermal synthetic emeralds and have not been reported in natural emeralds. The solid inclusions are related to the boundaries between the seed (natural colorless beryl or synthetic emerald) and the synthetic emerald. Needle-like tubes oriented almost perpendicular to the seed or to dominant growth faces are also characteristic for Chinese hydrothermal synthetic emeralds.

In addition, chlorine is diagnostic of the Chinese product and can be detected by both EDXRF analysis and infrared spectroscopy. The series of absorption bands in the 2500–3100 cm^{-1} region have never been seen in natural emeralds.

Unlike most natural emeralds, the Chinese hydrothermal synthetic emeralds examined did not contain any iron detectable by either EDXRF analysis or absorption spectroscopy in the visible to near-infrared range. However, some natural emeralds are almost iron-free and, consequently, do not show any iron absorption bands. A similar overlap of gemological characteristics such as refractive indices and specific gravity exists for Chinese hydrothermal synthetic emeralds and low-alkali natural emeralds from various localities.

REFERENCES

Aurisicchio C., Grubessi O., Zecchini P. (1994) Infrared spectroscopy and crystal chemistry of the beryl group. *Canadian Mineralogist*, Vol. 32, pp. 55–68.

Barton M.D. (1986) Phase equilibria and thermodynamic properties of minerals in the BeO-Al$_2$O$_3$-SiO$_2$-H$_2$O (BASH) system, with petrologic applications. *American Mineralogist*, Vol. 71, No. 3/4, pp. 277–300.

Brown G., Snow J. (1984) Inclusions in Biron synthetic emeralds. *Australian Gemmologist*, Vol. 15, No. 5, pp. 167–171.

Bukin G.V., Godovikov A.A., Klyakhin V.A., Sobolev V.S. (1986) Growth of emerald single crystals. *Growth of Crystals*, Vol. 13, pp. 251–260.

Delé-Dubois M.L., Dhamelincourt P., Poirot J.P., Schubnel H.-J. (1986a) Differentiation between natural gems and synthetic minerals by laser Raman micro-spectrometry. *Journal of Molecular Structure*, Vol. 143, pp. 135–138.

Delé-Dubois M.-L., Poirot J.-P., Schubnel H.-J. (1986b) Identification de micro-inclusions dans des rubis et émeraudes de synthèse par spectroscopie Raman. *Revue de Gemmologie*, No. 88, pp. 15–17.

Flamini A., Gastaldi L., Grubessi O., Viticoli S. (1983) Contributo della spettroscopia ottica ed EPR alla distinzione tra smeraldi naturali e sintetici. *La Gemmologia*, Vol. 9, No. 1/2, pp. 6–11.

Flanigen E.M. (1971) Hydrothermal process for growing crystals having the structure of beryl in an alkaline halide medium. United States Patent No. 3,567,642; March 2.

Flanigen E.M., Breck D.W., Mumbach N.R., Taylor A.M. (1965) New hydrothermal emerald. *Gems & Gemology*, Vol. 11, No. 9, pp. 259–264, 286.

Flanigen E.M., Breck D.W., Mumbach N.R., Taylor A.M. (1967) Characteristics of synthetic emeralds. *American Mineralogist*, Vol. 52, No. 5/6, pp. 744–772.

Franz G., Morteani G. (1981) The system BeO-Al$_2$O$_3$-SiO$_2$-H$_2$O: Hydrothermal investigation of the stability of beryl and euclase in the range from 1 to 6 kb and 400 to 800°C. *Neues Jahrbuch für Mineralogie Abhandlungen*, Vol. 140, No. 3, pp. 273–299.

Fritsch E. (1996) Chinese synthetics: The anonymous crowd. *Jewelers' Circular-Keystone*, Vol. 167, No. 3, pp. 51–52.

Fritsch E., Muhlmeister S., Birkner A. (1992) A preliminary study of the Biron synthetic pink titanium-beryl. *Australian Gemmologist*, Vol. 18, No. 3, pp. 81–82.

Galia W. (1972) Diagnostische Merkmale Synthetischer smaragde von Linde. *Zeitschrift der Deutschen Gemmologischen Gesellschaft*, Vol. 21, No. 2, pp. 112–117.

Geng G.L., Ou-Yang C.M. (1995) How to indentify hydrothermal synthetic emerald from China. *Jewellery News Asia*, No. 130, p. 92, 94.

Gübelin E. (1986) Die diagnostischen Eigenschaften der neuesten Synthesen. *Goldschmiede und Uhrmacher Zeitung*, Vol. 84,

No. 11, pp. 69–76.

Hänni H.A. (1993) Hydrothermalsynthesen aus Australien: smaragd und rosaberyll. *Swiss Jewelry and Watchmaker Journal*, April 1993, pp. 45–48.

Hänni H.A., Kiefert L. (1994) AGEE hydrothermal synthetic emeralds. *JewelSiam*, Vol. 5, No. 5, pp. 80–85.

Hänni H.A., Kiefert L., Chalain J.-P., Wilcock I.C. (1996) Ein Renishaw Raman Mikroskop im gemmologischen Labor: Erste Erfahrungen bei der Anwendung. *Zeitschrift der Deutschen Gemmologischen Gesellschaft*, Vol. 45, No. 2, pp. 55–69.

Hänni H.A., Kiefert L., Chalain J.-P., Wilcock I.C. (1997) A Raman microscope in the gemmological laboratory: First experiences of application. *Journal of Gemmology*, Vol. 25, No. 6, pp. 394–406.

Henn U., Lind T., Bank H. (1988) Hydrothermal grown synthetic emeralds from USSR. *Canadian Gemmologist*, Vol. 9, No. 3, pp. 66–72.

Hosaka M. (1990) Hydrothermal growth of gem stones and their characterization. *Progress of Crystal Growth and Characterization*, Vol. 21, pp. 71–96.

Kane R.E., Liddicoat R.T. Jr. (1985) The Biron hydrothermal synthetic emerald. *Gems & Gemology*, Vol. 21, No. 3, pp. 156–170.

Kiefert L., Schmetzer K. (1991) The microscopic determination of structural properties for the characterization of optical uniaxial natural and synthetic gemstones. Part 1: General considerations and description of the methods. *Journal of Gemmology*, Vol. 22, No. 6, pp. 344–354.

Klyakhin V.A., Lebedev A.S., Il'in A.G., Solntsev V.P. (1981) Growing of hydrothermal beryl (in Russian). In *Sintez i Vyrashchivanie Optich*. Kristallov i Yuvelir. Kamnei, Novosibirsk, pp. 45–66.

Kodaira K., Iwase A., Tsunashima A., Matsushita T. (1982) High-pressure hydrothermal synthesis of beryl crystals. *Journal of Crystal Growth*, Vol. 60, pp. 172–174.

Koivula J.I., Kammerling R.C., DeGhionno D., Reinitz I., Fritsch E., Johnson M.L. (1996) Gemological investigation of a new type of Russian hydrothermal synthetic emerald. *Gems & Gemology*, Vol. 32, No. 1, pp. 32–39.

Lebedev A.S., Askhabov A.M. (1984) Regeneration of beryl crystals (in Russian). *Zapiski Vsesoyoznogo Mineralogicheskogo Obshchestva*, Vol. 113, No. 5, pp. 618–628.

Lebedev A.S., Il'in A.G., Klyakhin V.A. (1986) Hydrothermally grown beryls of gem quality (in Russian). In *Morphology and Phase Equilibria of Minerals. Proceedings of the 13th General Meeting of the International Mineralogical Association, Varna 1982*, Vol. 2, Sofia, Bulgaria, pp. 403–411.

Leung C.S., Merigoux H., Poirot J.P., Zecchini P. (1986) Use of infrared spectrometry in gemmology. In *Morphology and Phase Equilibria of Minerals. Proceedings of the 13th General Meeting of the International Mineralogical Association, Varna 1982*, Vol. 2, Sofia, Bulgaria, pp. 441–448.

Nassau K. (1976) Synthetic emerald: The confusing history and the current technologies. *Journal of Crystal Growth*, Vol. 35, pp. 211–222.

Nassau K. (1978) Did Professor Nacken ever grow hydrothermal emerald? *Journal of Gemmology*, Vol. 16, No. 1, pp. 36–49.

Nassau K., Nassau J. (1980) The growth of synthetic and imitation gems. In Freyhart H.C., Ed., *Crystals: Growth Properties and Applications*, Vol. 2, Springer, Berlin, pp. 1–50.

Nikol'skaya L.V., Samoilovich M.I. (1979) Optical absorption spectra of beryls in the near infrared (900–2500 nm). *Soviet Physics-Crystallography*, Vol. 24, No. 5, pp. 604–606.

Pough F.H. (1965) A new hydrothermal synthetic emerald. *Journal of Gemmology*, Vol. 9, No. 12, pp. 426–433.

Schmetzer K. (1986) An improved sample holder and its use in the distinction of natural and synthetic ruby as well as natural and synthetic amethyst. *Journal of Gemmology*, Vol. 20, No. 1, pp. 20–33.

Schmetzer K. (1988) Characterization of Russian hydrothermally grown synthetic emeralds. *Journal of Gemmology*, Vol. 21, No. 3, pp. 145–164.

Schmetzer K. (1989) Types of water in natural and synthetic emerald. *Neues Jahrbuch für Mineralogie Monatshefte*, Vol. 1989, No. 1, pp. 15–26.

Schmetzer K. (1990) Two remarkable Lechleitner synthetic emeralds. *Journal of Gemmology*, Vol. 22, No. 1, pp. 20–32.

Schmetzer K. (1996) Growth method and growth-related properties of a new type of Russian hydrothermal synthetic emerald. *Gems & Gemology*, Vol. 32, No. 1, pp. 40–43.

Schmetzer K., Kiefert L. (1990) Water in beryl: A contribution to the separability of natural and synthetic emeralds by infrared spectroscopy. *Journal of Gemmology*, Vol. 22, No. 4, pp. 215–223.

Schrader H.-W. (1983) Contributions to the study of the distinction of natural and synthetic emeralds. *Journal of Gemmology*, Vol. 18, No. 6, pp. 530–543.

Sechos B. (1997) Identifying characteristics of hydrothermal synthetics. *Australian Gemmologist*, Vol. 19, No. 9, pp. 383–388.

Sosso F., Piacenza B. (1995) Russian hydrothermal synthetic emeralds: Characterization of the inclusions. *Journal of Gemmology*, Vol. 24, No. 7, pp. 501–507.

Stockton C.M. (1987) The separation of natural from synthetic emeralds by infrared spectroscopy. *Gems & Gemology*, Vol. 23, No. 2, pp. 96–99.

Sunagawa I. (1982) Gem materials, natural and artificial. In Kaldis E., Ed., *Current Topics in Materials Science*. Vol. 10, North-Holland Publishing Company, Amsterdam, pp. 353–497.

Wood D.L., Nassau K. (1967) Infrared spectra of foreign molecules in beryl. *Journal of Chemical Physics*, Vol. 47, No. 7, pp. 2220–2228.

Wood D.L., Nassau K. (1968) The characterization of beryl and emerald by visible and infrared absorption spectroscopy. *American Mineralogist*, Vol. 53, No. 5/6, pp. 777–800.

AQUAMARINE, Unheated Carving

Aquamarine is usually heat treated at a low temperature to change its inherent green-to-blue color to one that is predominantly blue (see Lab Notes, Spring 1997, p. 58, and references therein). On rare occasions, however, we receive predominantly green aquamarine for testing. Such occasions always spur us to question whether the material is unheated, a substantial gemological challenge because there are few differences in the properties of natural-color and heat-treated aquamarine.

The carving shown in figure 1, seen last fall in the East Coast Gem Trade Laboratory, is a gemologically interesting (and visually attractive, with its fish-and-sea motif) example of untreated aquamarine. Although the curved surface made it impossible to obtain a clear refractive index, we saw a uniaxial optic figure with the polariscope. The carving showed vit-reous luster, and testing in an inconspicuous spot revealed a hardness greater than 7 on the Mohs scale. It was inert to both long- and short-wave ultraviolet radiation. With magnification, we saw sparse crystals and fractures, as well as intact two-phase inclusions. These properties suggested that the object was aquamarine, and the color and inclusions pointed to unheated material, but further testing was required to confirm this identification.

Using a desk-model spectroscope, we saw an unexpected, rather strong, narrow absorption band at 537 nm, in addition to the strong line at 427 nm that is normally present in aquamarine and the weaker one at 456 nm that is often visible. A check of the literature changed this observation from a source of concern to one of confirmation. In the several editions of Webster's *Gems* (e.g., 4th ed., Butterworth, London, 1983, p. 119), it is reported that this 537 nm line is seen only in untreated aquamarines and in yellow and colorless beryls. Because we observed the spectrum through a large thickness of material, this usually weak absorption line showed up quite strongly.

GRC and TM

Figure 1. The predominantly green color and diagnostic absorption spectrum of this aquamarine carving, which measures approximately 16.0 × 11.0 × 9.0 cm, indicates that the material was not heat treated, unlike most aquamarine seen in the trade.

BERYL,
Treated Color

Last fall, the East Coast lab was asked to identify the 16.40 ct violetish blue cushion-shaped stone shown in figure 2, which was being sold as a tanzanite simulant. The stone had the color appearance of tanzanite, for which there are several simulants, but ultimately we proved it to be a new twist on an old treatment of a different gem mineral. A uniaxial optic figure was seen easily, with the axis making an angle of about 30° to a line from the culet through the center of the table. We measured refractive indices of 1.575 and 1.580, and we obtained a specific gravity of 2.74 using the DiaMension noncontact measuring system. These three properties indicate the mineral beryl, which is known to occur in many colors.

Most colors of beryl are referred to by their own gem variety name, such as emerald (saturated green), aquamarine (pale to medium dark bluish green to blue), and morganite (pink). Dark blue beryl was found in the Maxixe mine of Minas Gerais, Brazil, in 1917. However, interest in the material waned when it was discovered that the color faded with exposure to light. Decades later, in

Figure 2. This 16.40 ct highly saturated treated-color violetish blue beryl was being sold as a tanzanite simulant. Unfortunately, this color in beryl is unstable to light and heat.

the late 1960s, it was found that irradiation with X-rays, gamma rays, or neutrons could produce a strong dark blue color in some near-colorless or pale yellow, pink, or blue beryls. Consequently, gemological interest in this color of beryl was revived (see K. Nassau and D. L. Wood, "Examination of Maxixe-type Blue and Green Beryl," *Gems & Gemology*, Spring 1973, pp. 130–133, and references therein). At that time, treated-color dark blue beryl was offered in the trade as aquamarine, or more rarely as sapphire (Winter 1972/73 Lab Notes, p. 111). Nassau, Prescott, and Wood compared some of the original Maxixe material (which had been kept in the dark over the decades) with some of the new, treated material and some natural-color aquamarine. They identified three properties unique to all dark blue beryl ("The Deep Blue Maxixe-Type Color Center in Beryl," *American Mineralogist*, Vol. 61, 1976, pp. 100–107).

The stone we examined at the East Coast lab clearly exhibited two of the three properties described in the 1976 article: (1) strong pleochroism, with blue seen along the ordinary ray (looking parallel to the optic axis) and light brown along the extraordinary ray (looking perpendicular to the optic axis); and (2) six sharp, closely spaced lines in the visible spectrum, as viewed with a desk-model spectroscope, across the orange and red wavelengths from 575 to 690 nm. In contrast, aquamarine shows a blue pleochroic color along the extraordinary ray, and one or more "iron" lines in the blue region of the spectrum.

The third distinctive property of dark blue beryl is that stones cut from either the original natural material or treated-color dark blue beryl fade readily on exposure to mild heat or strong light. Nassau and co-authors found that one week of exposure to a 100 watt light bulb at a distance of 6 inches (15 cm) diminished the blue color by at least 50%, and that heating to 235°C removed any remaining blue color. The color can be restored

by irradiation. Although we did not test our stone for this third property, we did add a comment on the report stating that this color in beryl is not stable.   *IR and TM*

DIAMOND

Acting as a Heat Sink

In addition to being an important gem material, diamond has many industrial applications, and occasionally we see manifestations of diamond's physical properties in the Gem Trade Laboratory. One property that is used to distinguish diamond from most of its imitations is that of thermal conductivity: Heat is rapidly transferred from one side of a diamond to the other, and diamond is more efficient at transferring heat than any other material. Because of this property, blocks of either synthetic or natural diamond are used as "heat sinks" in some electronic circuit boards, transferring heat away from components that generate it, thereby cooling down the hot component and its local area. Faceted diamonds also conduct heat rapidly; otherwise, jewelers would have to take far more precautions when working on diamond-set jewelry. In general, however, this property is taken for granted in the gem trade.

A 2.40 ct round brilliant that came into the West Coast laboratory this summer served as a reminder that diamonds should never be taken for granted. The diamond was stored in GTL's standard transparent plastic box with its pavilion sunk into dark gray plastic foam. When the preliminary grader went to examine the diamond, he saw that the box had warped around the table of the diamond (figure 3). The box label, which was made from a piece of thermally activated paper (similar to thermal facsimile-printer paper), had discolored locally in the area near the stone. The inside surface of the lid showed a perfect impression of the diamond's table and adjacent facets (figure 4). The diamond itself had typical proportions and color, and was not "hot"

Figure 3. This 2.40 ct round brilliant diamond melted the lid of the plastic box in which it was held and discolored a piece of thermal paper nearby, shown here at the bottom.

Figure 4. The inside surface of the plastic lid shown in figure 3 carried an impression of the 5.56 mm table of the diamond that had transferred heat to it.

to the touch; nor did it demonstrate any radioactivity when tested with a handheld Geiger counter. So another explanation was required for the "meltdown."

We believe that the following scenario accounts for the deformation of the plastic box: Evidently, the box had been on top of the grader's stack of work items, directly in the beam of a high-intensity Tensor desk lamp, at a close distance. The dark plastic foam absorbed radiation from the Tensor lamp and grew hot. The diamond transferred this heat to the lid of the box, which melted locally; however, the stone itself was not damaged by this event.   *MLJ*

Fracture-Filled Pink Diamond

A 1.39 ct square-emerald-cut diamond that we saw numerous times over the last year (both before and after several fracture-filling treatments) gave us a new perspective on the difference in color as well as clarity that such treatment can produce. Before filling, this emerald-cut stone showed a saturated pink color that was somewhat obscured by the abundant fractures, which created a white appearance across a large portion of the crown (figure 5, left). The pink graining and 415 nm line seen with a desk-model spectroscope unit proved that the color was natural, and in this state (before treatment) the stone

Figure 5. The many white fractures in this 1.39 ct Fancy Intense Pink emerald-cut diamond (left) detract from the color. After the diamond was subjected to several episodes of fracture filling, most of the fractures appeared to be transparent and the stone revealed a highly saturated pink color in the face-up color-grading position (right). However, now that the diamond has been treated, the Gem Trade Laboratory can no longer issue a color grade for it.

received a grade of Fancy Intense Pink.

Because there were many fractures of different thicknesses, some of which were interconnected, it took several treatments to produce the desired effect. Although the clarity of the diamond after treatment was not significantly improved, the color appearance was much better (figure 5, right). The fracture-filling procedure made most of the fractures appear transparent rather than white, allowing the inherent color to show more fully when the stone was viewed in the face-up position. (As we have stated many times in the past, however, the GIA Gem Trade Laboratory does not offer grading services for clarity-enhanced diamonds, so no new color grade was issued.)

The durability of diamonds that have undergone fracture-filling treatment is a continuing concern to many in the trade, and this diamond also provided one example in that regard. Like many other pink diamonds, this one showed strong anomalous birefringence with high-order colors, an indication of high levels of strain within the original crystal. As mentioned previously, the treatment process was repeated several times to achieve the final result. Although the fracture-filling process involves heat and some changes in pressure (as discussed in R. C. Kammerling et al., "An Update on Filled Diamonds: Identification and Durability," *Gems & Gemology*, Fall 1994, pp. 142–177), this particular diamond survived the treatment intact.

IR

Mysteriously Fractured Diamonds

Occasionally, clients ask us whether fractures can appear in diamonds spontaneously, without any apparent cause. Typically, they report that a diamond of documented clarity is stored under ordinary conditions in a safe with other diamonds, and sometime later it is observed to be substantially fractured. The 2.93 ct crystal and the 0.73 ct polished round brilliant shown in figure 6 were loaned to

the East Coast laboratory by a client who made this very claim. Both diamonds showed large eye-visible fractures and cleavages. The cut stone had no polishing drag lines emanating from the fractures where they reached the surface, which indicates that the fracturing occurred subsequent to the last polishing. Further examination with magnification did not reveal any kind of surface trauma, as often occurs if the diamond is subjected to some kind of blow. These observations support the client's claim that the fracturing was recent, but they do not eliminate the possibility that the stone was damaged from exposure to stress during setting or another circumstance.

The case of the crystal is even more perplexing, since it had not undergone any manufacturing and probably had never been exposed to any jewelry-setting procedure. On the basis of the available information, we can only surmise that both diamonds were highly strained and that the fracturing was spontaneous. Examination of both stones between crossed polarizing filters showed moderate strain but no high-order interference colors. It is possible that some of the strain was relieved when the fracturing occurred. Although we are not certain exactly what happened to these diamonds, this is the first time we have been able to examine two stones that appear to have fractured spontaneously. We have not yet been able to document such an occurrence firsthand, but we have found one reference in the literature supporting this possibility (see Yu Orlov, *Mineralogy of the Diamond*, John Wiley & Sons, New York, 1977, p. 140). Perhaps one of our readers has had a similar experience and can provide further insight into this conundrum. *TM and GRC*

Figure 6. The owner of these two diamonds, a 2.93 ct crystal and a 0.73 ct round brilliant cut diamonds, hoped that GTL could explain why the stones had apparently fractured spontaneously during routine storage.

GARNET,
A Very Dark Pyrope-Almandite Identified by Raman Spectroscopy

A ring mounted with a large, very dark red oval cabochon was submit-

ted to the West Coast lab for identification. We were able to determine some gem properties on the mounted stone, that is, that it was singly refractive, with a spot R.I. of 1.75, and was inert to both long- and short-wave UV radiation. Because this information was not sufficient to identify the piece, we advised the client that the stone would have to be unmounted.

The loose cabochon measured 21.12 × 16.22 × 11.33 mm and weighed 38.92 ct. Although quite dark, the material was transparent; nevertheless, most of the light entering the stone was absorbed by it, and the absorption spectrum revealed by the spectroscope showed only a narrow transmission region in the red. The specific gravity was 3.76 (measured hydrostatically). When the cabochon was immersed in methylene iodide and viewed with direct transmitted light and magnification., straight parallel bands were visible through the side of the piece.

At this point, we had two possible candidates for the identity of this material: a very dark garnet or a high-refractive-index glass. Five minutes with GIA's new Renishaw Raman spectrometer answered our identification question: the Raman spectrum—with peaks at 360, 560, and 919 cm^{-1}—matched that of pyrope-almandite

garnet (and not glass), as confirmed by comparison with reference samples in our collection as well as with two compendia of spectra (a library file that comes with the Raman spectrometer, and "Utilité de la Microsonde Raman pour l'Identification non Destructive des Gemmes," by M. Pinet et al., *Revue de Gemmologie*, June 1992, pp. 12–60). The color and R.I. of this garnet were also consistent with pyrope-almandite.

To confirm the Raman results, we also analyzed the cabochon using energy-dispersive X-ray fluorescence (EDXRF), which showed elements consistent with pyrope-almandite (and no heavy elements such as lead, bismuth, or gold which might be found in a glass with such a high R.I.). Nor did the infrared spectrum match any of the spectra of glasses that we had on file. We therefore concluded that the cabochon was pyrope-almandite garnet.

MLJ, SFM, and JIK

Figure 7. The lenses in these unusual sunglasses were fashioned from synthetic sapphire. They measure 32.77 mm in diameter and 3.50 and 3.90 mm thick.

SYNTHETIC SAPPHIRE, Sunglasses

The sunglasses shown in figure 7 represent one of the more unusual uses for a gem material that we have ever seen. Created for British rock star Elton John, the glasses were submitted to the East Coast laboratory by the manufacturer of the lens material for a report to identify the material and document the item.

The blue color and the refractive indices of 1.76 and 1.77 indicated sapphire. Examination between crossed polarizing filters showed a uniaxial flash figure (as described in Wm. R. Phillips, *Mineral Optics: Principles and Techniques*, W. H. Freeman and Co., San Francisco, 1971), which indicates that the optic axis lies in the plane of the lens. Such an orientation allows for easy observation of dichroism—in this case, blue and blue-green—over polarized light (without a dichroscope). The lenses were inert to long-wave UV radiation, and fluo-

resced a weak, chalky green to short-wave UV. These latter two properties proved that the material was synthetic sapphire.

The client shared with us some details on the growth of the synthetic sapphire and manufacture of these lenses. The proprietary growth method is carefully controlled to minimize the stress across the growing crystal, producing large areas of synthetic corundum that are free from any inclusions and show no color variations or growth lines (curved striae). To choose a specific area optically suitable for lenses, the manufacturer examined a section of the rough material while it was immersed in oil to reduce light scattering at the as-grown surface. Next, two slabs were sawn from adjacent areas of the rough and with the same optical orientation. They weighed a total of 194 grams (970 ct). A core drill and carborundum slurry were used to cut circles (lens blanks) from the slabs, and parallel faces were ground on the blanks with a steel lapidary wheel that was charged with the slurry.

These parallel-sided rounds were then polished with diamond abrasives of successively finer grade (smaller particles) over a period of about a month. The final polish was done at an aerospace company, by a specialist in the machining of hard materials, to achieve high optical quality.

From the dimensions of 32.77 mm in diameter and 3.50 and 3.90 mm thickness for the two lenses, we estimated finished weights of 59.05 and 65.80 ct, respectively. The hand-made frames are sterling silver, and have been engraved with the first name of the silversmith, Behrle Hubbuch III. Because of the way these lenses are oriented, they function well as polarizing sunglasses. However, the combined weight of the lens material and the frame might limit the length of time that they could be worn comfortably. *IR*

THE 26TH INTERNATIONAL GEMMOLOGICAL CONFERENCE

On the occasion of its 500-year anniversary as a world leader in the gem-cutting industry, Idar-Oberstein, Germany, was a fitting site for the 26th International Gemmological Conference. The anniversary was commemorated by the German government through the issuance of an official postage stamp (figure 1).

In 1497 the gemstone industry in and around the towns of Idar and Oberstein was mainly concerned with the cutting of agate and other types of chalcedony. Today a wide variety of gem materials are cut in the Idar-Oberstein region. The area further prides itself on its role as a center for various kinds of training and commerce related to all types of gemstones, including diamonds. The region is home to the German Gemmological Institute, German Gemmological Association, German Foundation for Gemstone Research, German Gemstone Museum, the Diamonds and Gemstone Bourse, the Intergem trade fair, and numerous internationally acclaimed gem cutters and goldsmiths. A detailed history of Idar-Oberstein as a gem center has been published by Dr. Hermann Bank ("500 Jahre Edelsteinregion Idar-Oberstein [1497–1997]," *Zeitschrift der Deutschen Gemmologischen Gesellschaft*, Vol. 43, No. 3, pp. 129–152, 1997).

The first International Gemmological Conference was organized by Professor Karl Schlossmacher and Dr. Edward J. Gübelin in 1952. It has since become a biennial event, to which laboratory gemologists and gemological researchers from around the world are invited to present their latest discoveries.

This, the 26th IGC, was organized by Dr. Hermann Bank and Gerhard Becker, with assistance from Drs. Ulrich Henn and Claudio Milisenda, of the German Gemmological Association and German Foundation for Gemstone Research, and Dr. Jan Kanis of Veitsrodt, Germany. The conference took place from September 27 to October 3 and was attended by 50 official delegates from 24 countries. A total of 44 papers were presented. We are pleased to present abstracts from several of these presentations.

This section was prepared by Gem News editor John I. Koivula with the assistance of IGC participants Dr. Alfred A. Levinson and Michael E. Gray. Given space limitations, not all of the selected abstracts could be presented in this issue; some will appear in the Spring 1998 Gem News section.

DIAMONDS

Cathodoluminescence of yellow diamonds. Up to now, determination of "diamond type" has been based on spectroscopy. Junko Shida, of the Gemmological Association of All Japan, showed how cathodoluminescence can be used to classify yellow diamonds.

Diamonds are classified into the four main types (Ia, Ib, IIa, and IIb) based on their nitrogen contents; yellow diamonds are typically type Ia or Ib. However, mixed type diamonds (e.g., Ia + Ib + IIa) are well known. Substitution of elements other than nitrogen (e.g., hydrogen) also affects the properties of diamond, but these substitutions are not addressed in this classification system.

Ms. Shida described how, by interpreting zonal or sector structures and other features discernible by cathodoluminescence, one can distinguish various types of yellow diamonds (natural or synthetic), as follows:

- Type Ia ("cape" series): Blue and yellow zoned fluorescence.

- Type Ia (hydrogen rich): Irregular patchy blue and slightly chalky yellow fluorescence.
- Type Ib: Yellow, yellowish green, and orange-1yellow fluorescence; fine lines due to plastic deformation in the direction of octahedral faces are also seen.
- Mixed type: Irregular patchy fluorescence of various colors.
- Irradiated diamonds (type not specified): Chalky blue and dull yellow fluorescence.
- Synthetic (type Ib): Different colors of fluorescence in every crystallographically distinct sector.

Diamond inclusions in corundum. Using laser Raman microspectrometry, George Bosshart of the Gübelin Gemmological Laboratory in Lucerne, Switzerland, has identified inclusions of diamond with graphite in sapphires from Ban Huai Sai, Laos. Diamonds and corundum have been found in the same secondary deposits, such as the sapphire-rich alluvial deposits of New South Wales, Australia. However, recognition of the coexistence of these two minerals as inclusions within one another is both relatively recent and rare.

An inclusion of ruby in diamond was first reported in 1981 (sample locality unknown) by Meyer and Gübelin (*Gems & Gemology*, Vol. 17, No. 2, pp. 153–156), and later by Watt (*Mineralogical Magazine*, Vol. 58, 1994, pp. 490–493) from Brazil. The reverse association—diamond inclusions in corundum—is a more recent discovery, as it was reported first by Dao et al. (*Comptes Rendus de la Academie de Science, Paris*, Vol. 322, No. IIb, pp. 515–522) only in early 1996. In this case, diamond inclusions accompanied by graphite and lonsdaleite (also a high-pressure polymorph of carbon) were identified in seven rubies from Vietnam. Later in 1996, Dr. I. Wilcock and G. Bosshart tentatively identified minute diamond inclusions (accompanied by graphite

only) in two sapphires from Laos by Raman analysis.

The diamond inclusions in Ban Huai Sai sapphires are particularly important because the coexistence of diamond and corundum in the most significant primary diamond source rocks—deep-seated (peridotitic) ultramafic rocks—is considered unlikely, although theoretically possible. Diamond and corundum have been found in the same metamorphic (eclogitic) rocks on several continents. Knowledge of the conditions of coexistence of these phases (i.e., mechanisms by which the necessary temperature and pressure were obtained), and thus the likely geologic situation that accounts for their formation (e.g., metamorphic or igneous origin), should be forthcoming as newer analytical techniques become available.

The diamond pipeline into the third millennium. This two-part paper was presented by Menahem Sevdermish of Israel and Dr. Alfred A. Levinson of the University of Calgary, Alberta, Canada. In part 1, Mr. Sevdermish explained that De Beers's single-channel diamond marketing pipeline, which had been operative since the mid-1930s, is now obsolete. He suggested that it has been replaced by a pipeline that consists of three marketing channels: (1) the traditional channel for high-valued gem-quality diamonds, for which De Beers continues to maintain stability; (2) a channel based on small, low-quality diamonds cut in India; and (3) the Russian channel, which began to evolve in the early 1990s, but is as yet of undetermined status and potential. Each of the above channels operates—or is capable of operating—essentially independently, and each has its own organizational and distribution system. Mr. Sevdermish emphasized the role that small, Indian-cut diamonds play in the trade and how these have facilitated the creation of a homogenized mass market for inexpensive diamond jewelry, particularly in the United States.

In part 2, Dr. Levinson expanded on the modern dia-

Figure 1. This complete sheet of postage stamps was issued in 1997 by Germany to commemorate 500 years of gem cutting in the Idar-Oberstein region. Notice the various gemstone cuts depicted on the upper and lower margins of the sheet. Photo by Maha DeMaggio.

mond-cutting industry of India and its position in the world diamond trade. Using statistics on the world production of rough, Indian import data on rough, and export data on polished diamonds, he traced the evolution of the modern Indian cutting industry from its inception in the early 1960s to the present. In 1996, India accounted for about 70% of the world's polished diamonds by weight and 40% by value. Calculations show that Indian cutters now produce about 800 million polished diamonds annually (about 8 out of 10 polished in the world), the vast majority of which are less than 0.03 ct (3 points). These small, generally low quality stones have spawned a new segment of the diamond jewelry market, which is readily affordable and amenable to mass marketing. Presently, about 50% of world retail diamond jewelry sales by value—and perhaps 75% by number of pieces—are based on diamonds cut in India. Approximately 700,000 people cut diamonds in India, but only about 200,000 do so full-time.

Mineral inclusions in large Yakutian diamond crystals. Representing the Institute of Mineralogy and Petrography in Novosibirsk, Russia, Dr. Nikolai Sobolev presented results of a study conducted with E. S. Yefimova and O. V. Sukhodolskaya on the mineral inclusions in a special collection of large (>10 ct) diamonds from the three major Yakutian mines: Mir, Udachnaya, and Aikhal. Nearly all of the 2,334 specimens studied were sharp-edged octahedral crystals typical of Yakutian diamonds.

Sulfides, olivine, and chromite are the major mineral inclusions in the diamonds from these three mines; however, the proportion of each varies from mine to mine. Sulfide inclusions dominate in diamonds from Mir, whereas olivine and chromite dominate in diamonds from Udachnaya and Aikhal. Peridotitic inclusions (fig-

Figure 2. Pyrope (red) and chrome diopside (green) are among the peridotitic inclusions identified in Yakutian diamonds. Photomicrograph by John I. Koivula; magnified 15×.
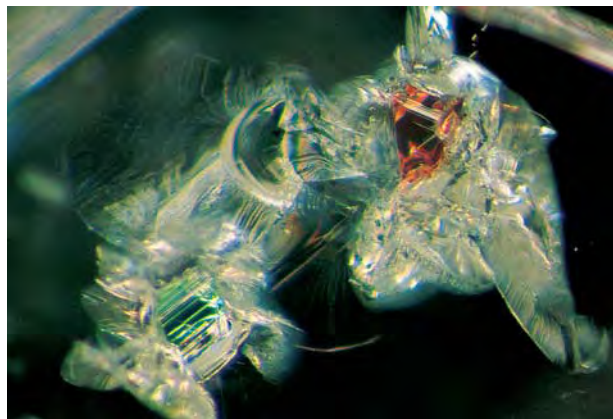
ure 2) were found to be far more common than eclogitic inclusions (the latter were identified in about 3%–14% of the diamonds from the various mines), confirming the dominant influence of peridotites (particularly harzburgite) in the formation of diamonds from this locality.

The morphology of natural gem diamond. Dr. Emmanuel Fritsch, of the University of Nantes, France, gave a status report on a study of the morphology of natural gem diamonds that he conducted with M. Moore and Dr. B. Lasnier. Although the morphology of natural diamonds has been studied for centuries, new analytical techniques and advances in our knowledge of crystal growth justify a revisit of this subject. Such studies are applicable to diamond faceting, the interpretation of diamond formation, and the differentiation of natural from synthetic diamonds. Dr. Fritsch reported that three growth morphologies are typical for natural diamonds: octahedral, cuboid, and fibrous.

Octahedral growth is common for most natural gem diamonds; such diamonds formed under conditions of low supersaturation of carbon. However, perfect octahedra are rare (most of those that are found come from the mines of Yakutia, Russia). Most octahedral diamonds are partially dissolved (etched) by kimberlite magma. Dissolution of the octahedral edges results in crystals that *look* like rounded rhombic dodecahedra. *Cuboid growth* does not mean growth of cube faces; rather, it refers to growth by undulating surfaces, each having a mean orientation corresponding to a cubic face. This type of growth is poorly understood, and only a portion of such a crystal is ever of gem quality. *Fibrous growth* forms opaque aggregates, and is the result of supersaturation of carbon and/or the presence of numerous inclusions that prevent the formation of octahedral faces. Fibrous growth never yields gem-quality material, but it can form overgrowths on gem diamonds (i.e., "coated crystals"). It is interesting that many large, valuable, nitrogen-free (type II) diamonds do not show any particular shape, for reasons that are still unknown.

All of the basic growth morphologies can be modified by various processes including dissolution, twinning, cleavage, fracture, and deformation. Thus, unusual shapes can result, such as that shown in figure 3. Note that perfect cubes and dodecahedra, composed of flat faces, do not exist in natural gem diamonds even though they may be depicted in idealized drawings in some reference books.

COLORED STONES AND INORGANIC MATERIALS

Identification of amber by laser Raman microspectroscopy. Thye Sun Tay, of the Far East Gemmological Laboratory in Singapore, discussed the results of a study conducted with Z. X. Shen, S. L. Yee, L. Qin, and S. H. Tang on the separation of amber from its various imitations, specifically more recent natural resins such as

Figure 3. This 0.60 ct slightly etched natural cleavage of a cuboid diamond from the Jwaneng mine, Botswana, shows the "skeletal" appearance that is sometimes formed during cuboid diamond growth. Courtesy of the Diamond Trading Company Research Center, Maidenhead, England; photo by John I. Koivula.

copal. Tay and his colleagues used a Renishaw Micro-Raman spectroscopy system with a near-infrared [782 nm] laser to help eliminate fluorescence problems encountered with lasers that operate in the visible-light region. They found the extended continuous scan feature of the Renishaw system useful to enhance weak Raman peaks, since peak strength and position are important for differentiating amber from amber-like substances.

New Zealand 'Kauri Gum.' Following a visit to the Otamatea Kauri Museum, North Island, New Zealand, Professor Herbert S. Pienaar, of the University of Stellenbosch in South Africa, reexamined the natural fossil exudate from the Kauri conifer, *Agathis australis*, known as "Kauri gum." In terms of polymerization and degree of solubility in methanol, this substance can be regarded as being either copal or amber, depending on its geologic age; amber is at least Middle Tertiary, while copal is younger.

To botanists, a gum is a water-soluble colloidal polysaccharide of plant origin (such as gum arabic), that becomes gelatinous when moist, but hardens on drying. Since "Kauri Gum" does not absorb water in this fashion, perhaps it should be referred to as "Kauri resin."

Inclusion-related fluorescence zoning in amber. Gem News editor John Koivula showed a series of slides illustrating distinctly zoned ultraviolet fluorescence patterns surrounding the legs of an arthropod within amber that appeared to be the remains of a whip scorpion (figure 4). This type of zoned fluorescence has been observed in several samples of natural amber containing fauna inclusions. It is most easily seen at and near the surface of the amber, immediately surrounding inclusions that have been cut through during lapidary treatment. The fluorescence patterning is probably the result of a chemical reaction between the amber resin and the animal. As this type of fluorescence has not been observed in any amber substitute or imitation, the reaction probably takes place over an extended period of time during the fossilization process. As such, when it is detected, inclusion-related zoned fluorescence is an indicator of natural origin.

New chrysoberyl deposits in India. Dr. Jayshree Panjikar, of the Gemmological Institute of India, Bombay, drew from research conducted with K. T. Ramchandran in her report on three new deposits of chrysoberyl that were discovered almost simultaneously in 1996, in the states of Madhya Pradesh, Orissa, and Andhra Pradesh, near the
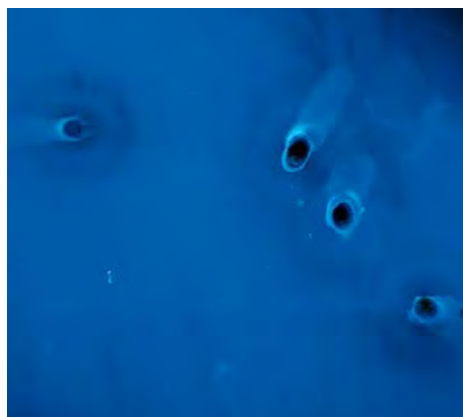

Figure 4. The legs of what appeared to be a whip scorpion are exposed on the surface of this piece of amber (left). The ultraviolet fluorescence of the host amber is visibly zoned around the legs of the arthropod where they reach the surface (right). Photomicrographs by John I. Koivula; magnified 10×.

eastern coast of India. Geologically, this entire region consists mostly of Precambrian age garnet-sillimanite and garnet-biotite gneisses. Chrysoberyl is found within cross-cutting pegmatites or along their contact zones, and also in gravels derived from weathering of the pegmatites. Alexandrite, yellow chrysoberyl, and cat's-eye chrysoberyl have been recovered. Alexandrite is typically found in the contact zones, yellow chrysoberyl occurs within the pegmatites, and the cat's-eye variety occurs is scattered throughout the pegmatites.

Alexandrite with a moderate to intense color change has been found at Deobhog in the Raipur district of Madhya Pradesh; yellow chrysoberyl also occurs in this region. In Orissa, occurrences at Jerapani, Surjapalli, and Dakalga produce mainly yellow chrysoberyl. Alexandrite with a slight to moderate color change has been found at Surjapalli. Large quantities of cat's-eye chrysoberyl are found in the southern part of Orissa.

The Vishakhapatnam district of Andhra Pradesh has produced yellow chrysoberyl, small alexandrites with a moderate color change, and large quantities of cat's-eye chrysoberyl. Most of this material is heavily included.

All the varieties of chrysoberyl show typical refractive indices of 1.746 to 1.755, with a birefringence of 0.009. The specific gravity is slightly lower than normal, at 3.69. In the visible-light absorption spectrum, the alexandrite shows weak to intense chromium lines, whereas the yellow chrysoberyl shows a clear absorption line at 444 nm. Common internal features are sillimanite, rutile, biotite, apatite, and liquid-filled "feathers," as well as straight and angular zoning.

Although the three new chrysoberyl localities are separated from one another by hundreds of kilometers, they probably formed at approximately the same geologic time. The apparent continuation of the pegmatite series farther south, in the state of Kerala, suggests the possibility of additional deposits there.

Gem corundum from Australia and Southeast Asia. Dr. F. Lynn Sutherland, of the Australian Museum in Sydney (in collaboration with E. A. Jobbins, R. R. Coenraads, and G. B. Webb), and Dr. Dietmar Schwarz, of the Gübelin Gemmological Laboratory, presented two papers on similar topics: the chemical and gemological characteristics of gem corundum from the basaltic fields of Barrington, Australia, and Pailin, Cambodia. Both fields have remarkably similar gem suites, in that both suites represent two distinct geologic origins: "metamorphic" and "basaltic" (or magmatic). The two origins for corundum can be distinguished by mineral inclusions and chemistry (trace and minor elements). These distinctions are indicative of two different underlying corundum sources tapped by rising basaltic magmas, which transported the corundum to the surface.

"Metamorphic" corundum from both localities is characterized by inclusions of magnesian spinel and sap-

phirine (figure 5), whereas "basaltic" corundum contains inclusions of ferrian spinel, zircon, and Nb-Ta-U- and/or Th-rich oxide minerals such as pyrochlore. Chemical differentiation between the two types of corundum is possible using the elemental ratios Cr_2O_3/Ga_2O_3 and Fe_2O_3/TiO_2 (figure 6).

Dr. Schwarz extended the study to sapphires from Thailand and Laos and obtained similar results—a bimodal distribution of the sapphires on the basis of chemistry and mineral inclusions. Such similarities in the corundum suites suggest that sapphires of metamorphic origin coexist with sapphires of basaltic origin at other localities.

Bactrian emeralds. An ancient country in what is today northern Afghanistan bore the name Bactria, after its main city (now Balkh). In 314–305 BC, Theophrastes wrote in his famous handbook on mineralogy, *Peri Lithon*, that Bactria was a source for "smaragdos." This word, however, was used to describe not only emerald, but other green stones as well. Since that time, Pliny the Elder and others have repeated this information in their writings. D. E. Eicholz, who prepared the English translation of Pliny's *Natural History*, book 37 (1962), stated that "the Bactrian *smaragdus* is . . . a fiction."

D. H. Piat of Paris and F. H. Forestier of Beaulieu, France, reviewed the reality-or-myth question of the existence of Bactrian emeralds in light of some relatively recent discoveries, especially the 1970 discovery of emerald deposits in the of Panjshir Valley, 120 km northeast of Kabul. The geology of those deposits, and the physical, chemical, and gemological properties of emeralds found there were compared to those of other deposits. Also con

Figure 5. The intergrowth of sapphirine (an Mg-Al silicate; not to be confused with sapphire) in this 3 mm ruby specimen indicates a metamorphic origin. The specimen, from Gloucester Tops, Barrington volcanic field, New South Wales, Australia, was brought to the surface by an alkali basalt. Courtesy of G. B. Webb.
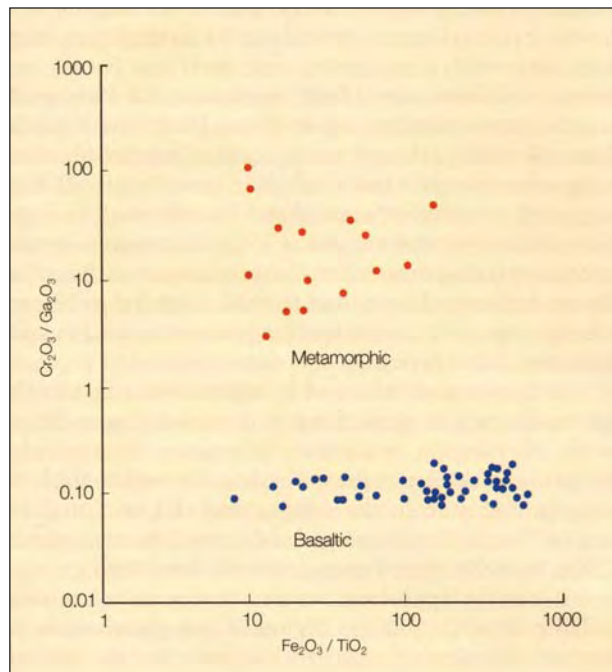
Figure 6. This graph illustrates the chemical distinction between corundum of metamorphic and basaltic origin based on ratios of the abundance of chromium, gallium, iron, and titanium as oxides. Corundum samples of metamorphic origin plot in the upper part of the diagram, while those of basaltic origin plot in the lower part. The data are based on samples from the Barrington field in Australia.

sidered were geographic factors: the presence of the Panjshir River drainage northeast of Kabul, the location of archaeological sites in the region, and the distribution of emeralds in the treasures of the historic kingdoms of the Indian peninsula. On the basis of this newly discovered evidence, the conclusion was reached that true emeralds could have been known in the country of Bactria in ancient times.

Emerald origin. To study the origin of emeralds, Israel Z. Eliezri and his colleague, Y. Kolodny, both of Israel, measured the isotopic composition of 10 emeralds from five major deposits. The geologic environment of emerald formation is primarily constrained by the availability of beryllium and chromium. Sources for these elements may be indicated by the oxygen isotopic composition ($\delta^{18}O$) of beryl. This composition is determined by the isotopic composition of the mineralizing fluid and by the temperature of formation.

Of the samples tested, the Colombian emeralds were the most $\delta^{18}O$ enriched, at $\delta^{18}O$ = 22‰ (per mil), which reflects their association with sedimentary rocks

and a relatively low temperature of formation. The Brazilian and Zambian emeralds were noticeably lower ($\delta^{18}O$ = 12‰), which reflects their contact metamorphic origin at higher temperatures in association with pegmatites and schists. The Tanzanian emeralds, which are closely associated with basic volcanic rocks, had the lowest $\delta^{18}O$ values (8‰); whereas the Nigerian emeralds had a slightly higher value of $\delta^{18}O$ = 9.5‰, which probably reflects their relationship to granitic rocks.

The results of this study show a general correspondence between the isotopic composition of oxygen of the various rock types and the emeralds found in association with these rocks. The authors feel that isotopic analysis of oxygen in emeralds can serve as a means of determining their country of origin, in particular to distinguish Colombian emeralds from those of other deposits.

Origin of ancient Roman emeralds. In collaboration with C. Aurisicchio and L. Martarelli, Professor Giorgio Graziani of the University of Rome has studied the geographic origin of emeralds that were found in funeral stores at a necropolis of ancient Rome.

Nondestructive analytical techniques, such as infrared spectroscopy and scanning electron microscopy, were used to characterize these emeralds. The resulting characteristics were compared to those of emeralds from known localities that ancient Romans might have had access to, such as Habachtal (Austria), India, Upper Egypt, and the Ural Mountains in Russia. The most useful information came from two regions in the infrared: 3,500–3,700 cm^{-1} and 400–1,100 cm^{-1}. The spectral features suggested that these emeralds probably came from Upper Egypt.

Blue quartz from Madagascar. Decorative quartz from Madagascar, showing a blue color caused by inclusions, was discussed by Dr. Emmanuel Fritsch, of the University of Nantes, France. Using a combination of SEM-EDXRF and Raman analysis, Dr. Fritsch and his colleague, Professor Bernard Lasnier, identified numerous inclusions in this material. Lazulite (figure 7) apparently causes the blue color. Other inclusions present are: ilmenite or titanomagnetite as rounded black grains, rutile as reddish brown rounded grains, apatite as colorless rounded grains, zircon as colorless-to-gray rounded grains, celestine and anhydrite as corroded colorless inclusions, hematite as red-brown hexagonal platelets, a monoclinic amphibole species as colorless elongated prisms, colorless mica as platelets with rounded edges, and svanbergite as a corona around some of the lazulite inclusions.

Lazulite is not the only mineral inclusion known to cause blue color in quartz. Finely disseminated inclusions of ajoite, azurite, chrysocolla, dumortierite, papagoite, and tourmaline have also been seen to cause visible blue coloration in otherwise colorless quartz.
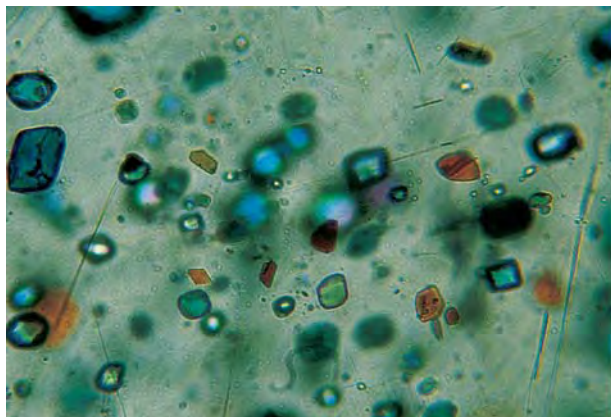
Figure 7. Blue lazulite and red-brown hematite are among the inclusions seen in quartz from Madagascar. The lazulite inclusions impart an overall blue color to the quartz. Photomicrograph by Bernard Lasnier; magnified 60×.

Ornamental stones and other gems from Bolivia. Dr. Jaroslav Hyrsl, of the Mineralogy Department of Charles University in Prague, Czech Republic, reported on the gemstones of Bolivia, which he divided into four basic groups: economically important gemstones, rare collector's stones, ornamental stones used by ancient Indians, and ornamental stones that are mined today.

Although numerous economically important gemstones are present in Bolivia, few of the deposits are large enough to mine. Bicolored amethyst-citrine ("ametrine"), the most important gem material of Bolivia, comes from the La Gaiba region. The Anahí mine is the best-known occurrence of ametrine; it also produces amethyst and natural (not heated or irradiated) citrine. Small diamond crystals weighing up to 1 ct occur in Permian glacial sediments in several rivers in the northern part of Bolivia. These alluvial deposits were prospected in the 1920s and considered uneconomic; several kimberlites have since been discovered in Ayopaya Province. A few opaque to translucent blue sapphires were found recently in alluvium in the Potosí Department, but they do not exceed a few millimeters. Very dark almandines up to ~1 ct are also present in alluvium in the Potosí area. Aquamarine is known from pegmatites in the San Ramon area, but the cut stones (up to 2 ct) are very pale. Crystals of smoky quartz (up to 50 cm long) and green tourmaline are also known from these pegmatites. Emerald crystals up to 1 cm long are known from the eastern Santa Cruz area, but no cuttable material was found until recently. The second significant modern occurrence of dark green chromium chalcedony (the first being the "mtorolite" deposit in Zimbabwe) is in eastern Bolivia's Chiquitania region, where this ornamental gem occurs as veinlets in a silicified laterite overlying ultrabasic intrusives.

Among the rare collector's stones are transparent purple apatite crystals from a tin deposit at Llallagua; yellowish hydroxyl-apatite crystals up to about 10 cm long, sometimes with a transparent core, from near Potosí; and cassiterite from the Viloco mine near La Paz, with faceted stones reaching up to 25 ct. Danburite crystals from Alto Chapare very rarely contain parallel fibers of magnesio-riebeckite (an amphibole group mineral) that can yield a strong cat's-eye effect. Phosphophyllite from Cerro Rico de Potosí can reach 75 ct. Transparent pyrargyrite crystals come from Colquechaca, southeast of Oruro, and several have been faceted. Large (up to 20 cm) siderite crystals with transparent portions recently came from the Colavi deposit near Potosí.

Ornamental stones used by ancient Indians, mostly for beads, include chalcedony with native copper inclusions, chrysocolla, malachite, blue-green fluorite, and turquoise. The chalcedony, chrysocolla, and malachite were probably from the copper deposits of Corocoro and/or Turco. Turquoise probably came from northern Chile, with the other materials mostly from Peru.

Recently exploited ornamental stones include sodalite from Cerro Sapo (figure 8) and stromatolite (a layered sedimentary-algal rock) from near the city of Potosí.

Cultured pearls from Indonesia. In this report, prepared with H. C. Zwaan, Dr. Pieter C. Zwaan of the Netherlands Gemmological Laboratory in Leiden noted that while conditions in Indonesia are generally good for the cultivation of saltwater pearls, actual production is restricted to a limited number of localities.

Earlier operations, between 1950 and 1960, produced a significant quantity of large cultured pearls, up to about 15 mm in diameter, from the Aru Islands in the Arafura Sea. Named after the most important trade center in that area, these pearls are commercially known as Dobo pearls.

Examination of a collection of these pearls, ranging from 9.2 to 15.3 mm in diameter, gave a density between 2.691 and 2.755. The nacre thickness varied from 1.0 to 2.0 mm, which by European laboratory standards is considered very good. Dobo pearls are produced by the silver-lipped mollusk *Pinctada maxima*. Recent information indicates that important pearl trade activities are now going on in that area.

Cultivation of blister pearls on *Pinctada maxima* shells started several years ago near the coast of Lombok island, in particular in Street Lombok, around the very small island Gili Air. Three shells from this area with a total of nine mabe "pearls" were examined and found to have hemispherical bead nuclei composed of artificial resin instead of mother-of-pearl or soapstone. These cultured blister pearls are sold on Lombok and Bali islands as natural pearls. At first glance, however, they resemble imitation pearls, because the relatively thin, translucent nacreous layer causes a deceiving sheen, which is produced by light reflection from the artificial nucleus. The

specific gravity of these blister pearls is also extremely low, ranging from 1.815 to 1.905.

Sapphires from northern Madagascar. In the past few years, several new and important sapphire deposits have been discovered in Madagascar. Dr. Margherita Superchi, of CISGEM, Milan, Italy, described a new occurrence at Ambondromifehy, in Antsiranana Province, in the northern part of the island. The sapphires found to date were alluvial, having been weathered from basaltic rocks that were emplaced intermittently during the period from the Upper Oligocene to the Pleistocene. The sapphires are thought to be xenocrysts; that is, they did not crystallize from the basaltic magma, but simply were transported by it. They are associated with zircon, spinel, pyroxene, and olivine.

Dr. Superchi and her colleagues (A. Donini, D. Muzzioli, and E. Roman) obtained detailed gemological data, chemical compositions, and optical and Raman spectra for 74 crystals (the largest being 182.59 ct) and 13 cut stones. Among the more interesting discoveries were inclusions of pyrochlore, zircon, and sodic plagioclase, which, with the chemical data (e.g., high gallium contents) confirm the "basaltic" association of these sapphires (see the earlier abstract on gem corundum).

Tunduru-Songea gem fields in southern Tanzania. Dr. Claudio Milisenda of the German Gemmological Association, using research done with Dr. Ulrich Henn and Dr. Hermann Bank, discussed the spectacular new gem occurrences that were discovered in late 1993 and early 1994 in the Tunduru-Songea area of extreme southern Tanzania. These alluvial deposits are located along tributaries of the Ruvuma River, which forms Tanzania's southern border with Mozambique. The area produces a large variety of gem materials, in particular blue and fancy-colored sapphire (including "padparadscha" and color-change stones), ruby, many colors of spinel, garnet (such as rhodolite, hessonite, and color-change), chrysoberyl (including cat's-eye, alexandrite, and cat's-eye alexandrite), various quartz and beryl varieties, tourmaline, zircon, kyanite, scapolite, peridot, and diamond.

The first gem rough appeared on the market in 1994, and included sapphire, spinel, garnet, chrysoberyl, and zircon, reportedly from an area east of Songea, where the Muhuwesi and Mtetesi rivers converge. Shortly afterwards, an even richer alluvial deposit was discovered near Tunduru, a remote area in southeast Tanzania. Because thousands of people were involved in mining and trading gemstones at the outset, it is almost impossible now to tell if some rough gems are from the Songea or the Tunduru area.

With the exception of the diamondiferous Mwadui pipe within the Tanzanian craton, all of Tanzania's known gemstone occurrences (including the Tunduru-Songea gem fields) are situated within the Proterozoic Ubendian-Usagaran System, a medium- to predominant-

Figure 8. Sodalite is one of the ornamental materials that is currently being mined in Bolivia, from the ancient deposits near Potosí. This cabochon weighs 5.05 ct. Photo by Maha DeMaggio.

ly high-grade metamorphic unit that includes gneiss, marble, metapelite, and quartzite, which are intruded by numerous pegmatites. The Ubendian-Usagaran System forms the Tanzanian part of the Mozambique Belt. This gem-bearing complex experienced its main thermo-tectonic evolution during the Pan-African orogeny (approximately 600 million years ago), which affected the entire eastern part of the African continent as well as southern India and Sri Lanka.

Dr. Milisenda also reported on the gemological characteristics of corundum, spinel, chrysoberyl, garnet, and tourmaline from the Tunduru-Songea region, which were based on the study of hundreds of carats of rough and cut stones. A visit to the localities yielded information on the geology and recovery techniques. Iron- and titanium-oxide contents of the corundum were compared with similar gem materials from Sri Lanka and India. With the exception of the occurrence of diamond and an unusual mint-green, vanadium-colored chrysoberyl, the gem gravels of the Tunduru-Songea region strongly resemble the gem concentrates of Sri Lanka, and the two areas may be genetically related. However, the large variety of gems of contrasting genetic type suggests that the gems themselves were derived from different geologic sources in both locales.

SYNTHETICS AND SIMULANTS

Imitation pearls—so-called "I Pearls" from Japan.
Professor Akira Chikayama of Tokyo, Japan, discussed the modern production of imitation "I Pearls" in Japan. Although best known for its cultured pearl industry, Japan is also an important manufacturer of imitation pearls. During the production of most imitation pearls, spherical beads are given their pearly-luster coating through the application of a fish-scale extract known as *Essence d'Orient*. More recently, a lead-carbonate-based pearlescent coating material has also been used.

The least expensive manufacturing process for imitation pearls uses plastic bead centers formed by injection molding. Because of their low cost, such imitations are responsible for as much as 80% of the imitation pearl market. Their low specific gravity, however, makes them less desirable than those imitations with heavier centers. This is particularly obvious when plastic imitations are used in strands, since these bead strands do not lay evenly or move "naturally."

The most expensive imitation pearls manufactured

Figure 9. Machine manufacturing of alabaster glass beads has modernized the production of glass-based imitation pearls in Japan. Note the accidental "baroque" beads that occasionally form. Photo by Professor A. Chikayama.

in Japan use central beads formed from shell. They can be quite convincing in both appearance and heft, and have been variously called "shell pearls," "imitation cultured pearls," and "man-made pearls."

The third form of imitation pearl is produced from a bead center of white alabaster glass. In the past, these bead centers were hand blown. More recently, a modern automatic bead-forming machine was invented by Mr. Satake of Izumi City. Machine manufacturing of the alabaster glass beads (figure 9) is much more efficient than the previous hand-blowing methods, so these glass-based imitation pearls are much more economical.

Because of the confusion created by numerous commercial names, the Japan Imitation Pearl & Glass Articles Association has suggested a new nomenclature to describe imitation pearls manufactured in Japan: the use of "I Pearl" together with an indication of the base material, such as shell, glass, or plastic. The letter I stands for "imitation" and also for the place of production, Izumi City. "I" (Ai) also means "love" in Japanese.

Growth-induced imperfections and inhomogeneities in single crystals. The science of crystal growth is important for distinguishing natural from synthetic single-crystal gem materials. Natural, synthetic, and treated stones have the same basic chemical composition and crystal structure, but different growth or post-growth histories. Dr. Ichiro Sunagawa, of the Yamanashi Institute of Gemmology and Jewellery Arts in Kofu, Japan, explained how imperfections and inhomogeneities are induced into a crystal during the growth process, or modified through post-growth treatment. Since growth conditions and ambient phases different from those of natural stones are required for the synthesis of many single crystals, the two materials may have different imperfections and inhomogeneities.

In the synthesis of gem crystals, growth usually takes place at the seed crystal–nutrient phase interface. The external forms of a crystal (its morphology) and surface microtopography of the crystal faces represent the final stage of a growth process, although these features are usually removed during cutting. However, features within the crystal represent earlier growth surfaces; thus, they serve as a record of the events that took place at the interface during growth. These events include: fluctuation of growth rates, incorporation of impurities, entrapment of inclusions, generation of dislocations, and the like. Solid or nutrient-phase inclusions, subgrain boundaries, and twin boundaries are macroscopic imperfections. However, growth sectors, sector boundaries, growth banding, and associated color zoning either can be detected with a microscope or require special techniques to visualize, such as X-ray topography, cathodoluminescence, or laser-beam tomography. Detection of dislocations requires special techniques. Post-growth treatments, such as heat and irradiation, may modify the growth-induced imperfections and inhomogeneities. In
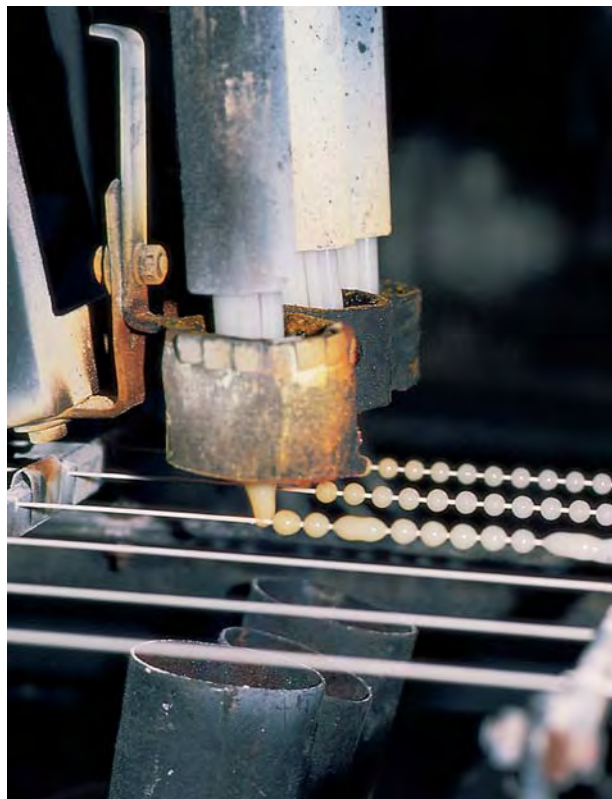
particular, the valence state of impurities may be detectably altered. As crystal-growth techniques become more sophisticated, gemologists may have to look to these signs more and more to make an identification.

Surface features and growth conditions of quartz crystals. The surface features of experimentally grown hydrothermal synthetic quartz were examined by Professor Takeshi Miyata, in collaboration with M. Hosaka, both also of the Yamanashi Institute. These researchers grew single crystals of synthetic quartz in sodium hydroxide solutions at 350°–515°C, and in sodium chloride solutions at 450°–490°C. They observed the morphology of the crystals and their surface microtopography using interference microscopy.

So that the shape of the seed would not influence the morphology of the grown synthetic crystal, spherical seeds of synthetic quartz were used. The growth rates were calculated by measuring the size of the seeds before growth and the size of the synthetic crystal overgrowths that formed within a specific time period. It is well known that the various shapes of natural quartz crystals from different localities are influenced by their growth conditions. So, too, are their macroscopic and microscopic surface characteristics. Comparison of shapes and surface features seen on synthetic quartz crystals grown under known, controlled conditions, to similar shapes and surface features observed on natural quartz crystals, may provide information on the growth conditions of the natural crystals.

Reversible twinning in an unusual synthetic material. Three pieces of an unusual synthetic material were loaned to Gem News editor John Koivula by Arthur T. Grant of Coast-to-Coast Rare Gems, Martville, New York. The samples constituted a well-formed 136.89 ct crystal, a 5.33 ct faceted sample (figure 10), and a 28.81 ct partially polished rectangular block. This material is

Figure 10. Illustrated here are the largest known crystal (136.89 ct) and the only known cut sample (5.33 ct) of neodymium penta-phosphate. Photo by Maha DeMaggio.

transparent and an intense, slightly purplish pink.

Twelve crystals of this material were grown about 10 years ago as an experimental material for the laser industry. The experiment was terminated when it was

Figure 11. Only slight finger pressure was required to cause a shift in the twin pattern in this block of neodymium penta-phosphate. Photomicrographs by John I. Koivula; polarized light, magnified 10×.
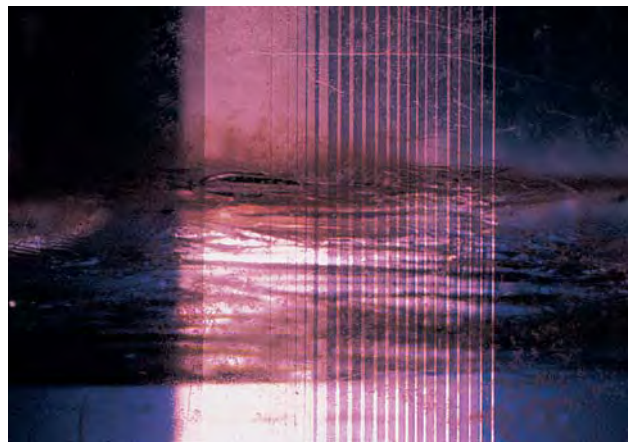
discovered that the crystals were difficult to cut because even slight pressure would cause a reversible elastic lamellar twin structure, which shifted position as the direction of pressure was changed. Hundreds of lamellar twin planes can be seen to appear and then disappear in polarized light (figure 11) when only slight finger pressure is applied. The shift in the twin planes is often accompanied by an audible clicking or cracking sound. Mr. Grant also encountered this twinning phenomenon when he faceted the 5.33 ct modified marquise shown in figure 10. During cutting, he noticed what appeared to be a cleavage plane form across the table facet which would alternately disappear and then reappear. Because the contour of the surface also shifts slightly when this occurs, it was very difficult to get a flat, well-polished table facet.

Qualitative EDXRF chemical analysis on the faceted sample by Sam Muhlmeister at GIA Research in Carlsbad, California, showed the presence of both neodymium and phosphorus. This analysis supported the stated chemistry as being neodymium penta-phosphate, with the formula NdP_5O_{14}. Gemological testing gave refractive indices of 1.608–1.632 and a birefringence o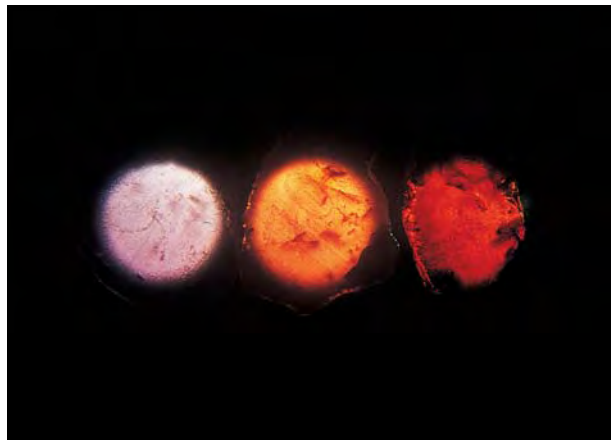f 0.024. The specific gravity obtained hydrostatically was 3.36. A strong typical rare-earth spectrum was observed using a handheld spectroscope. The material was inert to UV radiation, there was no reaction to the "Chelsea" color filter, and the pleochroism was weak, showing a shift between pink and purplish pink hues. Numerous two-phase inclusions visible with magnification in both the crystal and the block suggest hydrothermal growth.

TREATMENTS

Heat treatment of garnets. It is generally thought that garnets are not affected by treatment processes such as heating and irradiation, and therefore are not treated. Going against this convention, Gerhard F. A. Becker, of Idar-Oberstein, reported on the results of heat-treatment experiments he carried out on uncut rhodolite garnets from Brazil.

Mr. Becker conducted his experiments using a standard muffle furnace with the stones in air. The garnets were purple (figure 12, left) prior to heat treatment, and had gemological properties typical for rhodolite. Heating was conducted in 50°C increments, with the samples cooled and inspected between steps. The first noticeable change in color was observed at 700°C (figure 12, center), and the color continued to change up to 900°C (figure 12 right). Further heating resulted in the appearance of a metallic, hematite-like coating on the garnets (figure 13) that could be polished off.

Mr. Becker's research independently confirms earlier preliminary experiments done by Dr. Kurt Nassau (see *Gemstone Enhancement*, 2nd ed., 1994). Following up on an unpublished observation by G. V. Rogers, Dr. Nassau changed purplish rhodolite into a "hessonite-type brownish color" at a temperature of "about 600°C."

The metallic coating was probably the result of iron oxidation because the stones were heated in air. This coating might be similar to that reported in the Fall 1975 issue of *Gems & Gemology* on an emerald-cut almandine garnet that was misrepresented as cuprite. However, as heat treatment of garnets is generally not suspected, the stone seen in 1975 was thought to have been "sputter" coated (that is, to have had some material deposited on it) to give it the metallic coating.

Titanium and chromium diffusion-induced star sapphires. Gao Yan, of the National Gem Testing Center in Beijing, China, described some diffusion-treated star sapphires he and his colleagues, Z. Beili and L. Jingzhi,

Figure 12. Progressively hotter treatment of the untreated starting material on the left produced the changes in color shown in the two garnets on the right, at 700°C and 900°C, respectively. Photo by Gerhard Becker.

Figure 13. The metallic coating on these Brazilian garnets was the result of heat treatment above 900°C. Photo by Gerhard Becker.

received for identification in September 1996. All of the samples had essentially the same visual appearance, and all were approximately 5×7 mm. In daylight, the stones were translucent to opaque and showed a dark blue color with gray tone. They exhibited distinct six-rayed stars, very similar to those typically seen in synthetic star sapphires.

Measurements yielded an R.I. of approximately 1.76 and an S.G. of 3.97. All samples showed a distinct dichroism of blue and bluish green when viewed parallel to the girdle. A weak absorption line at 450 nm was visible with a hand spectroscope. The stones were inert to both long- and short-wave UV radiation. With magnification and darkfield illumination, three characteristics were observed: distinct color zoning, fingerprint-type healing fissures with two-phase inclusions, and tiny white spots scattered throughout. With the polariscope, almost all samples showed polysynthetic twinning. When viewed with fiber-optic illumination and high magnification, the surface revealed a very thin film of cotton-like material with spectral colors. A group of intense blue lines were concentrated along surface-reaching fractures that were produced by the polysynthetic twinning. When the samples were immersed in methylene iodide, a red halo appeared on the polished surface and a high-relief red outline was concentrated around the girdle.

EDXRF data from a cross-section cut across one of the samples showed that chromium was restricted to the sapphire's rim, and the titanium content was higher in the rim than in the core, although the sample was dark blue throughout. Iron was homogeneous throughout. With deep polishing of the dome of this sample, the asterism disappeared, confirming the conclusion that the material was diffusion-induced star sapphire.

Two distinctive characteristics were noted for these sapphires. First, instead of the colorless or pale blue treated corundum typically used as a starting material, the producer used dark blue sapphire with visible color banding. Second, it appears that chromium as well as titanium was part of the diffusion process, possibly to produce a thin red film that would deepen the blue surface color. On a dark blue background, the asterism becomes sharper and the color bands are less visible. Chromium may also enhance the asterism, although this remains to be verified.

These diffusion-induced star sapphires can be easily identified. The natural origin of the precursor material can be proved by internal characteristics such as the color banding and absorption spectra. The titanium and chromium diffusion process can be readily identified by blue lines along twin planes on the surface, a red halo on the surface, and a high-relief red outline around the girdle when the stone is immersed in methylene iodide. [Editor's note: See the Summer 1996 Gem News, pp. 136–138, for more information on diffusion-induced star sapphires.]

New hall opens at the Smithsonian Institution. The Janet Annenberg Hooker Hall of Geology, Gems & Minerals opened on September 20, 1997, at the National Museum of Natural History (Smithsonian Institution). The 20,000-square-foot exhibit features the renowned Hope Diamond along with the museum's superb collection of gemstones and jewelry (figure 14), including donations that had not previously been displayed. The hall features interactive computerized displays, animated graphics, special lighting effects, and touchable specimens. Its various galleries include the National Gem Collection; Minerals and Gems Gallery; Mine Gallery; Plate Tectonics Gallery; Moon, Meteorites and Solar

Figure 14. The famed Mackay emerald is on display in the new Janet Annenberg Hooker Hall of Geology, Gems & Minerals at the Smithsonian Insitution. The emerald weighs 168 ct and is set in an Art Deco diamond and platinum necklace. Photo courtesy of the National Museum of Natural History (Smithsonian Institution).

Figure 15. This Victorian-era brooch, mounted with two cabochon garnets, 35 rose-cut diamonds, and several pearls and half pearls, is among the pieces that will be displayed in the new Gem Room at the Cleveland Museum of Natural History, Cleveland, Ohio. Photo courtesy of the Cleveland Museum of Natural History.

System Gallery; and Rocks Gallery. For more information, visit their website at http:\\www.mnh.si.edu\collections.html. The National Museum of Natural History is located at 10th Street & Constitution Avenue Northwest, Washington, DC.

Diamonds at the American Museum of Natural History. *The Nature of Diamonds* exhibit opened on November 1, 1997, and runs through April 26, 1998. This comprehensive exhibit explores all aspects of diamond, from its geological origins to its place in history, art, adornment, and literature, including its uses in modern technology and research. A specially designed walk-in diamond vault houses some of the most dazzling objects in the exhibition. Other highlights include a hands-on model of the crystal structure of diamond, a mine tunnel leading to a re-created "diamond pipe," and a large-screen computer-animated illustration of how diamonds are formed. For more information, contact Holly Evarts, Department of Communications, American Museum of Natural History, Central Park West at 79th Street, New York, 10024–5192; or call 212-769-5099. The exhibit will be traveling to other museums after closing in New York.

New exhibits at the Cleveland Museum of Natural History. November 1 marked the opening of the Reinberger Hall of Earth and Planetary Exploration. This multi-sensory, permanent hall integrates earth science and planetary geology. Some of the thematic sections include Ores and Mining, Geology Beneath Your Feet, Rocks and Minerals, and the Gem Room. The Jeptha Homer Wade II Gem Room will open in the spring of 1998; this exhibit will showcase a permanent collection of gems, jewels (see, e.g., figure 15), and mineral specimens. The museum is at 1 Wade Oval Drive in University Circle, Cleveland, Ohio, 44106–1767. For more details, call 216-231-4600 or visit the museum's web site at http://www.cmnh.org.

***Gems & Gemology* wins ASAE award—again!** For the second year in a row—and the fourth time in the past six years—*Gems & Gemology* won first place for peer-reviewed journals in the Gold Circle competition of the prestigious American Society of Association Executives. *Gems & Gemology* Editor Alice Keller accepted the award in early December on behalf of the journal.

ERRATUM

The authors wish to make the following corrections to "Benitoite from the New Idria District, San Benito County, California," which appeared in the Fall 1997 issue of Gems & Gemology:

1. *In the geologic map in figure 7, "Blueschist" should refer to the dark blue unit, and "Altered blueschist" should refer to the light blue unit.*

2. *The reference suggesting that benitoite can be used as a standard for measuring dispersion in gemstones should be reported as: Hanneman W.W. (1992) Determination of dispersion using a refractometer.* Journal of Gemmology, *Vol. 23, No. 2, pp. 95–96.*

Book Reviews

SUSAN B. JOHNSON AND JANA E. MIYAHIRA, EDITORS

CREATIVE VARIATIONS IN JEWELRY DESIGN

By Maurice P. Galli, Dominique Rivière, and Fanfan Li, 527 pp., illus., publ. by Schiffer Publishing, Atglen, PA, 1997. US$69.95*

Creative Variations in Jewelry Design is the third book by these three authors. In their first book, *The Art of Jewelry Design* (1994), they outlined the principles of jewelry design and offered numerous design ideas for rings and earrings. In their second book, *Designing Jewelry* (1994), they presented hundreds of ideas for brooches, bracelets, necklaces, and accessories.

In this book, the authors develop original themes for 21 complete sets of jewelry, each of which includes matching necklace, bracelet, earrings, and ring. There are five illustrated plates for each theme. The first plate shows the source of the theme, and the next one presents the most affordable variation, with silver as the predominant metal. The third plate follows with a gold version, while the fourth plate uses gold, diamonds, and colored stones. The theme concludes with a presentation in platinum, diamonds, and high-end colored stones.

For example, for Fanfan Li's third design theme, she chose "Bianfu"—the Chinese bat—as her source illustrated in the first plate. The second plate shows her variation with polished silver and polished gold, using the Bianfu design for the ring, bracelet, necklace, and earrings. The third plate features matte yellow gold and polished yellow gold wire. In the fourth plate, Ms. Li uses yellow gold, carved emerald beads, pear- and round-shaped ruby cabochons, pavé-set diamonds, pearls, and black enamel. The final plate illustrates the use of platinum with marquise and pear-shaped prong-set diamonds and pavé-set diamonds. Not only is each variation beautifully illustrated, but each is also clearly described.

The quality of *Creative Variations in Jewelry Design* is excellent. The printing, resolution of images, and binding are greatly improved over the first two books. This book is ideal for students of design and counter sketching, as well as for the professional. However, I recommend that the novice read *The Art of Jewelry Design* first, to learn rendering techniques.

Creative Variations in Jewelry Design accomplishes just what it sets out to do clearly and concisely. As the authors state in their foreword, "Our past teaching experience has revealed in most students a tendency to not fully realize the whole potential of their ideas, neglecting to explore the use of a variety of metal textures and stones." In this book, they help the student learn to design a given theme at different price points, a skill that manufacturers will expect. This book is a must for the library of any jewelry design student or professional.

MELISSA WATSON-LAFOND
Gemological Institute of America
Carlsbad, California

VISUAL OPTICS: DIAMOND AND GEM IDENTIFICATION WITHOUT INSTRUMENTS—THE HODGKINSON METHOD

By Alan Hodgkinson, 50 pp., illus., publ. by Gemworld International, Northbrook, IL, 1995. US$25.00*

As stated on page one, "The target and attraction of Visual Optics is to provide gemological identification or information without the use of instruments." In the first half of the book, Mr. Hodgkinson provides procedures for estimating or determining optic character, birefringence, dispersion, and pleochroism using only a simple light source and a Polaroid filter. He maintains that these tests can be performed on faceted gemstones of any size that are loose or open-back mounted. Using the instructions, reference charts, and photographs, I performed the tests on some sample gemstones. I found the exercises accurate and, as the author suggests, "exhilarating."

The balance of the book outlines procedures for estimating or determining absorption spectrum and refractive index, with additional information on birefringence and dispersion. The R.I. estimation requires making or purchasing what appear to be simple accessories (suppliers are listed in the back of the book), and Mr. Hodgkinson recommends some not-so-simple stone and graph references to make adjustments for variations in stone proportion. I did not test these procedures.

It is essentially left up to the reader to decide how to use the information to aid in gem identification, with the exception of approximately a dozen common gem materials for which specific properties and photographs are featured. This book showed me numerous ways of viewing optical characteristics that I was previously unaware of, even with 18 years of gemological/appraisal experience.

DOUGLAS KENNEDY
Gemological Institute of America
Carlsbad, California

COLORED STONES AND ORGANIC MATERIALS

Control of crystal phase switching and orientation by soluble mollusc-shell proteins. A. M. Belcher, X. H. Wu, R. J. Christensen, P. K. Hansma, G. D. Stucky, and D. E. Morse, *Nature*, Vol. 381, May 2, 1996, pp. 56–58.

The authors studied the growth of abalone (*Haliotis rufescens*) shell materials *in vitro*—that is, in laboratory dishes rather than within the animal (*in vivo*). Abalone shell consists of layers of calcite, aragonite (another crystalline form of calcium carbonate), and proteins. Typically, proteins integral to the carbonate layers comprise less than 2 wt.% of the shell material. There is an abrupt switching between calcite and aragonite deposition, and distinct "populations" of proteins are associated with calcite and aragonite layers. Multiple layers of aragonite form nacre.

Calcium carbonate grows from saturated aqueous solutions as dense, well-organized, and well-oriented calcite layers on a sheet of nucleating proteins, but it will also grow (though not as well) on glass. The authors extracted water- and acid-soluble proteins from calcite and aragonite layers of natural *H. rufescens* shells; when they introduced these proteins into the carbonate growth environment, the proteins that were associated with the aragonite layer caused aragonite growth on the calcite layers. Aragonite formation could be switched on and off by adding or depleting these soluble proteins. The authors conclude that these proteins alone are sufficient to cause aragonite formation, and neither magnesium nor temperature/pressure changes are required to form the aragonite layers. This research is useful for understanding the development of nacre in shell materials. *MLJ*

Effect of ligand metal charge transfer and intravalence charge transfer bands on the colour of grossular garnet. T. Lind and H. Bank, *Neues Jahrbuch für Mineralogie, Monatshefte*, Vol. 17, No. 1, March 1997, pp. 1–14.

Garnets of the ugrandite solid-solution series generally include brown to yellow to green colors; previous studies linked these colors to different properties of ions involved in the chemical composition. *[Editor's note: "Ugrandite" is a group name for calcium garnets—**u**varovite, **gr**ossular, and **and**radite.]* The new grossular-andradites from Mali, however, all have a very similar bulk chemistry but still show a wide range of browns, yellows, and greens. The authors tried to find an explanation for this phenomenon by examining gem-quality grossular garnets from various Indian and African sources, including Mali. They looked at chemistry, absorption spectra, refractive indices, and density. On the basis of differences in absorption spectra, they distinguished three groups of garnets: (1) yellow and brown; (2) green to yellowish green with-

---

out chromium and/or vanadium bands; and (3) green with chromium and/or vanadium bands. The main part of the article discusses the properties and charge-transfer behavior of the ions involved, and the resultant effect on garnet color. *RT*

Garnet—January birthstone. H. Bracewell, *Australian Gold Gem & Treasure*, Vol. 12, No. 1, January 1997, pp. 48–49.

Birthstones are valued for their lore as well as their gemological properties. January's birthstone, garnet, is a group of minerals that occur in almost every color except blue. The name *garnet* probably comes from the Latin term *grantum* for the many-seeded pomegranate, whose red seeds resemble some garnet crystals. Garnets have been used in jewelry since ancient Egyptian, Greek, and Roman times. Some fashioned stones are hollowed out on the reverse side in order to make them less dark. Among the metaphysical properties claimed for garnets are guidance in the dark, and use as an antidote to snake bites and food poisoning; they have also been thought to calm anger. They are associated with constancy in the [Victorian?] "language of gems." For more about garnets, see Ezekiel 54:12 in the *Old Testament.* *MLJ*

DIAMONDS

Archangel confirmation. *Mining Journal, London*, Vol. 328, No. 8430, May 23, 1997, p. 409.

Archangel Diamonds is still evaluating its Pipe 441 kimberlite in northern Russia. The pipe "has the potential to have" an aerial extent greater than 40 hectares. The estimated average grade of the crater facies is 0.37 ct/ton, and that of the diatreme facies is 1.38 ct/ton, to give an average grade for the pipe of 0.71 ct/ton. *MLJ*

Botswana: A year of landmarks. *Mining Journal, London*, Vol. 328, No. 8427, May 2, 1997, pp. 357–359.
Although many companies are exploring for diamonds in Botswana, all production there now comes from Debswana's three mines: Orapa, Letlhakane, and Jwaneng. In 1996, these mines produced 5.64, 0.90, and 11.17 million carats (Mct) of diamonds, respectively, with ore grades of 71.7, 28.9, and 140.0 carats per 100 tons of ore. The average diamond value was $82 per carat. Plant capacity limits throughput at all three mines.

The Orapa (AK1) pipe was discovered in 1967 and began production in 1971. It has a surface area of 117 hectares; after 25 years of production, reserves are still calculated to last another 60 years. Botswana recently extended Debswana's lease to the year 2017. A second plant is expected to go on-line by the year 2000, adding 6 Mct to annual production; this would decrease the working lifetime of the open-pit mine to 32 years. However, the kimberlite pipe splits into two 20-hectare lobes at a depth of 210 m. These could be mined below 500 m by underground techniques, adding another 25 years to mine

life. The "ultimate configuration" of the Orapa pit is expected to be 500 m deep, 1.4 km wide, and 2.1 km long.

The two smaller pipes at Letlhakane, DK1 and DK2, about 40 km southeast of Orapa, started production in 1977. The Jwaneng kimberlite was buried under 50 m of Kalahari sand when it was found in 1973; sampling of termite mounds helped in its discovery. Production began in 1982; diamond yields increased 21% as a result of the "Fourth Stream" diamond recovery project, commissioned in 1995. Jwaneng is in the middle of a five-year initiative to reduce operating costs by 10%.

Diamondiferous kimberlites have been found at Martin's Drift, near Lerala, and at Falconbridge's Gope 25 pipe; De Beers is evaluating both deposits. Other companies looking for diamonds in Botswana include Auridiam, SouthernEra, Afriore, and Botswana Diamond Fields.
MLJ

Brazilian lamproites. *Mining Magazine*, Vol. 177, No. 1, July 1997, p. 81.
The Contendas structure, in the states of Minas Gerais and Goiás, Brazil, is a large (130 hectare) crater that is a source of eluvial diamonds. Joint-venture partners KWG Resources and Spider Resources have found "numerous" lamproite indicator mineral grains—including pyrope garnet, eclogitic garnet, chrome diopside, ilmenite, and olivine—in lake sediments within the crater. There are plans to drill the crater in order to delineate the lamproite vents which caused it (and to determine their diamond contents). The partners are also working with the current *garimpeiro* operator mining the southern exposure of the structure, in order to evaluate the recovered eluvial diamonds in a systematic manner. *MLJ*

Diamanten aus China [Diamonds from China]. G. Steiner and M. Steiner, *Lapis*, Vol. 22, No. 11, November 1997, pp. 13–17, 86 [in German].
Diamond deposits were first found in China only a few decades ago, and literature on the topic is still scarce. This article begins with information from historic sources in which diamonds are mentioned, and then summarizes some data about diamond prospecting and production, drawing mainly from recent Chinese reports. Unfortunately, these sources, like their predecessors, offer relatively imprecise information.

The discussion of the geology of the Chinese diamond occurrences features a geologic map showing 14 deposits. All are kimberlite pipes and dikes, together with related secondary deposits, in the Sino-Korean, Yangtze, and Tarim cratons. The formation of the easternmost deposits of the Sino-Korean craton (Mengyin) are related to the Tanlu Fracture Zone, which stretches over 2,400 km from Shandong and Liaoning south to Jiangxi. The balance of the article describes the Mengyin diamond field, the composition of its kimberlites, and diamond production there. Color photos show the "Mengyin No. 1," a 119.01 ct octahedron found in 1996, and other diamonds, as well as representative countryside. The article

also includes a photo and geologic map of the open-pit Changma diamond mine. *RT*

Diamonds are for . . . smuggling. *Mining Journal, London,* Vol. 327, No. 8384, August 2, 1996, pp. 93–95.

Smuggling is a fact of life in the diamond industry, because of diamonds' high value-to-volume ratio. Smuggled rough diamonds usually come from artisanal workings and small-scale producers in countries that may be unable or unwilling to control or even monitor such production. Areas of origin include Zaire, Angola, Sierra Leone, Ghana, Central African Republic, South America, and Namibia (in decreasing order of smuggling on a carat-weight basis). Artisanal diamond production is usually considered "outside goods"—the approximately 20% of the market that is not channeled through De Beers's Central Selling Organization (CSO)—although the CSO may purchase such stones. An estimated 9.69 million carats of diamonds are smuggled annually (almost half of the total "outside goods"). The "outside goods" market is typically much more volatile than the CSO, and dealers may buy stones at higher-than-CSO prices (in a strong market) or not at all (in a weak one).

The buying-price formula for artisanal goods is calculated as the international price; minus expenses for buying, treating, and selling; minus taxes; and minus profit margins. Currency volatility and market volatility for the "outside goods" also play roles. If the difference between buying price and international price is very large, artisanal operators are tempted to bypass regular selling channels. A digger normally receives 50%–60% of the export value of his goods from an established field diamond broker. Traders operating on a barter basis, or those who undervalue the foreign currency (usually dollars) on which the diamonds' worth is based, can offer more money to diamond miners than legitimate channels. (Money launderers—offering above-market prices for available stones—can precipitate chaos in a local diamond market.) Smuggling costs are estimated at 4%–5% of the value of the goods, so export duties that exceed this amount encourage smuggling, as do bureaucratic inefficiency and corruption. Sometimes operators select better-quality goods for smuggling, and sell their lower-quality stones through an "official" operation.

The article estimates that about 50% of diamonds (by weight) in the "outside goods" pool have been smuggled. Although artisanal mining and smuggling will likely remain inseparable, artisanal mining does have its pluses. Diggers work small and low-grade deposits that would be uneconomical for most mining companies. Also, these operations provide income for people in rural regions, and—if taxed intelligently—provide foreign exchange and tax revenue for the producing country. *MLJ*

Diamonds from warm water. R. C. DeVries, *Nature*, Vol. 385, February 6, 1997, p. 485.

Natural diamonds are "remarkably free" of the metallic inclusions so typical of synthetic diamonds, and most natural diamonds may have been formed by processes that require water (that is, hydrothermal processes). Silicate and sulfide mineral inclusions in natural diamonds give clues about how they form; still more evidence is available from liquid inclusions, especially from the poor-quality fibrous surface layers on "coated diamonds." These coatings suggest the presence of liquid carbon-hydrogen-oxygen (C-H-O) phases during diamond growth.

Additional evidence comes from chemical vapor deposition (CVD) of synthetic diamond coatings, where diamond can be deposited from C-H and C-H-O gases at 1000°C and low-deposition pressures. Even more evidence comes from the chemistry of the graphite-water system (if graphite is stable coexisting with water, diamond should be, too). Very small diamonds found in metamorphic rocks probably grew from C-H-O liquids.

Given all this evidence, the hydrothermal synthesis of diamond by Zhao et al. reported in *Nature* (abstracted in the Summer 1997 *Gems & Gemology*, p. 160) is plausible; however, a reliable method must be found to distinguish diamond seed crystals from new growth before this type of diamond synthesis can be confirmed. Zhao et al. imply a very slow growth rate: The Cullinan diamond, for instance, would require 30 million years to grow by their hydrothermal technique. *MLJ*

Diavik mine development at $750 Million. *Diamond Intelligence Briefs*, Vol. 13, No. 247, July 30 1997, p. 1545.

A valuation of 4,217 carats of diamonds from a bulk sample at Diavik, in Canada's Northwest Territories, yielded $60 per carat, with a grade of 2.8 ct/ton. Mining of the deposit [not to be confused with BHP-DiaMet's mine in the Northwest Territories] could begin in four years, and is estimated to cost $600 million to $750 million to develop. Two mining methods are being considered: construction of a ring dike around the property (cost: $60–$100 million), so that water could be pumped out and an open-pit mine developed; and underground mining.

The Diavik project is 60% owned by Rio Tinto, and Aber Resources has a 40% share. Aber has discovered 50 kimberlite pipes in the area, 12 with diamonds. The company is also exploring for diamonds in Greenland and at Victoria Island and Camsell Lake in the Northwest Territories. *MLJ*

Kelsey Lake's place in history. D. Clifford, *Mining Magazine*, Vol. 177, October 1997, pp. MNA 23, MNA 25–26, MNA 28.

The State Line kimberlite district, on the Colorado/Wyoming border, has about 30 kimberlites, almost all of which contain diamonds. However, only two of these pipes (KL-1 and KL-2), comprising Redaurum's Kelsey Lake deposit, are economic at present; these have already

gone into production. This deposit represents the first successful commercial kimberlite mine in the United States. *[Editor's note: The diamond mine at Murfreesboro, Arkansas, was never economic, even though it operated over a period of many years in the early part of this century.]*

The Kelsey Lake kimberlites were discovered in 1986–1987 after a diamond was found in a peridotite xenolith (a rock carried by igneous activity from deep within the earth). All the pipes in the state line district are about 390 million years old. The aerial extent of the two commercial pipes is greater than 9 hectares.

Assessing the economic potential of diamond deposits is expensive, and must be done early in the exploration cycle. At Kelsey Lake, gem-quality (rough) stones weighing 6.2 ct and 14.2 ct were recovered from the first 6,000 tons of ore processed. A resource of 16.9 million tons of ore to 100 m has been identified, and the weathered kimberlite in both pipes extends to even greater depths. Reserves are sufficient to support a 12-year mining operation.

The ore is processed simply and inexpensively in a plant that uses environment-friendly rotary pans for concentrating heavy materials and grease tables for the final separation of the diamonds. In 1996, 10,000 carats were recovered at a cost of less than US$10/ton of ore. Redaurum has also secured the rights to process ore from the nearby Maxwell kimberlite, should it prove to be economic.

Diamond marketing is relatively unattractive to many mining companies in terms of "adding value to the product," since profit margins for finished goods are low and the diamond business is highly subjective. However, Redaurum has registered the trademarks "Kelsey Lake Diamonds" and "Colorado Diamonds," in order to develop a niche market. Fashioned stones have been sold for an average of $173 per carat, and a 5.4 ct pear shape (illustrated on p. 54 of the Spring 1997 Gem Trade Lab Notes) sold for more than $16,000 per carat.   *MLJ*

Martapura diamonds. *Mining Journal, London*, Vol. 329, No. 8448, September 26, 1997, p. 252.

One hundred and three "gem and near-gem" diamonds weighing up to 1.63 ct have been recovered from the Upper Gravel Unit of the Martapura diamond project in southeast Kalimantan, Indonesia, by Indomin Resources. The stones were mostly "white to off-white" in color; no bort and no diamonds below "near-gem" quality were recovered. The amount of gravel from which these stones were recovered was not provided. Indomin has identified 8 million cubic meters of diamondiferous gravels in the Martapura area.   *MLJ*

Moonstar's marine diamonds. J. Chadwick, *Mining Magazine*, Vol. 177, July 1997, pp. 42, 45–47.

This article describes marine diamond mining aboard the *Moonstar*, a ship owned by Benguela Concessions and

Moonstone Diamonds. Benguela has the rights to several marine mining concessions off the northwest coast of South Africa, where diamonds that were transported by rivers from their original kimberlites are found along submerged benches (former beaches). The *Moonstar* will be used first to mine trenches in concessions off Wreck Point and Port Nolloth.

The ship, built in Scotland in 1966 and formerly known as the *Aberthaw Fisher*, was refurbished and refitted as a diamond mining vessel (her tonnage is not specified). Onboard are:

- Two 510 mm airlift mining heads (vacuum-cleaner-like machines); the first removes overburden, and the second pumps the slurried diamond ore up to the vessel.

- A series of multi-stage vibration screens (which separate gravel from clay, returning the latter to the water).

- Surge bins (to break up large clumps of ore still glued together by clay).

- A scrubber mill, a 50-ton-per-hour dense-media separation plant, and X-ray separation equipment.

The plant design has been customized to survive the corrosive marine environment and to deal with seashells in the gravels, which interfere with recovery. The vessel has helicopter support and a crew of 70, including 45 mining personnel.

In four days of tests, 35 diamonds (totaling 18.79 ct) were recovered. The *Moonstar* is expected to recover about 65,000 carats of diamonds (with an average value of $200 per carat) annually. The stones found to date average 0.32 ct; it is anticipated that the largest would be about 8 ct.   *MLJ*

NSW diamond find. *Mining Magazine*, Vol. 177, No. 2, August 1997, pp. 144–145.

Fifteen "gem-quality" diamonds (total weight 3 ct) have been found during trial mining at the Round Top prospect, in the Copeton Dam region of New South Wales, Australia. The mining company, Cluff Resources Pacific, also recovered 200 diamonds in May 1997 from the nearby Lucky Streak prospect. The Copeton–Mount Ross area was a major source of diamonds in the late 19th century, when an estimated 0.5 million carats were recovered.   *MLJ*

Platinova diamond. *Mining Journal, London*, Vol. 329, No. 8441, August 8, 1997, p. 116.

Platinova A/S has found a 1 point (0.01 ct) diamond in a 27.6 kg sample from kimberlite boulders on the shore of an unspecified lake near the coast of central west Greenland. "Abundant" diamond indicator minerals are found in till samples taken in the direction of ice movement from the lake. Platinova has also found kimberlite boulders and dikes in the lake's vicinity.   *MLJ*

Results. *Mining Journal, London*, Vol. 329, No. 8448, September 26, 1997, p. 263.

Rex Diamond Mining recovered 8,635 carats of diamonds (from 41,800 tons of ore) from the Ardo and Bellsbank mines in South Africa during the year ending June 30, 1997. The average value of these stones was US$256 per carat. Flooding at the mines limited production.   *MLJ*

Russian environmental agreement. *Mining Journal, London*, Vol. 328, No. 8417, February 21, 1997, pp. 149–150.

The republic of Sakha (Yakutia) has signed an agreement with the World Wide Fund for Nature, which will allocate US$350,000 to protect Arctic lakes and forests. Mining for diamonds and other commodities in the past has caused serious leaks of toxic chemicals into the Vilyuo River.   *MLJ*

Stresses generated by inhomogeneous distributions of inclusions in diamonds. T. R. Anthony and Y. Meng, *Diamond and Related Materials*, Vol. 6, No. 1, January 1997, pp. 120–129.

Inhomogeneous (nonuniform) distributions of inclusions in diamonds can generate long-range strains, with maximum magnitudes approaching the crushing strength of the diamond. These strains can either strengthen or weaken the diamond. The stresses generated by inclusions are proportional to the average size of the inclusions and to their concentration. If the diameter of a central inclusion cluster is greater than 20% of the diameter of the diamond, the inclusion cluster may "significantly" weaken the diamond crystal.   *MLJ*

Tracing diamonds looted by Nazis. C. Even-Zohar, *Mazal U'Bracha*, Vol. 13, No. 82, September 1996, pp. 21, 22, 24.

Documents produced by "Operation Safehaven," a U.S. intelligence effort that immediately followed World War II, were recently declassified by the U.S. National Archives. These documents show that the Nazis were probably extremely successful in obtaining diamonds (and $2.5 billion of gold, at today's prices) from conquered countries. On the basis of 1940–1942 documents specific to Antwerp, Nazis may have looted diamonds worth millions of dollars. Diamonds that were not needed directly for the war effort may have been sold through Switzerland and Spain.

Rough taken from Belgium in 1940 alone exceeded 340,000 carats, worth $10.5 million at 1940 prices. The combined total of stolen rough and polished goods probably exceeded $25 million, an astonishing amount considering that CSO sales for 1940 were £6.1 million (about $25 million).

These documents—which name specific German officials, diamond dealers, and buyers—also indicate that separate bureaus were responsible for polished goods and rough stones. It remains to be seen if renewed efforts to trace these items will succeed more than 50 years after their theft.   *AAL*

A wake-up call—diamond mining from the ocean. B. Dunnington, *The Diamond Registry Bulletin*, Vol. 29, No. 2, February 1997, p. 5.

Namibian Minerals Corporation, or Namco, is among the companies mining diamonds from beneath the waters off the Namibian coast. Namco has concessions from the Namibian government to dredge off of Luderitz Bay. (De Beers has the close-in concession at the mouth of the Orange River.) In 1996, Namco's two mining ships recovered 456,000 carats from the seafloor. Using a special dredging technology, they separate diamonds from the alluvial host material at the seafloor, so only the diamonds come to the surface; this minimizes disturbance to the environment.   *MLJ*

GEM LOCALITIES

Areas of greatest interest. *Queensland Government Mining Journal*, Vol. 97, No. 1132, March 1996, p. 14.

Some areas of greatest interest for field gem collectors ("fossickers") in Queensland, Australia, have been listed as Designated Fossicking Land, Fossicking Areas, or General Permission areas. This article lists highlights of the recent laws, which govern the conduct of field collectors at these sites. Gem materials that can be "fossicked" include: sapphires (several areas in the Anakie region, especially near Rubyvale, Sapphire, and Willows Gemfields); boulder opal (Yowah, Cunnamulla, Duck Creek, Sheep Station Creek, Quilpie, Opalton, and Winton); aquamarine (O'Briens Creek, Mount Surprise); topaz (the aquamarine localities, plus Swipers Gully in the Passchendaele State Forest); zircon (the sapphire localities); peridot (Chudleigh Park); and quartz varieties (amethyst at Kuridala, "amethystine quartz" at Castle Mountain, smoky quartz at Swipers Gulch, agate at Agate Creek and Forsayth, and petrified wood at Chinchilla).   *MLJ*

Bernstein der Lausitz [Amber from the Lausitz Region]. W. Sauer, *Der Aufschluss*, Vol. 48, No. 1, 1997, pp. 43–51 [in German].

During the ice ages, glaciers spread Baltic amber across the north German lowlands. This amber has become a popular by-product of open-pit lignite mining in the Lausitz region of Eastern Saxony. Because it is a by-product, amber production increases when lignite production is increased. Amber mainly occurs in the Tertiary and Quaternary sediments adjacent to the lignite. The article also contains information on the history of amber production in this area, amber's local use in jewelry, and the different types of amber (succinite and glessite) recovered. Color photos show several samples.   *RT*

Black pearls of French Polynesia. D. Doubilet, *National Geographic*, Vol. 191, No. 6, June 1997, pp. 30–37.

The lagoons in the Tuamoto Archipelago are famous for the black-lipped pearl oyster, *Pinctada margaritifera*, a source of black pearls. The author visited Robert Wan, whose company—Tahiti Perles—produced more than half of the million cultured pearls exported from French Polynesia in 1996.

The pearl oysters in French Polynesia spawn naturally in these lagoons (unlike Japanese Akoya oysters, which are conceived by combination of sperm and egg cells in a hatchery). These oysters require 75°F (about 24°C) unpolluted waters. The larvae attach themselves to plastic garlands, where they grow into oysters. After six months, they are transferred to hanging baskets. They remain in the lagoon for another two years, when they are collected for pearl culturing. A small piece of mantle tissue and a nucleus (a bead carved from an American freshwater mussel) are surgically introduced into each oyster, and the oyster is returned to the lagoon. The mantle tissue will form a sac in which the nacre that will cover the shell nucleus is generated. The oysters are harvested for pearls three years later.

French Polynesia had "pearl" fisheries at the turn of the century, but the main product was mother-of-pearl for inlay and buttons; pearls were very rare. In addition to Mr. Wan's large operation, about 500 other pearl farms operate throughout Polynesia. Different localities have some product variation; for instance, pearls with green overtones are grown in the cooler waters of the Gambier Islands. *MLJ*

Boulder opal—going, going . . . *Queensland Government Mining Journal*, Vol. 97, No. 1134, May 1996, p. 16.

The discovery of opal in Queensland, Australia, was first recorded in 1872, from sites at Listowel Downs, Adavale, and near Springsure. The Cragg mine, in the northern Queensland Mayneside area, was the first to be staked, in 1888. In the 1890s, commercial production began in opal fields at Kynuna (or Kymuna), Opalton, Kyabra, Ah, Koroit (or Korbit), and Hungerford. From 1900 until 1957, the Hayricks Mine in Quilpie was the most important producer of opal in Queensland. Many mines were developed from the 1960s to 1988, as opal increased in popularity and because of the growth of gemstone investment activities.

The Queensland Boulder Opal Association was formed in 1992 to promote these opals, and the first international boulder opal auction/sale was held in May 1993. Three such auctions were held in 1996 in Winton, Queensland. For the auctions, the opals are classified as boulder black, boulder crystal, boulder light, boulder matrix, and "ah nuts" (or Yowah nuts).

The Queensland fields extend about 1,000 km north to south (from Kynun to the New South Wales border) and over 300 km west from the centers at Longreach, Blackall, and Charleville. Other opal fields include Toom-pine, Kyabra-Eromanga, Bulgroo, Yaraka, Jundah, and Davenport-Palparara. *MLJ*

Chrysoprase from Warrawanda, Western Australia. T. Nagase, M. Akizuki, M. Onoda, and M. Sato, *Neues Jahrbuch für Mineralogie, Monatshefte*, Vol. 17, No. 7, July 1997, pp. 289–300.

The authors used optical and transmission electron microscopy, Fourier-transform infrared spectroscopy, and electron microprobe analysis to determine the origin of color in chrysoprase from Warrawanda, about 80 km (50 miles) southwest of Newman, Western Australia. Inclusions of kerolite, a talc-like mineral with a nickel content of about 10 wt.% NiO, were found to be the color source. The Ni is believed to come from the strongly weathered silicified serpentinite in which the chrysoprase veins and nodules occur. The Ni-bearing kerolite mainly occurs as fillings in the interstices between the quartz grains and as inclusions in quartz crystals. *RT*

Exploration and prospecting interest on the increase in Wyoming. W. D. Hausel, *International California Mining Journal*, Vol. 65, No. 11, July 1996, pp. 5, 6, 8.

Several Wyoming regions are being prospected for diamonds and other gem materials. Along the northern flank of the Seminoe Mountains of central Wyoming, kimberlitic indicator minerals (pyrope garnets) have been found in a dry gold placer. In addition, several diamond-iferous kimberlites have been located in the State Line diamond district of southeastern Wyoming: More than 120,000 diamonds [carat weight unspecified] have been produced so far, and some of the pyrope garnet and chrome diopside in the area also show gem potential.

"Hundreds" of kimberlite-indicator-mineral anomalies have been found in anthills, stream sediments, and Tertiary conglomerates in the Green River basin. Guardian Resources has reportedly discovered 10 kimberlite breccia pipes in the area, one diamondiferous. A few small diamonds have been reported from a coal bed in the Powder River Basin in northeast Wyoming, and kimberlite indicator minerals were reportedly recovered from stream sediments in the Bighorn Mountains in the early 1980s. *MLJ*

Flammenachat aus Brasilien—Zur Entstehung unge-wöhnlicher Chalcedon-Quarz-Geoden aus dem Paraná-Becken, Rio Grande do Sul, Brasilien [Flame agate—on the formation of unusual chal-cedony-quartz geodes from Paraná Basin, Rio Grande do Sul, Brazil]. R. Rykart, *Lapis*, Vol. 22, No. 5, May 1997, pp. 27–31 [in German].

The author describes the appearance, mineral composition, and formation of flame agate, snake agate, and irregularly formed chalcedony specimens that occur in sandstones of the Tupanciretá formation, in Soledade, Paraná Basin, Rio Grande do Sul, Brazil. The chalcedony geodes, called flame agate, measure 3–12 cm in diameter. The

cavities in which they occur are surrounded by characteristic bulges of colored chalcedony and typically contain small quartz crystals (rarely amethyst) and sometimes goethite, calcite, and zeolites. The geodes originated from "steam bubbles" that formed in layers of wet sandstones that were repeatedly covered by basaltic lava flows during the Jurassic era. Snake agate, small chalcedony disks 3–5 cm in diameter, and irregularly shaped chalcedony formations are assumed to originate from gelatinous polysilicic acid that precipitated in fissures in the host rock.   *Dr. Peter R. Buerki*

Green to envy. A. Wenk, *Modern Jeweler*, Vol. 96, No. 10, October 1997, pp. 33–34, 36, 38.

Since its discovery in the mid-19th century in Russia's Ural Mountains, the demantoid variety of andradite garnet has been touted by Tiffany and flaunted by Fabergé, its fiery green brilliance making it the best of the breed. Despite its beauty, however, demantoid's rarity has been its most important claim to fame. Since 1915, the Russian deposits have produced relatively few stones above one carat. In addition, limited production over the past 80 years has caused this brilliant green garnet to be of more interest to collectors than to jewelers.

A new deposit in Namibia has given hope that demantoid will be available in significant quantity and good quality for the first time, although it is doubtful that demantoid will ever be plentiful. The deposit is located in a large savanna, surrounded by mountains in the central area of the Precambrian Damara Orogen belt in central Namibia. At its best, Namibian demantoid is bright green and usually eye clean. Rough from the new deposit has thus far produced cut stones up to 9.89 ct, a size close to the record 10.40 ct demantoid from Russia in the Smithsonian Institution. The new demantoid from Namibia does not have the "horse-tail" chrysotile inclusions characteristic of the Russian material. In fact, demantoid is one of the few gems that is made more valuable by its internal features, as horse-tail inclusions prove Russian origin.   *MD*

Neues Vorkommen von Demantoid in Namibia [New occurrence of demantoid in Namibia]. T. Lind, U. Henn, A. Henn, and H. Bank. *Gemmologie: Zeitschrift der Deutschen Gemmologischen Gesellschaft*, Vol. 46, No. 3, 1997, pp. 153–159 [in German].

This is the first detailed technical study on the potentially important new demantoid deposit in central Namibia. Following a historical review of demantoid and a description of the geology of the Namibian deposit, the authors report the physical-chemical properties of the Namibian material.

The Namibian demantoid has a density of 3.81–3.85 gm/cm³. The refractive index was over the limits of the refractometer. Chemical analyses show a composition that is essentially pure andradite with very low concen-

trations of chromium, ranging between 0.02 and 0.13 wt.% Cr_2O_3. The visible-range absorption spectra show bands for Fe^{3+} and Cr^{3+}. Distinct growth zoning is seen with the microscope, as are unidentified ore-like (opaque) inclusions. "Horse-tail" chrysotile inclusions, so characteristic of the Russian demantoids, were not seen in the Namibian material.   *AAL*

On the topaz trail. P. O'Brien, *Australian Gold Gem & Treasure*, Vol. 12, No. 4, April 1997, pp. 26–30.

The Innot Hot Springs topaz locality is about halfway between Atherton and Mt. Surprise in North Queensland, Australia. The topaz comes from dumps left over from a rich tin deposit discovered in the late 1800s. Topaz, quartz, aquamarine, and sometimes sapphires were by-products of alluvial tin (cassiterite) workings in Australia; the tin miners had no interest in these gangue minerals and left them behind, much to the delight of modern-day fossickers.

Collecting is done by of dry-sieving. The topaz is unmistakable: "It literally pops out of the ground, clear, shiny, and definite." The author unearthed several "marble size and bigger" topaz crystals in about four hours. Most of this material was clear with "perfect" crystal forms; blue specimens were uncommon. About 30 years ago an 18 kg piece of topaz was found at Innot Hot Springs. Permission is required to enter the topaz digging area.   *MLJ*

Sapphire agreement. *Mining Journal, London*, Vol. 326, No. 8416, February 14, 1997, p. 136.

Montana sapphire producer Gem River Corporation entered into an agreement with Landstrom's Original Black Hills Gold Creations™, in which Landstrom will purchase between $1 million and $3 million in cut and polished sapphire over one year, beginning February 12th, 1997. For the first six months of that period, Landstrom was not to sell or market any of these sapphires. The agreement set prices for various colors, styles, sizes, and quality grades of sapphires, which were to average $55 per carat. Most stones were projected to be under 1 ct in weight. The stones were to be marketed as "Gem River Sapphires" and "Montana Sapphires" (both terms trademarked).

Gem River has identified proven reserves of 4 million carats. However, the company owns freehold over "substantial" ground around the deposits and was confident that adequate ore reserves could be proved to sustain mining.   *MLJ*

Gem River resumption. *Mining Journal, London*, Vol. 329, No. 8437, July 11, 1997, p. 27.

Gem River Corporation has resumed mining for sapphires at Lower Dry Cottonwood Creek in Montana for the 1997 season. Gem River produced 975,000 carats in 1996, and 1.5 million carats are anticipated in 1997.

MLJ

Surface geochemical techniques in gemstone exploration at the Rockland Ruby mine, Mangare area, SE Kenya. A. G. Levitski and D. H. R. Sims, *Journal of Geochemical Exploration*, Vol. 59, No. 2, June 1997, pp. 87–98.

Mineral and gem deposits that are covered by soils, alluvium, glacial deposits, or any other material are among the most difficult to discover. Geologists typically use indirect methods to find these buried deposits. The techniques vary, depending on the specific geologic situation (e.g., type of overburden or the mineral being sought).

This article describes exploration techniques used to find corundum mineralization in the Mangare area of southeast Kenya. The Rockland (John Saul) Ruby mine was the specific study site. This type of corundum mineralization is found in pegmatitic material adjacent to ultramafic bodies within gneiss. The area is covered by 1–3 m of overburden consisting of soils, gravels, and secondary calcareous material.

Bulk samples of the overburden were chemically analyzed. Also used was a special *in situ* selective chemical leach called "MDI" (Method of Diffusion Extraction). Both methods yielded unambiguous anomalies for nickel, cobalt, and chromium over the known extent of the ultramafic body; however, the MDI anomaly defined the ultramafic body more precisely.

Because a spatial and genetic relationship exists between the corundum mineralization, the pegmatitic material, and the ultramafic body, a two-step exploration sequence is recommended: (1) soil sampling and analysis on a 100 × 50 m grid to delineate the ultramafic areas; followed by (2) MDI measurements of a finer (50 × 25 m) grid over the ultramafic body to, one hopes, delineate individual corundum-bearing pegmatites. *AAL*

INSTRUMENTS AND TECHNIQUES

Raman spectra of various types of tourmaline. B. Gasharova, B. Mihailova, and L. Konstantinov, *European Journal of Mineralogy*, Vol. 9, 1997, pp. 935–940.

The authors characterized 25 natural tourmalines of known origin and chemical composition by polarized Raman spectroscopy in the spectral range 150–1550 cm^{-1}. They used a Raman microspectrometer (a Microdil-28) with an intensified diode-array detector in back-scattering geometry and argon laser excitation. Raman bands of the buergerite-schorl series are centered at about 230 and 670 cm^{-1}; in addition, the spectra are characterized by a single peak at 238 ± 2 cm^{-1} and three resolved peaks at 635 ± 3, 674 ± 3, and 697 ± 3 cm^{-1}. Elbaite tourmalines have a sharp peak at 224 ± 2 cm^{-1} and two well-separated peaks, one at 638 ± 3 cm^{-1} and the other above 707 cm^{-1}. The dravite-buergerite-uvite series is characterized by two peaks at 215 ± 3 and 237 ± 3 cm^{-1}, with a smooth spectral band centered at about 670 cm^{-1}.

Dr. Peter R. Buerki

JEWELRY HISTORY

Capturing the image of antique jewelry. R. Weldon, *Jeweler's Circular-Keystone*, Heritage section, Vol. 168, No. 6, June 1997, pp. 210–215.

Photographing gems and jewelry is surprisingly difficult, as anyone who has tried it will agree. Robert Weldon, a Graduate Gemologist and a writer for the jewelry trade press, is also an excellent gem and jewelry photographer. In this article, he generously shares his photographic knowledge, giving not only the basics but also insight into photographic pitfalls and tricks to avoid them.

The article is divided into eight sections: tools for the job, other considerations (e.g., set-ups and f-stops), choosing the piece, choosing the background, lighting, photographing shiny metal, photographing gems, and documenting the piece. There is also a table, "Matching Film to Light," in which specific film types are recommended and their idiosyncrasies listed.

The article is well illustrated with the author's photographs. In several cases, the same piece is shown under different lighting conditions, or with different backgrounds, to demonstrate points in the text. Mr. Weldon's writing style is engaging, and the article makes this exacting artform sound deceptively easy. *EBM*

Dates to remember. C. Romero, *Jeweler's Circular-Keystone*, Heritage section, Vol. 168, No. 2, February 1997, pp. 160–167.

In the estate jewelry business, questions always arise when a period piece is being dated. Knowing when a specific clasp was invented or when certain synthetic gems were put on the market can help pinpoint a piece's age. For this article, Christie Romero has compiled important dates for inventions and discoveries relevant to jewelry history. The data come from her book, *Warman's Jewelry* (Chilton Co., Radnor, PA, 1995), which presents the material chronologically. In the article, however, she arranges it in five categories: metals and metalworking techniques, inventions and patents, gemstone cutting and setting techniques, natural and synthetic gemstone discoveries, and other synthetic jewelry material. Caveats about what can be concluded from the information provided, together with a strong bibliography, frame the text, which is *packed* with useful facts. Included among the many items listed in the article are: patent dates for white gold, spherical cultured pearls, and the screw-backed earring, along with dates for the discovery of demantoid garnet, the flux-grown synthetic ruby process, and the development of Bakelite plastic. Ms. Romero has done a tremendous amount of work here, and she deserves the full respect and gratitude of jewelry dealers, researchers, and historians alike. *EBM*

The jewelry of John Paul Cooper. N. N. Kuzmanovic, *Jewelry: Journal of the American Society of Jewelry Historians*, Vol. 1, 1996–1997, pp. 41–51.

John Paul Cooper, a notable jeweler of England's Arts and

Crafts movement, was active between the late 1890s and 1933. Cooper began work in 1889 as an architect but segued into the decorative arts after encouragement from Henry Wilson, his boss at the firm. During the 1890s, Cooper made boxes and other decorative objects; his work with shagreen (shark skin) became a popular product of the firm's studio branch. His move into metalwork and jewelry coincided with the opening of his own studio in 1897. Cooper's jewelry is typical of the Arts and Crafts style—hand-fabricated gold and silver set with pearls and cabochon-cut gemstones (predominantly amethyst, moonstone, chrysoprase, and aquamarine). His motifs are mostly stylized florals, often incorporating the mystical or mythological. The author categorizes Cooper's jewelry into four periods with subtle stylistic differences:

- The Birmingham period (1902–1906)—characterized by chased (a form of metalwork) figures and scenes with a mythological theme.
- The Hunton period (1907–1910)—more opulent and colorful than the Birmingham period and using more gems; the metal is also more elaborately worked.
- The first Betsom's Hill period (1911–1919)—more elegant and refined.
- The second Betsom's Hill period (1920–1933)—simplified, cool, and detached.

Using Cooper's jewelry stockbook as a reference, the author chronicles his development as a jeweler and quotes from Cooper's personal journal to show how his interest in spirituality and mysticism influenced his work. Although the chances of finding Cooper's pieces on the open market today are slim, it is important to chronicle his work. Without being too biographical, the article is a scholarly overview of the jewelry made by this little-known artist. *EBM*

Margaret Craver: A foremost 20th century jeweler and educator. J. Falino and Y. Markowitz, *Jewelry: Journal of the American Society of Jewelry Historians*, Vol. 1, 1996–1997, pp. 8–23.

For the inaugural issue of the American Society of Jewelry Historians' journal in its new format, authors Falino and Markowitz give us a tidy introduction to the work of artist-jeweler Margaret Craver. Ms. Craver is a respected metalsmith and jeweler whose work is part of permanent collections at 11 major U.S. museums, including the Smithsonian Institution, where her tools, hallmarks, notes, and correspondence are now in the Archives of American Art.

Ms. Craver's jewelry style is strong and clean. She primarily used hand-forged silver, often incorporating enamel or gems that she cut herself (chiefly turquoise and varieties of quartz). In the 1950s, she became fascinated with *en resille*, a style of enameling used in France during the 16th and 17th centuries. This technique, of floating enameled foils in an enamel ground, had been lost, and Margaret Craver experimented for several years to recre-

ate it. Her success is evident in pieces made during the 1960s and 1970s that were shown in major art exhibitions nationwide and have since become part of various museum and private collections.

Ms. Craver also dedicated much time to teaching. As a volunteer at a Chicago hospital in 1944, she developed a rehabilitative metalsmithing program for disabled World War II veterans. This program brought her to the attention of the Worshipful Company of Goldsmiths in London, the Rhode Island School of Design, and the Rochester Institute of Technology, for whom she organized workshops and conferences that she also participated in. She filled the years between 1950 and her retirement in 1988 with exhibitions, lectures, and time devoted to her jewelry work.

This well-documented article is augmented by 14 illustrations. The authors also have thoughtfully provided Ms. Craver's hallmarks (one for 1934–43 and a second for 1944–88), a chronology of her professional life, and a list of museums that house her pieces. *EBM*

Splendor in the glass. E. C. Fisher, *Jeweler's Circular-Keystone*, Heritage section, Vol. 168, No. 6, June 1997, pp. 204–208.

The popularity of costume jewelry today has prompted a need for information about its historical background and development. This article focuses on glass made in Bohemia for use as gem substitutes in jewelry.

Bohemia, in central Europe, became Czechoslovakia after World War I. In 1993, it split into two independent states, the Czech Republic and Slovakia. This region has long produced glass for jewelry use. Ms. Fisher neatly capsulizes four centuries of this craft—from the mid-16th century to the present—sketching in the highlights of its evolution from cottage industry to mass production and international renown. Included in the highlights is the well-known name Swarovski, as Daniel Swarovski introduced machine technology to the manufacture of rhinestones in the late 1800s. Wars and economic depressions have increased the demand for costume jewelry. During the 20th century, it grew enormously in both acceptance and market value.

In addition to describing the development of Czech glassmaking, the author also touches on jewelry design and manufacture in the region. Typically made in brass filigree, the work was originally all done by hand, but the cost effectiveness of machine-stamped mounts soon revolutionized the industry. Ms. Fisher's article gives insight into, and instills respect for, Bohemian jewelry. Nine photographs handsomely illustrate the text, and a bibliography provides sources for more information about this interesting topic. *EBM*

The Stuart Jewel: A new acquisition for the National Museums of Scotland. B. Jackson and S. Honeyman, *Journal of Gemmology*, Vol. 25, No. 6, April 1997, pp. 428–430.

The National Museums of Scotland recently acquired a

rare example of 17th century Scottish jewelry with a well-documented history of ownership. The unusual piece is an enameled "trembler" gold hat ornament, set with rubies that are apparently of Burmese origin. The enameled flower (a Stuart rose?) attaches to its stem with a spring that permits the top to move; hence, the name "trembler." Information about the piece's creator is being sought.   *CMS*

JEWELRY RETAILING

The Israeli public owns $11.7 billion of jewelry. *Mazal U'Bracha*, Vol. 13, No. 83, October 1996, pp. 78, 80, 81, 83.

One independent organization, Gemolab, appraises 80% of Israel's jewelry. Gemolab experts estimate that Israelis own $11.7 billion of jewelry, or about $4,186 for every Israeli woman. Jewelry constitutes "10–12% of the belongings" of an average household, so the need for independent appraisers is high in Israel. Retail-store-based appraisers often have conflict-of-interest problems.

The main objective of home-insurance appraisals is to determine fair replacement value. This is a relatively straightforward process for unmounted stones. Gemolab appraisers use prices from the Rapaport list and the Israel Diamond Exchange; mark-ups and VAT (Value Added Tax) are also added.

Appraising set diamonds is far more complex because of difficulties in determining color, clarity, and weight; precise evaluations are usually impossible. Even more difficult is appraising the setting. The profit margin of the retail source must be factored in, as must the reputation of the designer and the store from which the jewelry was purchased. Designer reputation might be considered highly subjective, however, so Gemolab bases their appraisals on the local market and on local prices, enabling consistency and objectivity.

The Israeli appraisal market has two unusual aspects. First, the term "replacement value" means being able to buy the same or a similar object in the "same store again" (which is something that insurance companies elsewhere in the world might not accept). Second, appraisal value differs from place to place in Israel (similar to how an insurance policy costs more in a high-risk neighborhood).   *AAL*

Sri Lanka deregulates to raise exports. M. A. Prost, *Colored Stone*, Vol. 10, No. 6, November–December 1997, pp. 10, 12.

Responding to competitive market pressures, Sri Lanka last June lowered taxes and tariffs to help small and medium-size cutting and manufacturing companies increase productivity. The new policies allow manufacturers to import rough stones duty-free, paying only a 4.5% security levy that is refunded if the stones are reexported within six months. More important to manufacturers is that any company can trade gems locally and pay only

the security levy. The government is also offering a 100% tax exemption on imports of goods, such as machinery, to companies that export 50% of their production. To further assist the industry, the National Gem and Jewellery Authority, which regulates the jewelry industry in Sri Lanka, has allocated $4.2 million to develop heat-treatment facilities for milky corundum mined in Sri Lanka. All these measures are designed to help Sri Lankan industries compete internationally. According to the Sri Lanka Gem & Jewellery Exchange, the liberalization of import and export regulations—which began two years ago—has already had a positive effect on the industry. The export value of cut and polished gems reportedly increased from $13.64 million in 1996 to $18.79 million by the end of July 1997.

Although manufacturers are optimistic, they remain concerned about other restrictions, including the time-consuming paperwork in which goods are officially documented, valued, and cleared through the Gem Authority in Colombo. That process normally takes two days and is seen as the major remaining obstacle.   *MD*

PRECIOUS METALS

Metal boulders. A. Maslowski, *International California Mining Journal*, Vol. 66, No. 3, November 1996, pp. 15–19.

Among the metallic elements found worldwide as minerals are gold, silver, platinum, copper, and iron (or iron-nickel alloy). The largest gold nuggets usually are too valuable to preserve. Many have been found in Australia: One that contained more than three tons of gold was found in New South Wales in 1872. Native silver is found—sometimes as veins—in underground mines, but it reacts with air, water, and many elements far too rapidly to form significant placer nuggets. The largest platinum nugget in the Smithsonian Institution weighs 536.7 grams, and came from Chocó, Colombia; both Russia and Colombia are possible sources of still larger nuggets. Some masses of native copper have weighed more than 100 tons. One nickel-iron meteorite, Ahnighito, weighs about 31 metric tons. Found in Greenland, it now resides in New York's American Museum of Natural History. This article mentions several other sizable nuggets, including a glacier-transported 104.4 gram platinum nugget found in 1880 in Plattsburgh, New York.   *MLJ*

X-ray assays offer a non-destructive complement to traditional fire assays. F. Reilley, *American Jewelry Manufacturer*, Vol. 42, No. 7, July 1997, pp. 48–50.

A fast, accurate, and nondestructive way to determine metal purity is briefly described. X-ray assay will not replace fire assay techniques, but it complements them well. It could be helpful in jewelry manufacturing and in quality control of incoming goods, for example. In X-ray assay, analysis of the electromagnetic spectrum determines the test sample's elemental compositions by weight percentage. Accuracy depends on the accuracy of

the reference standards used, the length of time the standard is measured, the similarity of the standard to the unknown sample, and the shape and size of the item being tested. This article is worth at least a quick read because it describes an assay technique that could be widely used in different areas of the jewelry industry.

<div align="right">JM</div>

TREATMENTS

How to identify fillings in emeralds using Raman spectroscopy. H. A. Hänni, L. Kiefert, and J.-P. Chalain, *Jewellery News Asia*, No. 145, September 1996, pp. 154, 156.

Using a Renishaw Raman laser spectrometer-microscope system, researchers at the SSEF Swiss Gemmological Institute have successfully detected various organic materials used to fill emeralds. Such analyses are fast, nondestructive, and require no special sample preparation. According to the SSEF, the important features for these fillers are observed in the Raman spectra between 2800 cm^{-1} and 3100 cm^{-1}, with another region showing diagnostic peaks between 1200 cm^{-1} and 1700 cm^{-1}. The most important individual peaks in these regions, which are absent or extremely weak in natural resins or oils, are found at 3069 cm^{-1}, 3008 cm^{-1}, 1606 cm^{-1}, and 1250 cm^{-1}. However, the age of the organic fillers can affect Raman spectra. The spectra of older fillers may have an additional "hump" because of fluorescence in the region between 2800 cm^{-1} and 3100 cm^{-1}. This can mask characteristic peaks in this region and make the identification of an older filling very difficult—if not impossible—using this region alone. Fortunately, the region between 1200 cm^{-1} and 1700 cm^{-1} is not diminished by this fluorescence effect.

<div align="right">John I. Koivula</div>

Treated jadeite doublets confuse market. *Jewellery News Asia*, No. 156, August 1997, p. 38.

Ou-Yang Chiu Mei, of the Hong Kong Institute of Gemmology and President of Hong Kong Gems Lab, describes an assemblage (doublet) that is composed of a thin layer of jadeite over an epoxy resin. The material, sometimes called "egg crust jadeite" or "thin layer jadeite," is 10% jadeite and 90% epoxy resin. Dark jadeite with poor translucency is usually used. When this jadeite is cut into very thin layers and combined with the resin, material with enhanced transparency results. The infrared spectra of this assemblage are similar to those of B-jade. However, requests to call it "A-jade" or "B-jade" on laboratory certificates have been refused.

<div align="right">JM</div>

MISCELLANEOUS

A gem of an exhibition. M. Kernan, *Smithsonian*, Vol. 28, No. 6, September 1997, pp. 57–63.

The Janet Annenberg Hooker Hall of Geology, Gems and Minerals at the Smithsonian Institution, Washington, DC, opened in September 1997. In addition to the famous Hope Diamond, the 20,000-square-foot (6,096 m^2) hall features 40 of the best-known cut-stone creations in the world. Among the most ravishing is a diadem, Napoleon's wedding present to Empress Marie-Louise. This piece, which currently contains more than a thousand diamonds and 79 turquoise cabochons, originally held emeralds—instead of turquoise—which were removed by Van Cleef & Arpels and sold in the 1950s. Also on display are the Napoleon diamond necklace, given to Empress Marie-Louise on the birth of their son; the Hooker Starburst diamonds and Hooker emerald; the Star of Asia; the Marie Antoinette diamond earrings; the DeYoung red-and-pink diamonds; a 23,000 ct topaz; the 38 ct Chalk emerald; the 423 ct Logan Sapphire; and the 127 ct Portuguese diamond.

The Minerals and Gems Gallery has interactive displays and videos that explain many properties of gems and minerals. A 1,600-square-foot (488 m^2) "mine" contains zinc, copper, lead, and some gem minerals. Real ore veins and crystal pockets are set into rock-like walls, painted to resemble a working mine. The Rocks Gallery exhibition tells how rocks are formed and altered by wind, water, gravity, and powerful forces below the earth's crust. Granites, basalts and limestones, glacially striated rocks, and large garnets are displayed. The Plate Tectonics Gallery features video presentations that demonstrate how the movement of enormous plates cause most of the planet's geologic activities. A cutaway of an active volcano shows the mechanics of the heat from the earth's interior bursting to the surface and creating islands. The Moon, Meteorites, and Solar System Gallery includes a 4.5 billion-year-old meteorite.

<div align="right">MD</div>